SECONDARY ELECTRON EMISSION

Electronics and Waves Series

BALINT.
A BOOK I BORROWED IN 1963!
Someday.....

PROPERTY OF
ENGINEERING LIBRARY
WESTINGHOUSE ELECTRIC CORPORATION
ELECTRONIC TUBE DIV., ELMIRA, N. Y.

PERGAMON SCIENCE SERIES

ELECTRONICS AND WAVES—*a series of monographs*

EDITOR: D. W. Fry (Harwell)

PHYSICS AND APPLICATIONS OF SECONDARY ELECTRON EMISSION

PHYSICS AND APPLICATIONS OF SECONDARY ELECTRON EMISSION

By

Dr. H. BRUINING, M.B.E.

Philips Research Laboratories, Eindhoven

NEW YORK: McGRAW-HILL BOOK CO., INC.

LONDON: PERGAMON PRESS LTD.

1954

Published in Great Britain by Pergamon Press Ltd., Maxwell House, Marylebone Road, London, N.W.1

Published in U.S.A. by McGraw-Hill Book Co., Inc., 330 West 42nd Street, New York 36, N.Y.

Made in Great Britain at the Pitman Press

CONTENTS

EDITOR'S PREFACE

The aim of these monographs is to report upon research carried out in electronics and applied physics. Work in these fields continues to expand rapidly, and it is recognised that the collation and dissemination of information in a usable form is of the greatest importance to all those actively engaged in them. The monographs will be written by specialists in their own subjects, and the time required for publication will be kept to a minimum in order that these accounts of new work may be made quickly and widely available.

Wherever it is practical the monographs will be kept short in length to enable all those interested in electronics to find the essentials necessary for their work in a condensed and concentrated form.

D. W. Fry

AUTHOR'S PREFACE

The phenomenon of secondary electron emission was discovered fifty years ago. At first only little interest was shown, but when electronic tubes came into more general use, secondary electron emission was also more intensively investigated. Literature on this subject is of both an academic and a technological character. In this book a survey of the physics and applications of secondary electron emission is given.

In the first seven chapters the physical side of secondary electron emission is discussed. The first chapter is an introduction; the second treats methods and measurements. The third and fourth chapters give numerical results on the secondary electron emission yield of both metals and metal compounds. In these chapters some effects are discussed and their connection with the experimental technique explained. The fifth chapter deals with the influence of externally adsorbed foreign atoms and ions on secondary electron emission. Chapters 6 and 7 deal with the mechanism of

secondary electron emission. While it is evident that a complete theory does not yet exist, the author has endeavoured to give a survey comprising the various approaches to the problem. Results of experiments of fundamental importance are also discussed.

The three final chapters deal with the application side: Chapter 8 on the application of electron multiplication, Chapter 9 on the elimination of disturbing effects due to secondary electrons, and Chapter 10 on "storage" devices in which information on electrical charges is written on an insulating surface, often by making use of secondary electron emission.

Literature on this subject is rather extensive. In accordance with the contents of the book the list of references is divided into two parts, one being a chronological list of articles on the physics of secondary electron emission, and the other comprising articles on the application.

The author would like to express his thanks to Professor Dr. H. B. G. CASIMIR, director of the Philips Research Laboratories, for his permission to publish this book. He is much obliged to Professor Dr. J. L. H. JONKER, who read the manuscript and made several valuable suggestions. On the subjects treated in Chapter 10 he had many useful discussions with Dr. P. SCHAGEN.

Thanks are also due to the Pergamon Press for the handsome printing of the book.

EINDHOVEN,

November 1953

1

INTRODUCTION

1.1. DISTINCTION BETWEEN SECONDARY ELECTRONS OF A DIFFERENT CHARACTER

When electrically charged particles with sufficient kinetic energy hit the surface of a solid, the latter emits electrons. These electrons are called *secondary* electrons, and the bombarding electrons are called *primary* electrons. This book surveys the phenomenon of secondary electron emission from different kinds of substances in the solid state.

The phenomenon of secondary electron emission was discovered by AUSTIN and STARKE [8] in 1902. AUSTIN and STARKE were studying the reflection of cathode rays from metal surfaces and found that the metal target was able to emit a larger number of electrons than it was receiving. This was proof that the primary electrons liberated additional ones from the material itself; if mere reflection occurred, a number of secondary electrons at the most equal to that of the primary electrons would have been found.

Later on these phenomena were thoroughly studied by LENARD and his co-workers. LENARD [1] proposed the following distinction between different groups of electrons.

1. "Secondary electron radiation"; this was meant to be the result of ejection of electrons from a substance by the impact of primary electrons. Electrons which are able to leave the substance were called surface-secondary-electrons. When the substance under investigation has the shape of a thin plate, emission of secondary electrons on both sides can be found, namely on the side exposed to the bombardment of the primary electrons (emission on the entrance side) and also on the side through which the primary electrons are leaving the substance (emission on the exit side).

This book will mainly consider the emission of secondary electrons on the entrance side. The emission on the exit side has never been a subject for profound examination, although it might be of

importance for technical application (see Chapter 9). On the other hand, the emission on the entrance side has been examined thoroughly in numerous investigations; it is very important from a technical point of view, as it is found in all kinds of electronic valves or tubes where its effect is indeed essential for their operation.

2. "Re-diffusion" (LENARD's "Rückdiffusion"); the result of the bending of the path of an electron, caused by the penetration of atoms, LENARD called "diffusion". When the direction of the path was altered through more than 90°, he used the term "Rückdiffusion". Upon bombardment with primary electrons these "rediffused" electrons are found among the secondary electrons. The term "reflected electron" was used by LENARD for the special case of a rediffused electron which had suffered only one collision with an atom.

LENARD made this distinction because it was observed that among the secondary electrons there were different groups, namely a slow group with an energy of the order of magnitude 10 eV (this was approximately independent of the energy of the primary electrons) which was considered to consist of the secondary electrons, and a group with a greater energy being the rediffused electrons. An example of such a separation will be discussed in the next section.

Another way to differentiate between different kinds of "secondary electrons" which is often encountered in the literature is the following [5, 6]:

"true" secondary electrons	LENARD's secondary radiation
(primary) electrons which have suffered one or more inelastic collisions (primary) electrons which have been scattered elastically (without loss of energy)	rediffused and reflected radiation

From this one can see that the terminology used in the literature is quite different. The expressions used by LENARD refer to *the path or orbit of the primary electrons* in the substance under investigation; the words elastically and inelastically refer to *the loss of energy of the primary electrons.*

1.2. ENERGY DISTRIBUTION OF THE SECONDARY ELECTRONS

In this section we shall consider how it is possible to classify secondary electrons experimentally. The determination of their energy distribution can be carried out by two different methods:

(1) By means of a retarding electric field E, permitting the number of secondary electrons with an energy greater than E to be determined.

(2) By means of a magnetic deflecting field, leading to a determination of the number of secondary electrons with an energy between E and $E + dE$.

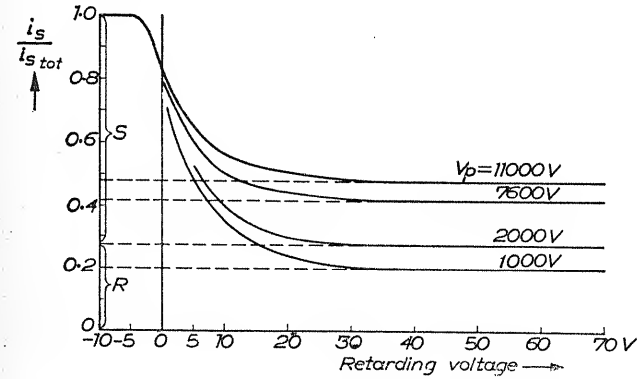

Fig. 1.1. Energy distribution of secondary and rediffused electrons emitted by gold; according to STEHBERGER [70]

In fig. 1.1 an energy distribution is shown measured by STEHBERGER with a retarding electric field. The abscissa gives the voltage, the ordinate the fraction of the secondary electrons capable of overcoming the retarding field. When the secondary electrons are all drawn to the collector (negative abscissa), the curve runs parallel to the abscissa. With a small retarding voltage the curve drops steeply, and then continues horizontally as the voltage is further increased. In this drawing the method of separation of secondary and rediffused electrons is also shown. According to the Lenard school this can be carried out by extrapolating back the horizontal section from a voltage of about 30 V, and determining the intersection with the ordinate axis. When $V_p = 2000$ V, 27% of the secondary electrons are then found to be rediffused electrons and the rest "secondary radiation".

Fig. 1.2 shows the energy distribution of secondary electrons emitted by copper, after FARNSWORTH [41]. Again the abscissa gives the retarding voltage; the ordinate is the number of secondary electrons per primary electron capable of overcoming the retarding field. The different curves are for different values of V_p, in this case much smaller than in fig. 1.1; there is again a steep fall at low retarding voltages, but this continues nearly rectilinearly with increasing voltage. As the retarding voltage approaches the value

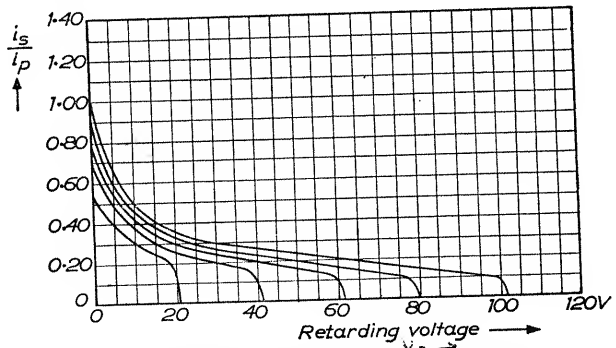

Fig. 1.2. Energy distribution of secondary electrons emitted by copper; according to FARNSWORTH [41]

of V_p a further steep fall occurs; the only electrons now able to reach the collector are elastically reflected primaries.

Unlike fig. 1.1 then, fig. 1.2 fails to show a separation into slow and fast electrons. Such a separation is not generally possible with slower primary electrons. An exact separation would be possible only if the orbits of the electrons in the substance could be observed, but this cannot be realized. It was suggested by STEHBERGER that the slow fraction consists only of "secondary radiation" and the faster part of rediffused electrons.

It is however possible to distinguish inelastically scattered primary electrons from the others. This can be done by measuring the energy distribution with the aid of a magnetic deflection method (RUDBERG [79, 103]). In fig. 1.3 the distribution curve is shown for a silver target; the ordinate is the number of electrons with an energy between E and $E + dE$, the abscissa the energy in eV. The curve shows four maxima.

The abscissa of the broad high maximum, marked S, is nearly independent of the energy of the primary electrons and is therefore

caused by the "true secondary electrons". The maximum marked R originates from the elastically scattered primary electrons. The distance between the maxima U and R is independent of the energy of the primary electrons. The maxima U are evidently caused by primary electrons which have lost a certain amount of energy, i.e. have been elastically scattered. It is of course possible

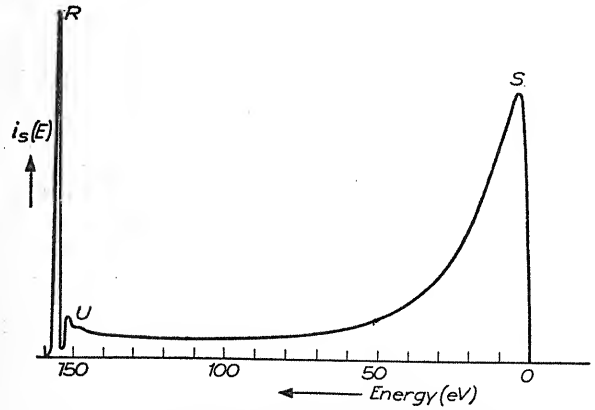

Fig. 1.3. Energy distribution of secondary electrons emitted by silver; according to RUDBERG [79, 103]

that the number of these electrons is greater, but it is not possible to recognize them as such. The section of the curve parallel to the abscissa consists presumably of a mixture of "true" secondary electrons with inelastically scattered primary electrons or, to use LENARD's terminology, of "secondary radiation" and rediffused electrons.

1.3. YIELD OF SECONDARY ELECTRON EMISSION

From the examples discussed in the previous paragraphs it will have become obvious that only the elastically reflected primary electrons can be separated with certainty. Fig. 1.2 shows that the elastic reflection decreases with increasing energy of the primary electrons; e.g. at $V_p = 20$ V 40% of the "total" secondary electrons consist of elastically reflected electrons, but this percentage drops below 10 for primary electrons with an energy of 100 eV.

As far as the inelastic scattering is concerned, it seems reasonable to assume with MCKAY [6] that all electrons with an energy greater

than 50 eV have been scattered, either inelastically or elastically. In Chapter 3 we shall give a further survey of the number of these electrons emitted by different substances, calculated on this basis. We shall repeat here that such a separation can only be carried out properly for $V_p > 2000$ V.

In the region $V_p < 2000$ V the slow electrons, i.e. true secondary electrons, are the larger fraction of the total secondary electron current. This has no doubt been the reason why many authors have fallen into the habit of calling all emitted electrons secondary electrons, and have thus tacitly assumed that all emitted electrons are liberated by the action of the impinging primary electrons. This assumption is of course incorrect, but it is useful when the aim is to find gross effects; e.g. if the question arises which substances are able to emit very many or very few secondary electrons, it is practical to define the yield of secondary emission *as the proportion δ of the total emitted secondary electron current to the primary electron current*. This definition will be followed also in this book. If, however, measurements are carried out with slow primary electrons or if small effects are traced, one always has to take into account that the supposition mentioned above is not strictly correct, that is to say, that the total secondary current always contains both elastically and inelastically scattered electrons. This fact has been neglected in some cases.

Only in a few cases will it be necessary to consider the following correction:

In order to get the most correct value for the true secondary emission coefficient, it is reasonable to make corrections when using either very slow primary electrons (~ 10 eV) or high energy primary electrons (several kV). In the former case the coefficient of elastic scattering is important, and from a physical point of view it is logical to count the number of true secondary electrons not per primary hitting electron but per primary electron penetrating into the substance.

Calling the total secondary electron i_s, the current of elastically scattered electrons i_{refl} and the primary current i_p, δ_{true} can be written as:

$$\delta_{\text{true}} = \frac{i_s - i_{\text{refl}}}{i_p - i_{\text{refl}}} \equiv \frac{\delta - \delta_{\text{refl}}}{1 - \delta_{\text{refl}}}. \tag{1.1}$$

With high energy electrons (several kV) the number of rediffused primary electrons is important. In order to get the correct number of true secondary electrons released by the action of each primary electron, it is not sufficient only to subtract the current of the primary electrons being scattered back; it is necessary also to subtract the number of

true secondary electrons released by the rediffusing or inelastically scattered primary electrons. This fact was pointed out by PALLUEL [304, 305] who worked the correction in the following way.

If r is the coefficient of rediffusion, a coefficient η can be defined:

$$\eta = \delta - r$$

in which η means the true secondary emission coefficient due to ionization by the primary impinging and rediffusing electrons. In order to separate both kinds of electrons a rough estimation has been carried out by the author by assuming that the mean voltage V_r of the rediffused electrons is a constant fraction of the mean voltage V_p of the primary electrons, that is to say

$$\chi = \frac{V_r}{V_p}.$$

Now if $(\delta_{\text{true}})_{V_p}$ is the true secondary emission coefficient for electrons released by the action of the primary electrons one can write

$$(\delta_{\text{true}})_{V_p} = \eta_{V_p} - r(\delta_{\text{true}})_{\chi V_p}.$$

Although (δ_{true}) is not known, the above assumption leads to an analogous equation for $(\delta_{\text{true}})_{\chi V_p}$:

$$(\delta_{\text{true}})_{\chi V_p} = \eta_{\chi V_p} - r(\delta_{\text{true}})_{\chi^2 V}$$

but this is only possible, of course, if r is constant in the region of V_p under consideration.

By successive approximation a series for $(\delta_{\text{true}})V_p$ can be derived:

$$(\delta_{\text{true}})_{V_p} = \eta_{V_p} - r\eta_{\chi V_p} + r^2\eta_{\chi^2 V_p} - r^3\eta_{\chi^3 V_p} + \ldots \tag{1.2}$$

An approximation like this cannot pretend to be more than a very rough estimate of the true secondary emission at high primary energies. It illustrates again how complicated the phenomenon of secondary electron emission is from a mere theoretical point of view, and also from the point of view of interpretation of experimental results.

2

METHODS AND MEASUREMENTS

2.1. METHODS FOR MEASURING THE YIELD OF SECONDARY ELECTRON EMISSION

2.1.1. Tube with Electron Beam [167].

The yield of secondary electron emission is expressed by the symbol δ giving the number of secondary electrons emitted by the action of one primary electron. This factor δ can be determined with the apparatus shown in fig. 2.1. The tungsten filament F is the source of the primary electrons; it is surrounded by a cylinder C which concentrates the electrons on the aperture of the gun G. The electrons leaving the opening in C are formed into a beam by means of the gun G, and hit the target T; T is covered with the substance from which the secondary electron emission yield has to be determined. The secondary electrons emitted by T are collected on the spherical collector S. To permit the coating of T with different substances it is attached to a rod R, at whose other end an iron piece IP is fixed, so that with a magnet the target plate can be drawn into the neck N of the tube. The substances to be investigated are brought on to filaments F_1 and F_2 and can be evaporated on to the target plate. By this construction it is possible to accomplish the preparation and the measurement in the same tube without exposing the prepared target to the action of the air.

The secondary electrons from T are all drawn to S, when the potential of S is raised above that of T; in this way the total secondary electron current is measured. If the potential of S is lower than that of T, it is not possible for all electrons to reach S. Only those can reach S, which have been emitted with a kinetic energy sufficient to overcome the retarding potential difference between S and T. If the potential of S is some volts higher than that of F, only the electrons with an energy approximately equal to the energy of the primary electrons can reach S; in this way it is possible to separate the primary electrons, which are elastically reflected.

One may ask whether the possibility exists in this kind of device that the primary electrons, after leaving the upper aperture of the gun G, can reach the collector S directly, bypassing the target T. When the surface of T is perpendicular to the axis of G there will

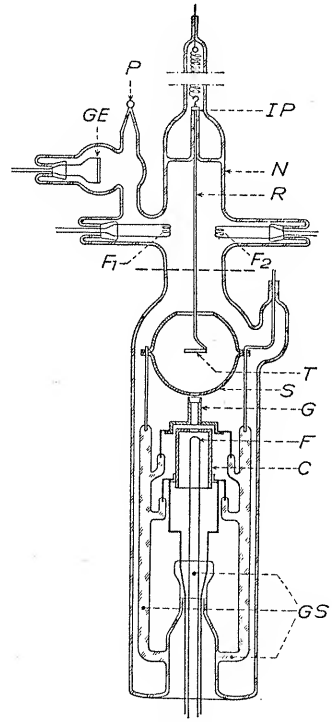

Fig. 2.1. Apparatus for measurement of secondary emission yield and energy distribution [167]. F = tungsten filament, source of primary electrons; C = cylinder; G = electron gun; T = secondary emitting target plate; S = sphere, collector for secondary electrons emitted by T; R = rod; IP = iron piece; N = neck; F_1F_2 = heaters; GE = plate containing getter material; P = scaling off point; GS = glass support.

be very little chance, as the field strength perpendicular to the direction of the beam is then zero. This field strength has a finite value, however, if the target is not perpendicular to the beam, owing to the variation of the angle of incidence of the primary electrons; one then has to take into account the possibility of primary electrons being drawn to S, if its potential is higher than the potential of T.

There are many devices described in the literature which closely resemble the tube of fig. 2.1, and this should be considered just as a typical example. Attention is drawn to a tube constructed by FARNSWORTH [41], especially designed for experiments with slow moving primary electrons. Another method is to use an ordinary cathode ray tube, the screen of which has been replaced by the target to be investigated, with a suitable collector for the secondary electrons.

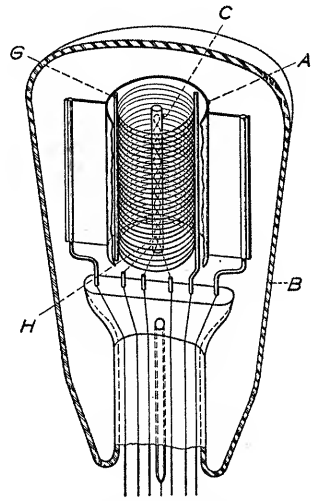

Fig. 2.2. Triode for measurement of secondary emission yield of the anode. C = cathode; H = heater filament; G = grid; A = anode; B = glass bulb

2.1.2. Triode.

It is also possible to measure the coefficient δ with an ordinary triode. One cannot attain the same degree of accuracy, as by using the apparatus described in the previous paragraph, nor can one separate the elastically scattered electrons. The construction of a triode is however much simpler.

The primary electrons in a triode, as shown in fig. 2.2 are delivered by a cathode C, which can be heated by a filament F. The substance under investigation is applied to the inner surface of the anode A. The potential difference V_g between the grid G and the cathode C is made greater than the potential difference V_a between the anode A and C, as the secondary electrons from the anode have to be drawn to the grid.

Let us call the primary current emitted by the cathode i_c. A fraction si_c is then intercepted by the grid before reaching the anode. The fraction of the cathode current to the anode $(1 - s)i_c$ causes a current of secondary electrons. If δ is the coefficient of secondary emission of the anode surface we can write

$$i_s = \delta(1 - s)i_c. \tag{2.1}$$

If the current to the grid i_g and the current to the anode i_a are measured, we can determine δ as follows:
The current to the anode is

$$i_a = (1 - s)i_c - i_s. \tag{2.2}$$

The current to the grid is

$$i_g = si_c + i_s. \tag{2.3}$$

Elimination of i_c and i_s from the equations 2.1, 2.2, 2.3 gives

$$\delta = 1 - \frac{i_a}{(1 - s)\,(i_g + i_a)}. \tag{2.4}$$

It is of course a drawback that a fraction si_c of the cathode current is intercepted by the grid, because it is not an easy procedure to determine accurately the factor s. The device described in the previous paragraph, if properly constructed, does not suffer from this disadvantage. A second difficulty is that smaller values of δ will be found than with the apparatus provided with an electron beam. The reason is that secondary electrons liberated from the anode are drawn through the meshes of the grid, return between grid and cathode and hit the anode after bypassing the grid wires for a second time. Thirdly, the angle of incidence of the primary electrons is not well defined because some of them are deflected by the wires of the grid.

In spite of these disadvantages, the triode is a useful measuring instrument, especially for technical purposes. We shall therefore consider some methods of determining the "shadow" factor s, i.e. the distribution of the cathode current between grid and anode. The ideal way would be to construct a triode of a similar geometry, but with electrodes without any secondary electron emission. No known substance has zero secondary emission, however, and one has to look for another method.

TANK [33] and VAN DER POL [36] have tried to solve this problem by making use of the fact that, if the initial velocities of the electrons are neglected, the ratio of the primary currents to grid and anode is a function only of the quotient V_g/V_a. In other words, the distribution of the primary electrons between grid and anode remains constant as long as V_g/V_a is constant. If i_g and i_a are measured for low V_g and V_a, with a small coefficient of secondary emission, it is possible to find by extrapolation the distribution of the primary currents at increasing V_g and V_a. This method, however, only partly eliminates the secondary electron emission because the secondary current consists mainly of elastically reflected primary electrons; and if $V_g = 5$ V, for example, δ is of the order of 0·20. For more accurate measurements a correction has to be applied for the initial energies of the primary electrons and the difference in contact potential.

The method proposed by DE LUSSANET DE LA SABLONIÈRE [96] is better in this respect, since it allows the current distribution between grid and anode to be determined at greater values of V_g and V_a. The assumption is made that the velocity of the secondary electrons is negligible compared with the velocity of the primary electrons, so that with a given configuration of the electric field both primary and secondary electrons travel along the same orbits. DE LUSSANET'S method is illustrated in fig. 2.3*.

In this figure the anode current i_a is drawn as a function of V_g/V_a. (The shape of the curves will be explained in more detail in the next section, 2.2.) For each curve V_g is kept constant. The dotted curve gives the still unknown course of the primary anode current i_{ap}. In the region where $V_a > V_g$ the secondary electrons are drawn from the grid to the anode. The anode current consists therefore of the secondary electrons emitted by the grid (i_{gs}) and the electrons emitted by the cathode (i_{ap}).

According to DE LUSSANET it is possible to express the current of secondary electrons emitted by the grid (corresponding with the points A_1, B_1, A_2 and B_2) as a product of two factors: (a) the secondary emission coefficient δ, constant along each curve because V_g is constant, and (b) a saturation coefficient γ, constant for each value of V_g/V_a.

* The author has used this method to determine the current distribution in a tetrode. For simplicity's sake it is described here for a triode.

For the secondary electron current emitted by the grid, i_{gs}, we can write for each of the points A_1, B_1, A_2 and B_2 the following equations:

$$i_{gs}(A_1) = \delta_1\gamma_A = i_a(A_1) - i_{ap}(A)$$
$$i_{gs}(A_2) = \delta_2\gamma_A = i_a(A_2) - i_{ap}(A)$$
$$i_{gs}(B_1) = \delta_1\gamma_B = i_a(B_1) - i_{ap}(B)$$
$$i_{gs}(B_2) = \delta_2\gamma_B = i_a(B_2) - i_{ap}(B).$$

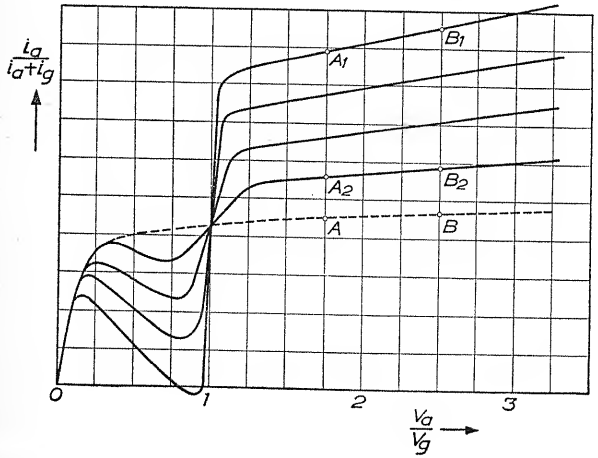

Fig. 2.3. $\frac{i_a}{i_a + i_g}$ as a function of $\frac{V_a}{V_g}$. Method of determining the distribution of the primary electron current between grid and anode in a triode; according to DE LUSSANET [96]

From these four equations the following relation can be derived:

$$\frac{i_a(A_1) - i_{ap}(A)}{i_a(A_2) - i_{ap}(A)} = \frac{i_a(B_1) - i_{ap}(B)}{i_a(B_2) - i_{ap}(B)}. \qquad (2.5)$$

If an arbitrary value for $i_{ap}(A)$ is assumed, it is possible to find any other B-point on the curve through A. The following method is proposed by DE LUSSANET to find the curve for the primary currents. In the regions where $V_a < V_g$ and also in the regions where $V_a > V_g$ a bundle of possible curves is drawn using relation (2.5). The correct curve can be found by choosing out of each bundle a line in such a way that both lines coincide if elongated. An example of this method is shown by fig. 2.4.

Another method, starting with the assumption that the velocities of the secondary electrons are negligibly small, has been described by LANGE. LANGE recognized that because of the difference in velocity of primary and secondary electrons it was practical to separate them by the application of a magnetic field so that the

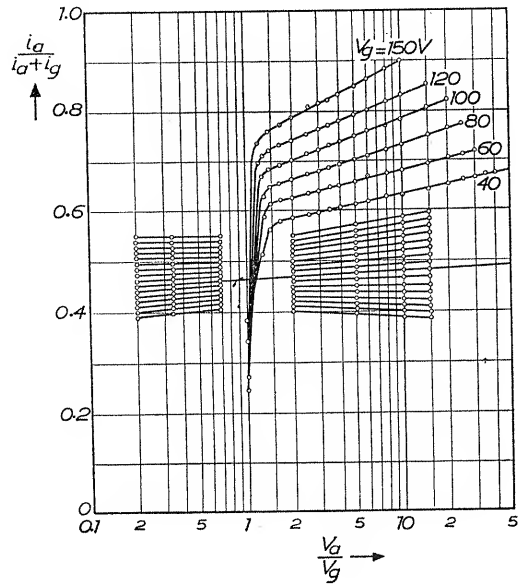

Fig. 2.4. Determination of the primary anode current i_{ap}; according to DE LUSSANET [96]

secondary electrons are bent to the electrodes from which they originate, whereas the primary electrons are deflected only slightly. Such a separation can be properly carried out if the potential difference between grid and anode is not too high, i.e. if the secondary electrons are not much accelerated.

It is also possible to determine the current distribution in a triode if the energy dissipation is measured in grid and anode. This method has been used by SCHWARZENBACH [104] and MYERS [161]. In order to describe the method in its fundamental and most simple form, we shall again neglect the initial energies of the secondary electrons. Let us consider the case where $V_a > V_g$, so that all secondary electrons from the grid are drawn to the anode.

If W_a and W_g are the energies dissipated in the anode and the grid the following relation exists:

$$W_a = i_{ap}V_a + i_{gs}(V_a - V_g)$$

or
$$W_a = i_a V_a - i_{gs}V_g \tag{2.6}$$

and
$$W_g = i_{gp}V_g. \tag{2.7}$$

When $V_a < V_g$ the relations become:

$$W_g = i_{gp}V_g + i_{as}(V_g - V_a)$$

or
$$W_g = i_g V_g - i_{as}V_a \tag{2.8}$$

and
$$W_g = i_{gp}V_g. \tag{2.9}$$

Considering the case $V_a > V_g$, the measurement of W_a alone would be sufficient to determine i_{gs} by equation (2.6); if i_{gs} is known the primary currents i_{ap} and i_{gp} are also known. In practice however the anode receives also radiated energy from the grid. To correct for this MYERS measured W_g. There is also an "evaporation" heat of the secondary electrons, so that an extra negative term has to be added on the right of equation (2.7).

By means of experiments of this kind we can prove experimentally that the distribution of the primary current is a function of V_g/V_a.

A method founded on another principle has been elaborated by HYATT [64, 65]. He used a triode, in which the "cathode" did not emit electrons, but positive ions (caesium ions). The measurement was in two parts. In the first part the grid was at a negative potential with respect to the cathode, and the anode at a positive potential. The secondary electrons liberated by the ions from the grid were drawn to the anode. So it was possible to determine the number of secondary electrons per primary impinging positive ion. In the second part both grid and anode were negative with respect to the cathode; in this situation it was possible to determine the distribution of the ion currents between the two electrodes. The distribution of the electron currents was now also known, since the orbits of ions and electrons are similar with the same configuration of the electric field. HYATT showed in his first paper that the distribution was independent of the applied voltages, if $V_a > 0{\cdot}2\ V_g$; in his second paper he reported that the criterion was $V_a > 0{\cdot}75\ V_g$. This difference was presumably due to the difference in geometrical

construction of the tubes used in his experiments. The fraction of the current reaching the grid was in both cases equal to the fraction of the anode surface covered by the grid as seen from the cathode (fig. 2.5).

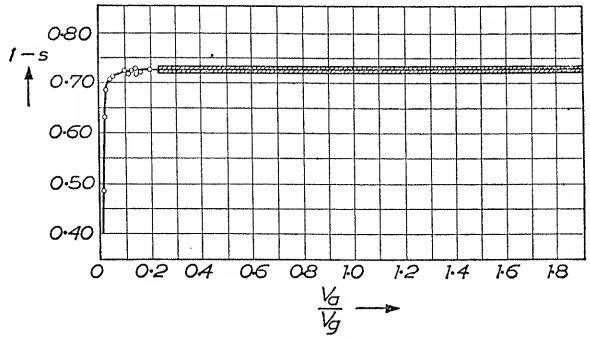

Fig. 2.5. Distribution of the primary electron current between grid and anode in a triode; according to HYATT [64, 65]

Along theoretical lines JONKER and TELLEGEN* derived a formula giving the current distribution in a triode:

$$i_g = \frac{2c}{l}\sqrt{\frac{V_g}{V_s}}\, i_c \left[1 + \frac{V_g - V_s}{2V_s \ln (l/2\pi c)}\right] \qquad (2.10)$$

in which $2c$ = diameter of the grid wire,

l = spacing between the grid wires,

V_s = mean potential of the grid surface,

$i_c = i_g + i_a$.

This formula applies in the case of an indefinitely extended flat cathode.

All methods described above are obviously approximation methods. It is not correct, for example, to neglect the starting energies of the secondary electrons which are always some eV in magnitude. How far it is permissible to do so has never been fully discussed. In most methods it is assumed that the fraction of the electrons hitting the grid is equal to the fraction of the anode surface covered by the grid (for this "shadow factor", see the result obtained by HYATT, fig. 2.5). There may also be objections to the method

* J. L. H. JONKER and B. D. H. TELLEGEN; *Philips Res. Repts.*, **7**,13, 1945.

proposed by HYATT; for he has not taken into account the possibility that secondary electrons released by the ions from the grid wires can be drawn to the ion source.

2.1.3. Measurement of the Secondary Electron Emission using a Triode with a Photoelectric Cathode and a Photosensitive Secondary Emitting Electrode (PENNING and KRUITHOF).

In fig. 2.6 an example of a tube used by PENNING and KRUITHOF is shown. The cathode and anode are prepared on the inner side of the glass envelope and are both of the type [Ag] — Cs_2O — Cs (the significance of these symbols will be explained in detail in

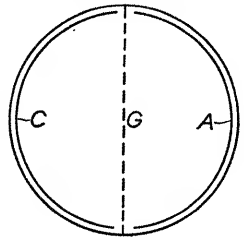

Fig. 2.6. Photo-electric cell with secondary emitting electrode and anode; according to PENNING and KRUITHOF [116]

Chapter 4). Irradiation with light causes an electron emission (photoelectric emission) from the anode A, which serves as a secondary emitter.

The expression for the coefficient δ of the anode becomes in this case

$$\delta = 1 - \frac{i_a + i_{aph}}{(1 - s)\,(i_a + i_g)} \qquad (2.11)$$

in which i_{aph} is the photoelectric current emitted by the anode.

2.1.4. Measurement of the Secondary Electron Emission of Wire-shaped Bodies.

In the previous sections measuring devices have been described in which the substances whose secondary emission was under investigation had the shape of a plate or had been evaporated on to a plate. If for one reason or another the substance has to be heated to a high temperature, the use of a plate may give difficulties. A considerable amount of energy is needed to raise a plate to a high temperature, and other parts in the tube may also be raised in temperature causing a release of gas.

In these cases it is more appropriate to carry out measurements on wires, which can be heated very simply by applying a current. In such a device it is however impossible that all the primary electrons from the cathode hit the wire-shaped target. The surrounding electrode for collecting secondary electrons will also be hit by primary electrons. The distribution of the primary electrons then has to be measured, and this is possible in principle with the methods described in section 2.1.2.

A special method giving more accurate data has been worked out by TRELOAR [135]. His apparatus is shown in fig. 2.7. C is

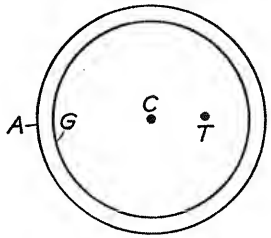

Fig. 2.7. Apparatus for determining secondary electron emission yield of a wire; according to TRELOAR [135]

the primary cathode, T the wire under investigation, G a grid at cathode potential and A the anode. In order to determine the coefficient δ of T, the potential difference V_a between A and C is increased until the potential in the plane of the grid is sufficiently high to attract all secondary electrons from T to A. If V_a is reduced a potential minimum arises between T and A and the secondary electrons from T cease to reach A. In this situation the distribution of the primary electrons is measured; it appears that the current of primary electrons is proportional to

$$i_p \sqrt{\frac{V_p}{V_a}}$$

where V_p is the potential difference between T and C; a result which can be predicted from theoretical considerations. Values of δ found by TRELOAR correspond well with data obtained with plates by other authors. With increasing V_p however somewhat higher values of δ are found, because the electrons do not all approach the wire perpendicularly (see Chapter 7).

2.2. DETERMINATION OF THE SECONDARY ELECTRON EMISSION FROM BAD CONDUCTORS (INSULATORS)

The determination of the secondary emission coefficient of dielectrics suffers complications as electron transport is not in general possible; the methods described in the previous sections can only be used if the conductivity of the layer is large. (1942, 493)

A method that has been used by GEYER and others employs a thin layer evaporated on to a metal plate or, if a metallic compound is to be investigated, the metal is evaporated first and then a layer of the compound is formed on it. The conductivity of a target can also be increased by heating or by irradiation with infra-red light. In Chapter 6 it will be shown that the process of energy transfer of the primary electrons to the electrons of the lattice is independent of the temperature.

If the dielectric in question is, however, too thick and its conductivity is too small, other methods have to be used. To understand these better, we must first consider the potential which a surface of an insulator can assume under electron bombardment. For such a surface there may be two different situations:

(a) no electrons are able to reach the surface;
(b) the number of secondary electrons emitted by the surface is equal to the number of primary electrons.

The following experiment indicates at which energy of the primary electrons the number of secondary electrons reaching the collecting electrode is equal to the number of primary electrons. In a triode the anode current i_a is determined as a function of the anode voltage V_a, the grid voltage being constant. In fig. 2.8 three characteristics are drawn for three different values of V_g. It is assumed that the emission of the cathode is saturated and that the energy eV_p of the primary electrons is smaller than the energy at which δ has its maximum value. As V_a increases from zero there is an initial increase of i_a due to the change of the electrostatic field in the grid plane (cf. eqn. 2.10). As V_a increases still more, the anode current i_a passes a maximum and decreases again. This behaviour of i_a is caused by the increasing number of emitted secondary electrons being captured by the grid. At still higher values of V_a, i_a passes through a minimum and then rises rapidly. This rise begins when the field between grid and anode is reversed in direction. Electrons emitted by the anode are not able to reach

the grid whereas secondary electrons from the grid are drawn to the anode. When V_a is very large, i_a becomes constant. The complete curve is often referred to as the "dynatron characteristic".

If we consider now the three curves I, II and III, corresponding to three different values of V_g, curve I intersects the abscissa only at the origin, curve II touches the abscissa again, but curve III has three points of intersection, at the origin, and at P and R. Let us consider curve III first. If the anode is covered with an insulating layer its surface can only be at cathode potential or at the potential

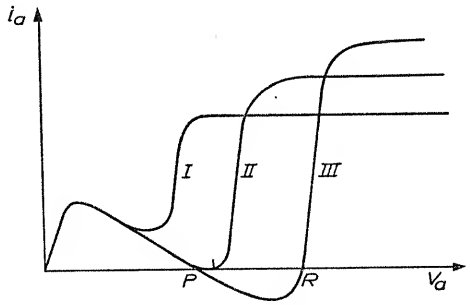

Fig. 2.8. Dynatron characteristics in a triode

corresponding to R. The situation at P is unstable. This has been shown by H. BARKHAUSEN (*Elektronenröhren*, p. 105, Leipzig 1931): a consequence of the rise in potential in situation P is an increasing positive charge, which further increases the potential, and so on. In the same way it can easily be proved that the situation at R is stable.

There are therefore two possible situations. If the anode starts at the voltage R, which can be observed with an electrostatic voltmeter, its potential drops with decreasing V_g. But if V_g drops below the grid voltage of characteristic II no intersection is left, except that at the origin. The anode then jumps to cathode potential.

It is obvious that measurements of this kind require a reliable method to determine the surface potential. To measure screen potential in cathode ray tubes, NELSON [186a] connected the outside wall of the tube with an electrostatic voltmeter. HAGEN and BEY (151) stretched a thin wire as in an electrometer opposite the bombarded surface. Other authors measured the deflection of an electron beam passing parallel to the surface.

As will be discussed later, the secondary emission yield goes through a maximum as a function of the primary voltage V_p. This means that there exists a second (higher) value of V_p where $\delta = 1$. This second value can also be measured with an electrostatic voltmeter, if the potential of the collector of secondary electrons is raised beyond this value of V_p, the surface potential of the target remains constant. The two values of V_p where $\delta = 1$ are often indicated in literature respectively as V_{p1} and V_{pII}.

The value of V_{p11} is important from a technical point of view as it gives a natural limitation to the energy with which the primary electrons strike the screen in a cathode ray tube (Chapter 10).

Considering curve III in fig. 2.8, the difference between the potential at point R and the potential of the collecting electrode will be in most cases of the order of some volts. The shape of the curves in fig. 2.8, besides depending upon the coefficient δ, also varies with the geometry of the electrodes. If, for example, the collecting electrode surrounds the target as shown in fig. 2.7, the potential of the target surface will be somewhat higher than the potential of the collector; on the other hand in a triode, with a grid that is a poor collector of secondary electrons, the reverse will be found. We may thus conclude:

(*a*) *If the secondary emission yield of the target is equal to or greater than* **1**, *it is possible to stabilize the potential of the target surface at or near the potential of the collector.*

(*b*) *The potential of the target surface can always be stabilized at the potential of the cathode delivering the primary electrons.*

These properties are very important; they enable the secondary emission coefficient of insulating substances to be measured, as is shown in fig. 2.9. The primary electrons are delivered by a cathode and hit the insulating target. The secondary electrons are collected by the collector. Let us suppose $\delta > 1$. To start the measurement the switch is put in a position, so that the target surface is stabilized at collector (e.g. earth) potential. After switching over to the other position (+100 V) the secondary electrons are drawn to the collector and an instantaneous current $i_p - i_s$ flows through the resistance R causing a potential difference, which can be measured by the oscillograph; however the target potential, and thus V_p, rises during the measurement. The original situation is restored if the switch is put in the first position, after which the measurement can be repeated. In the case of $\delta < 1$, the surface has to be stabilized at cathode potential; the switch is then inserted in the target circuit.

The method described here is essentially a pulse technique. Its basic principle is that after each pulse the surface potential of the target returns to its original value. A method described by SALOW [229] achieves this with the aid of a second electron beam, which

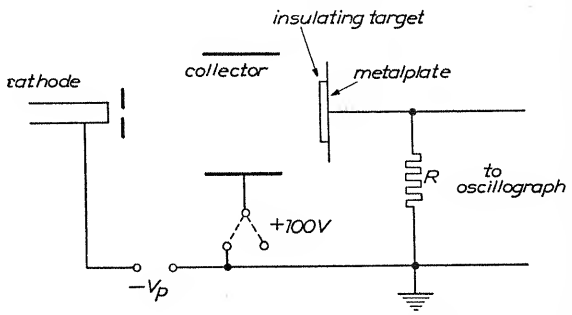

Fig. 2.9. Determination of the secondary emission yield of an insulating material

brings the surface potential back to its original value during the interval between two pulses. Pulse methods have also been described by SCHERER [231], HEIMANN and GEYER [218], JOHNSON [302] and POMERANTZ [300].

2.3. DETERMINATION OF THE ENERGY DISTRIBUTION OF SECONDARY ELECTRONS

2.3.1. Use of a Retarding Electric Field.

This method was considered at the beginning of this chapter. If the potential of the spherical collector in the tube in fig. 2.1 is V_s volts lower than the potential of the target T, only those secondary electrons can reach the target whose energy E is equal to or greater than eV_s. If the energy distribution is given by the function $F(E)$, the current to S is equal to

$$i_s = \int_{eV_s}^{\infty} F(E)\mathrm{d}E.$$

Therefore

$$F(E) = -\frac{\mathrm{d}i_s}{\mathrm{d}(eV_s)}. \tag{2.12}$$

With the apparatus in fig. 2.1 the energy distribution for all electrons emitted into the "hemisphere" is measured. A similar determination is of course possible for electrons emitted in a particular direction.

An inexactitude in measurements of this kind is caused by the fact that the electrons emitted by T, when they hit the collector S, release from S more secondary electrons, which are drawn towards T. In any retarding potential apparatus it is therefore advisable to cover the inner surface of S with a substance poor in secondary emission, like a soot layer.

From equation (2.12) it can be seen that the actual energy distribution curve can be obtained only by differentiating the experimental curve with respect to energy. The method is therefore not very accurate compared, for instance, with the method to be described in the next paragraph. It is however possible to get the distribution curve directly with a retarding field method if, according to VAN DER POL and WEIJERS,* an alternating voltage of small amplitude is added to the retarding voltage and the amplitude of the first harmonic, present in the secondary electron current, is measured. The amplitude of the first harmonic is proportional to the differential quotient $\mathrm{d}i_s/\mathrm{d}(eV_s)$.

2.3.2. Measurement of the Energy Distribution with a Magnetic Field.

A well known way to determine the energy spectrum is to use a magnetic field (fig. 2.10). The secondary emitting target T is bombarded by an electron beam; the secondary electrons are deflected by the force of a transverse homogeneous magnetic field and are forced to follow a circular path. Between the radius r of the path, the magnetic field H, and the velocity v of the particle, the following well known relation exists:

$$H \cdot \frac{e}{m} \cdot r = v. \tag{2.13}$$

The current entering the cage, I_{cage} is measured as a function of the magnetic field H. This is given by

$$I_{\text{cage}} \sim \varphi(v)\Delta v, \tag{2.14}$$

if $\varphi(v)$ is the velocity distribution of the secondary electrons. The

* *Physica, 's Grav.*, **1**, 481, 1934.

velocity interval Δv is determined by the aperture of the cage Δr

$$\Delta v = H \cdot \frac{e}{m} \Delta r. \tag{2.15}$$

Eliminating Δv from equations (2.14) and (2.15) and using (2.13) one finds for $\varphi(v)$:

$$\varphi(v) = I_{\text{cage}} \frac{m}{eHr \dfrac{\Delta r}{r}} = \frac{I_{\text{cage}}}{v} \frac{1}{f} \tag{2.16}$$

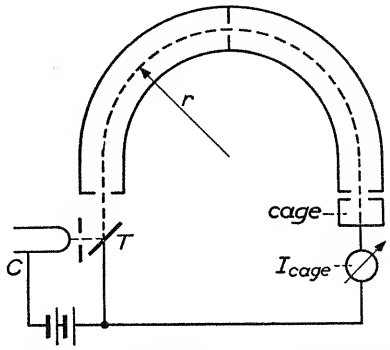

Fig. 2.10. Device to determine the energy distribution of secondary electrons

where $f = \dfrac{\Delta r}{r}$ is a constant of the apparatus. The current to the cage divided by the velocity of the electrons is proportional to the velocity distribution. From this the energy distribution can be derived, if the abscissa is multiplied by mv and the ordinate divided by mv.*

The apparatus, as shown in fig. 2.10, is of a complicated character and is rather extensive in its dimensions. An elegant method with a longitudinal magnetic field has been worked out by KOLLATH [222], fig. 2.11. He uses the following well known principle: If a point source emits electrons with the same energy all at the same angle to the lines of force of a homogeneous magnetic field, the electrons will meet again at a point. The distance from this image point to the point source is proportional to the velocity of the electrons and

* R. KOLLATH; *Ann. Physik*, **27**, 721, 1936.

inversely proportional to the magnetic field. The device acts therefore as a velocity selector in the same way as the one mentioned before.

For the special purpose of measuring the velocity (or energy) distribution of secondary electrons a gun delivering the primary electrons is placed along the axis of the apparatus. The secondary electrons travelling in the space between two cones (determined by the slits) are focussed into the hole in a Faraday cup collector. The current to the collector gives the distribution of the secondary electrons in the same way as in the apparatus of fig. 2.10.

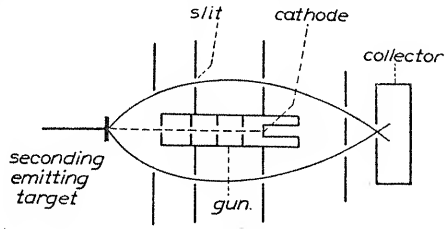

Fig. 2.11. Determination of energy distribution of secondary electrons; according to KOLLATH [222]

The relative low energy of the secondary electrons makes it necessary to eliminate stray fields and to correct for contact potential differences.

It is obvious that magnetic deflection methods give only the distribution curve of electrons emitted in one specified direction, whereas the retarding electric field measures all emitted electrons.

2.4. EXPERIMENTAL TECHNIQUE

As will be pointed out repeatedly in the following chapters, secondary electrons are emitted from the outer atomic layers of a substance. It is therefore necessary to take care that the substance to be investigated has the cleanest possible surface. The work function is also of some influence, although not to the same degree as in thermionic and photoelectric emission. The contamination consists mainly of absorbed atoms and molecules of foreign gases. Substances with a considerable chemical activity, such as alkali metals, easily form superficial compounds.

For the same reason it is necessary to have as good a vacuum as possible and never to use polished glass parts with grease in between.

In general, substances with a high vapour pressure should be avoided in the construction of the tube.

From the cathode, which is the source of the primary electrons, contaminants may evaporate on to the target. This is a well known difficulty especially with the "oxide-cathode" usually composed of a mixture of barium oxide and strontium oxide. Barium atoms and barium oxide molecules evaporate continuously and hit the target. A tungsten wire may be considered as the source of primary electrons least liable to give contamination.

The pumping practice mostly used is the following: The tube is first baked at a temperature as high as possible (for degassing the glass envelope) and the metal parts are afterwards heated by high frequency induction during constant pumping. By firing a suitable getter (magnesium or better barium) any gases still remaining can be removed. After sealing off absorption charcoal cooled in liquid nitrogen is often used to improve vacuum conditions. It is not possible to give general rules. It is necessary to have a vacuum of such a quality as to get reproducible results and to get secondary emission coefficients remaining constant for a considerable time. It is difficult to give any figures for the pressures required, since some gases (like oil vapour) can be extremely reactive with the substances under investigation, and others (like the rare gases) do not show any reaction at all.

3

SECONDARY ELECTRON EMISSION FROM METALS; REVIEW OF RESULTS

3.1. INTRODUCTION

This chapter is devoted to an experimental survey of the secondary electron emission coefficient from metals. The numerical results here quoted have been obtained only by careful experiments carried out by different authors. We shall take the opportunity to associate

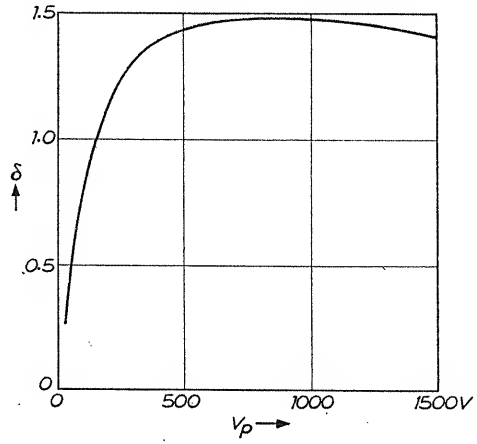

Fig. 3.1. Secondary electron emission yield of silver; according to WARNECKE [137]

δ with other physical properties of the metal in question, but shall leave the detailed explanation to be treated in Chapters 6 and 7. We shall discuss some measurements carried out with high voltage primary electrons, in which case the scattered or rediffused primary electrons form the major part (see Chapter 1), and shall briefly survey the secondary emission on the "exit side".

3.2. SECONDARY ELECTRON EMISSION COEFFICIENT δ FOR V_p FROM 0 TO 1500 VOLTS

In this range of V_p δ passes a maximum. A detailed discussion will be given in Chapter 6, but the maximum can be explained briefly by the fact that an increasing primary energy increases the number of secondary electrons generated, but the depth at which secondary electrons are released also increases and there is thus an increasing loss by absorption. Figs. 3.1 to 3.29 give a complete survey of the secondary emission yield for V_p between 0 and 1500 V.

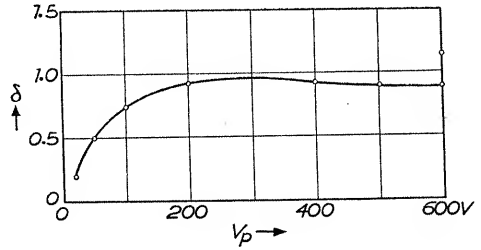

Fig. 3.2. Secondary electron emission yield of aluminium; according to BRUINING and DE BOER [167]

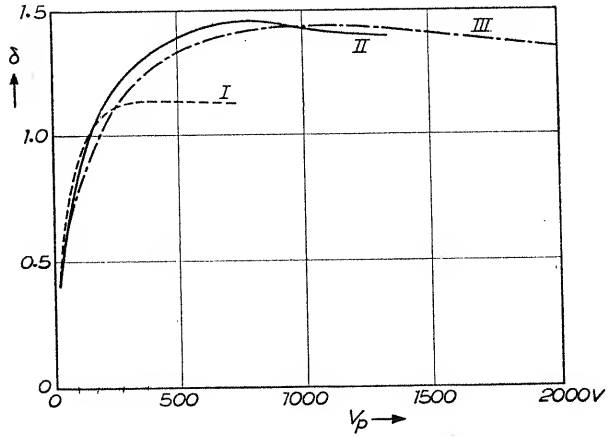

Fig. 3.3. Secondary electron emission yield of gold; according to: I. PETRY [51]; II. WARNECKE [137]; III. COPELAND [109]

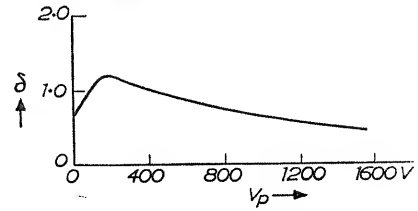

Fig. 3.4. Secondary electron emission yield of boron; according to KOLLER and BURGESS [298]

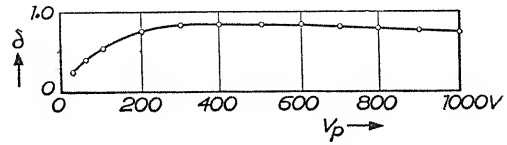

Fig. 3.5. Secondary electron emission yield of barium; according to BRUINING and DE BOER [167]

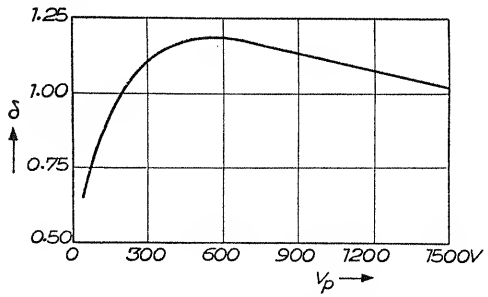

Fig. 3.6. Secondary electron emission yield of bismuth; according to MOROZOV [262]

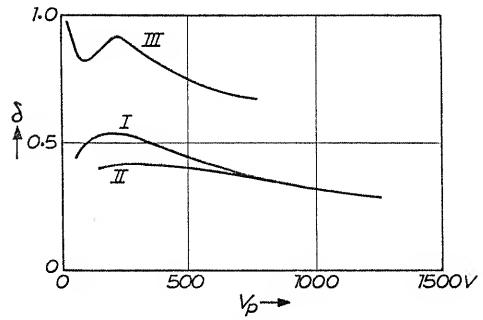

Fig. 3.7. Secondary elcctron emission yield of beryllium; according to: I. BRUINING and DE BOER [167]; II. KOLLATH [180]; III. SCHNEIDER [190]

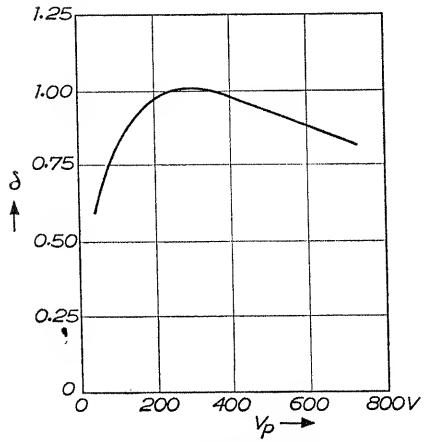

Fig. 3.8. Secondary electron emission yield of carbon; according to BRUINING [171]

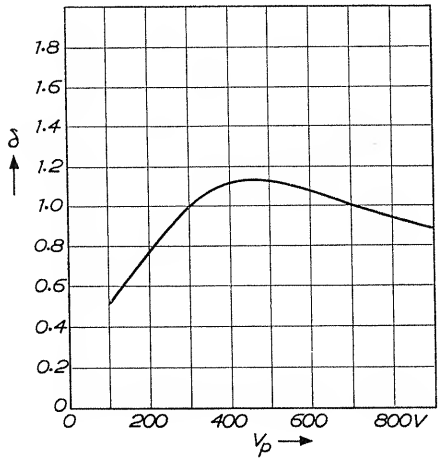

Fig. 3.9. Secondary electron emission yield of cadmium; according to SUHRMANN and KUNDT [284]

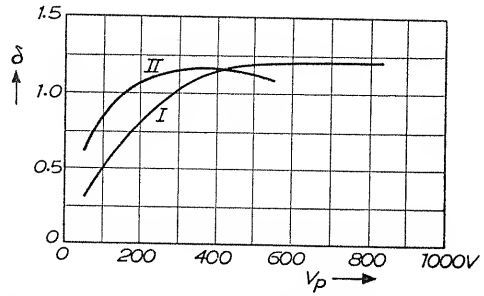

Fig. 3.10. Secondary electron emission yield of cobalt; according to: I. WOOLDRIDGE [213]; II. TRELOAR and LANDON [191]

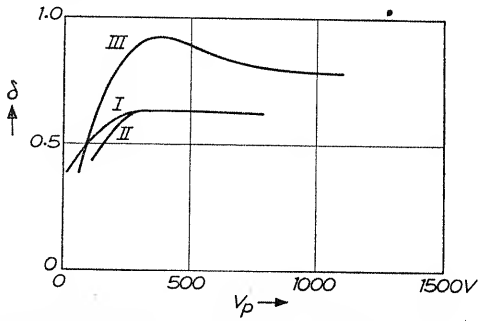

Fig. 3.11. Secondary electron emission yield of caesium; according to: I. BRUINING and DE BOER [167]; II. MAHL [204]; III. KHLEBNIKOW and KORSHUNOVA [176]

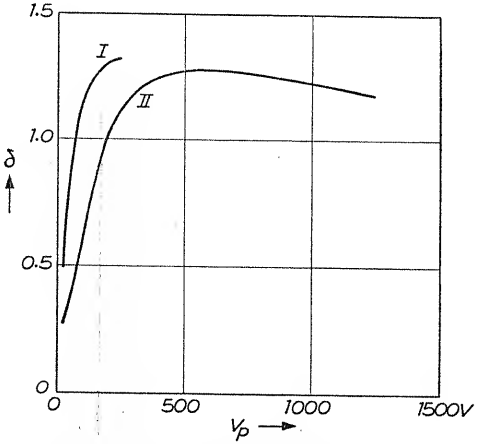

Fig. 3.12. Secondary electron emission yield of copper; according to: I. PETRY [51]; II. WARNECKE [137]

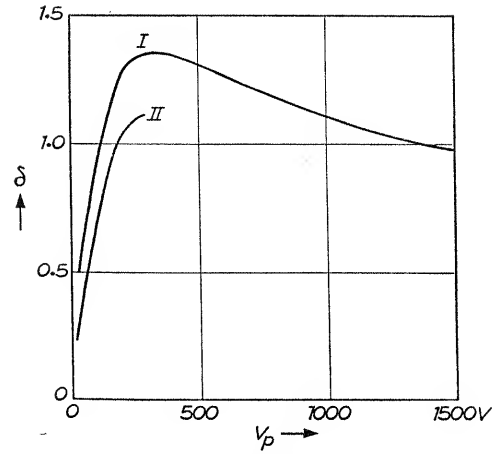

Fig. 3.13. Secondary electron emission yield of iron; according to I. PETRY [44]; II. WARNECKE [137]

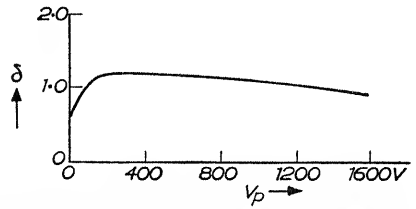

Fig. 3.14. Secondary electron emission yield of germanium; according to KOLLER and BURGESS [298]

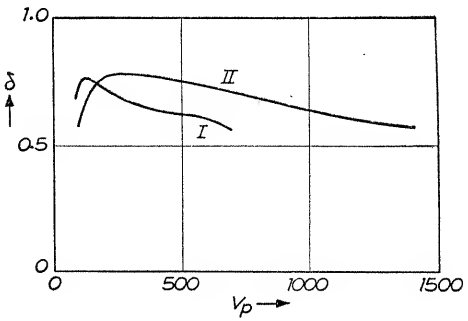

Fig. 3.15. Secondary electron emission yield of potassium; according to I. MAHL [204]; II. AFANASJÈWA and TIMOFEEW [144]

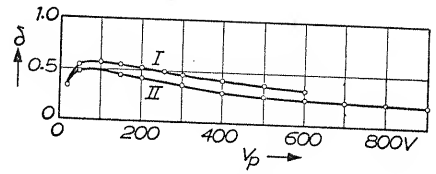

Fig. 3.16. Secondary electron emission yield of lithium; according to BRUINING and DE BOER [167]

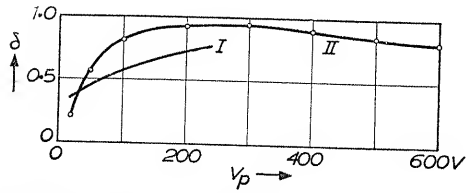

Fig. 3.17. Secondary electron emission yield of magnesium; according to: I. FARNSWORTH [41]; II. BRUINING and DE BOER [167]

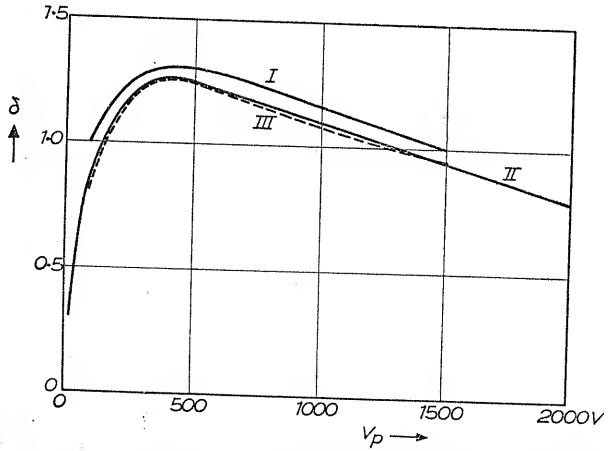

Fig. 3.18. Secondary electron emission yield of molybdenum; according to: I. PETRY [44]; II. COPELAND [93]; III. WARNECKE [137]

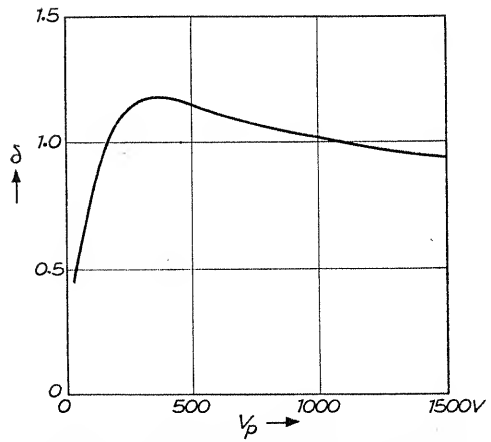

Fig. 3.19. Secondary electron emission yield of niobium; according to WARNECKE [137]

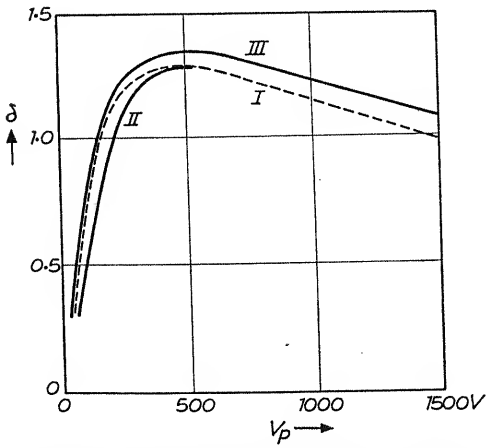

Fig. 3.20. Secondary electron emission yield of nickel; according to: I. PETRY [44]; II. RAO [76]; WARNECKE [137]

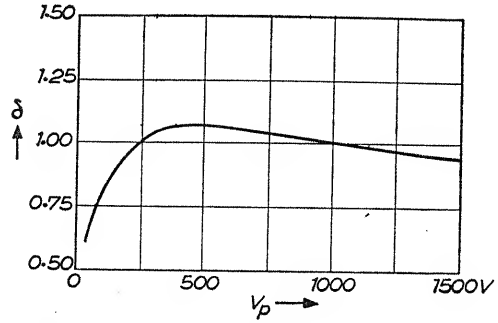

Fig. 3.21. Secondary electron emission yield of lead; according to MOROZOV [262]

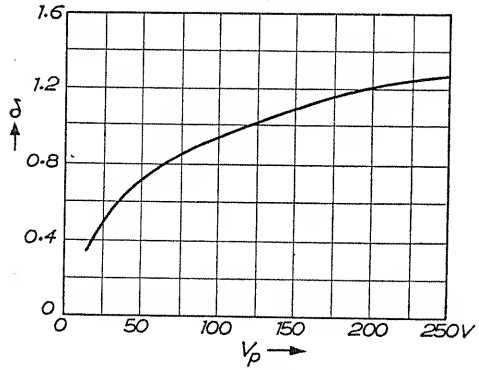

Fig. 3.22. Secondary electron emission yield of palladium; according to FARNSWORTH [41]

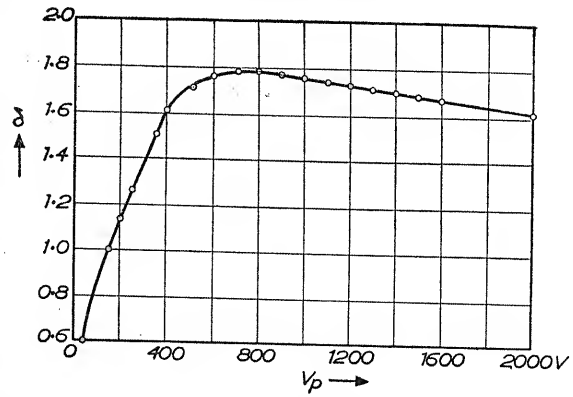

Fig. 3.23. Secondary electron emission yield of platinum; according to COPELAND [83]

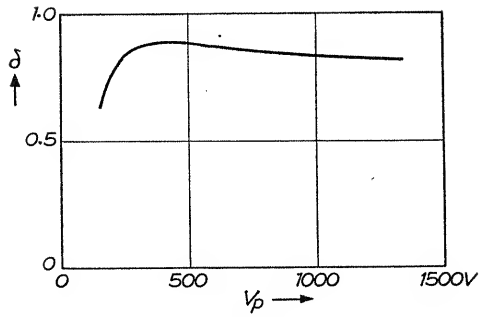

Fig. 3.24. Secondary electron emission yield of rubidium; according to AFANASJÈWA and TIMOFEEW [144]

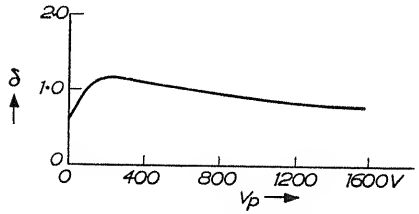

Fig. 3.25. Secondary electron emission yield of silicon; according to KOLLER and BURGESS [298]

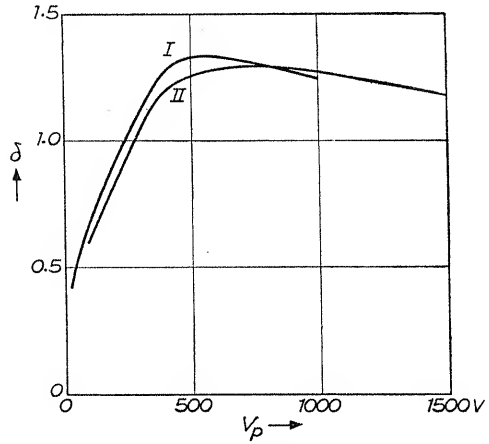

Fig. 3.25a. Secondary electron emission yield of tantalum; according to WARNECKE [137]

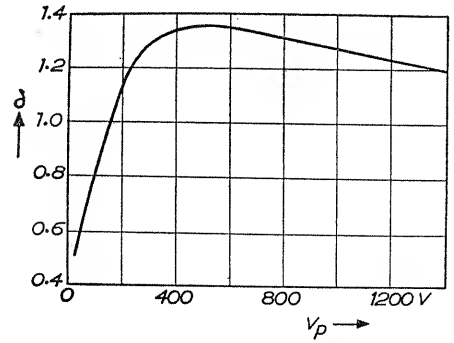

Fig. 3.26. Secondary electron emission yield of tin; according to MOROZOV [262]

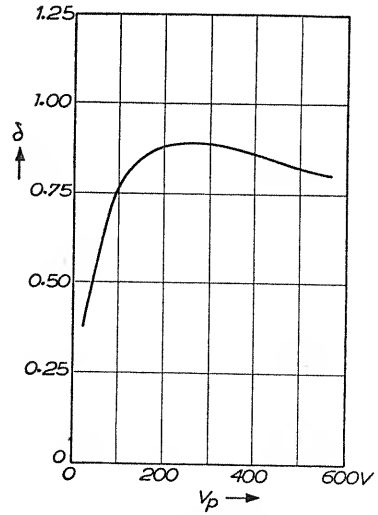

Fig. 3.27. Secondary electron emission yield of titanium; according to BRUINING [170]

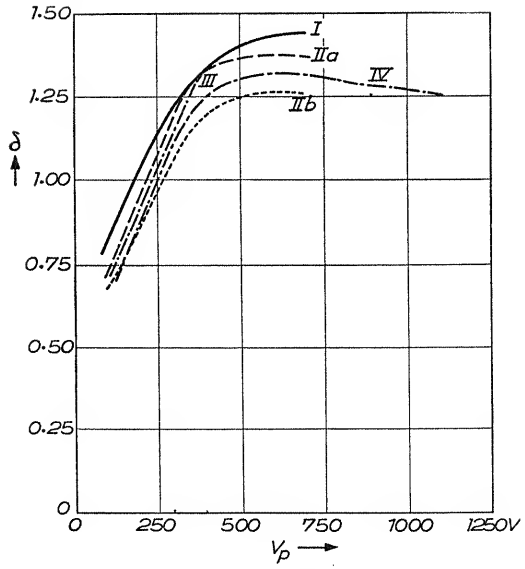

Fig. 3.28. Secondary electron emission yield of tungsten; according to: I. PETRY [51]; IIa and b. KREFFT [68]; III. AHEARN [82]; IV. WARNECKE [137]

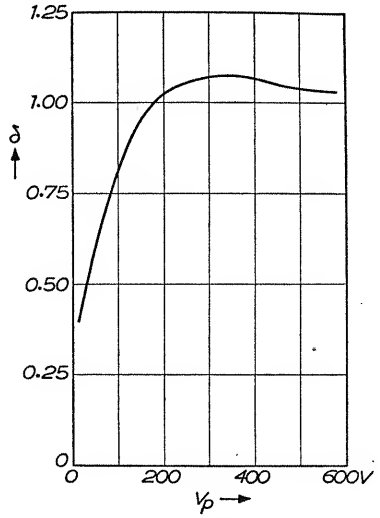

Fig. 3.29. Secondary electron emission yield of zirconium; according to BRUINING [170]

3.3 DATA

Table 3.1 is a list, from the data given in the different graphs, of the maximum secondary emission yield δ_{max} with the corresponding $V_{p(max)}$.

TABLE 3.1. MAXIMUM SECONDARY ELECTRON EMISSION YIELD δ_{max}, AND CORRESPONDING $V_{p(max)}$, FOR DIFFERENT ELEMENTS

Element	δ_{max}	$V_{p(max)}$	*Fig. No.*	*Ref.*
Ag	1·5	800	3.1	137
Al	1·0	300	3.2	167
Au	1·46	750	3.3	137
B	1·2	150	3.4	298
Ba	0·83	400	3.5	167
Bi	1·15	550	3.6	262
Be	0·53	200	3.7	167
C	1·0	300	3.8	171
Cd	1·1	400	3.9	284
Co	1·2	700	3.10	213
Cs	0·72	400	3.11	167
Cu	1·3	600	3.12	137
Fe	1·3	350	3.13	137
Ge	1·2	400	3.14	298
K	0·75	200	3.15	144
Li	0·5	85	3.16	167
Mg	0·95	300	3.17	167
Mo	1·25	375	3.18	137
Nb	1·2	375	3.19	137
Ni	1·3	550	3.20	137
Pb	1·1	500	3.21	262
Pd	>1·3*	>250*	3.22	41
Pt	1·8	800	3.23	83
Rb	0·9	350	3.24	144
Si	1·1	250	3.25	298
Sn	1·35	500	3.26	262
Ti	0·9	280	3.27	170
W	1·4	700	3.28	51
Zr	1·1	350	3.29	170

* $\delta = 1{\cdot}3$ at $V_p = 250$ V is not maximum value of δ.

One might expect to find a high yield of secondary electrons from metals with a low work function, but this is not in accordance with the experimental results. MCKAY [6] has plotted δ_{max} as a function of the work function of different metals and the result is just the contrary, namely a high work function corresponds to a high δ_{max}. MCKAY observes rightly that the work function itself plays a relatively minor role in determining the secondary emission yield, but other physical properties such as the density are probably of more importance. We shall discuss this question in Chapter 6.

3.4. INFLUENCE OF CRYSTAL AND SURFACE STRUCTURE ON δ

3.4.1. Secondary Electron Emission from different Crystal Faces.

So far, the secondary emission yield from metals in polycrystalline form has been discussed.

One may ask whether a single crystal shows a different δ—or to put the question more accurately, whether different crystal faces give a different δ. This could be expected, since the work function of tungsten varies from 4·35 V for the (111) crystal direction to 4·65 for the (110) direction.

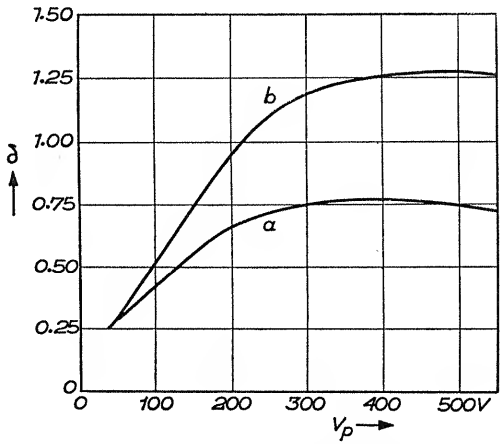

Fig. 3.31. Secondary electron emission yield of (b) polycrystalline nickel and (a) the 100-face of a nickel single crystal; according to RAO [77]

It seems that the use of electrons to form optical images of a polycrystalline surface is the best way to investigate this question. KNOLL and THEILE [203] (fig. 3.30) have got some striking results by forming a television picture of a silicon iron target, using the emitted secondary electrons for generating the signal. The different crystals can be distinguished, and this would not have been possible if all crystal faces had exhibited the same yield.

Only one other quantitative measurement has been published. RAO [77] (fig. 3.31), determined the factor δ for a (100) face of a nickel single crystal. This face apparently emits a much smaller number of secondary electrons than nickel in the polycrystalline state. The experiment seems however to indicate that at lower

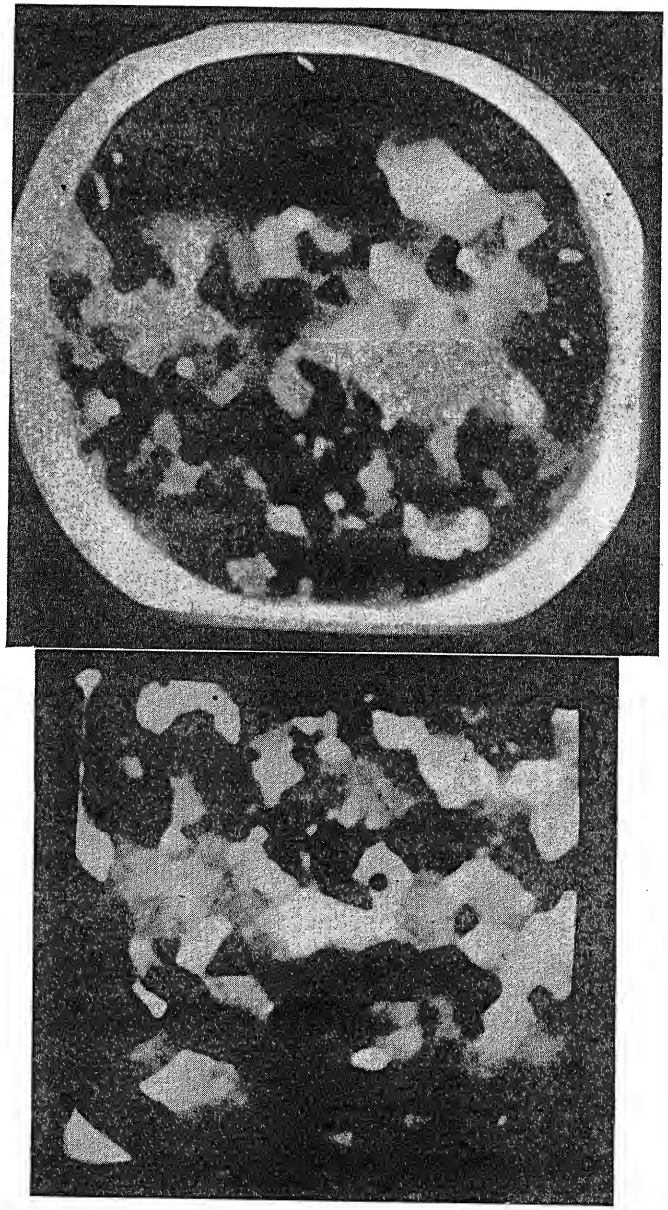

Fig. 3.30. Television image of the structure of a silicon-iron plate; according to KNOLL and THEILE [203]

To face page 40

primary energy the (100) face shows the higher yield, but it is possible that in this case the fraction of elastically scattered primary electrons is greater. More quantitative experiments are needed to settle this problem, which may be important for the understanding of the mechanism of secondary emission from metals.

Another question is whether the yield changes when, as the temperature of the target is varied, the crystal structure undergoes a transformation. The experiments of TRELOAR [191] and WOOLDRIDGE [241–243] show little or no change at the hexagonal to face centred transformation of cobalt at 410°C or at the body centred to face centred transformation of iron at 910°C.

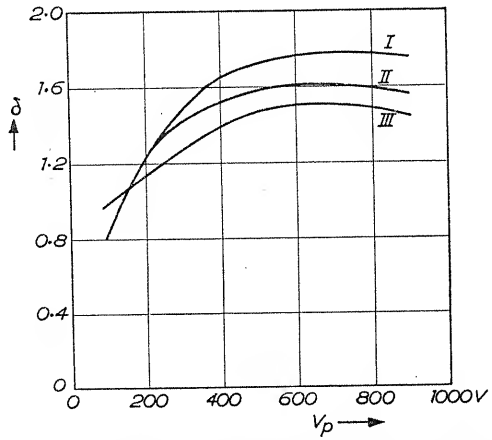

Fig. 3.32. Secondary electron emission yield of gold in disordered state (curve I) and the ordered state (curves II and III); according to SUHRMANN and KUNDT [283]

3.4.2. Secondary Emission Yields of Targets in the Ordered and Disordered State.

SUHRMANN and KUNDT [283] have carried out some interesting experiments comparing the secondary emission coefficients of metals in the ordered and disordered state. They obtained the disordered state by evaporating a metal layer on a cooled plate at 83°K and the ordered state by heating the target to room temperature. As can be seen from fig. 3.32 the yield of a gold layer in the disordered state (curve I) is greater than in the ordered state (II and III). It is remarkable that the difference in yield becomes greater with increasing V_p, which may mean that the difference is due to

the greater absorption of the secondary electrons in the ordered state.

3.4.3. Comparison of the Secondary Emission Yield of Targets consisting of Metal in Bulk and Targets provided with a Metal Layer obtained by Evaporation in Vacuo.

There has been ample discussion of the question whether the yield of targets consisting of a metal in bulk is equivalent with the yield of evaporated layers. The difficulty is that metals with a low work function, i.e. metals with a considerable affinity for oxygen, hydrogen, carbon dioxide etc., cannot be obtained in bulk without an oxide layer, which of course influences the factor δ considerably. It has been stated unjustly by KOLLATH [178] and WARNECKE and Miss LORTIE [195] that oxide layers on these metals can be removed by heating in vacuo. These authors found a considerably higher yield for metals with a low work function than other authors who investigated samples of evaporated layers.

There is, however, considerable evidence that layers evaporated in vacuo are equivalent to metals in bulk. There is not much difference to be observed between the yield from evaporated layers of copper or silver and from the same metals in bulk [167]. If the ever present oxide layer is removed from an aluminium metal plate by sputtering in an argon atmosphere, the yield is about the same as from an evaporated aluminium layer [247].

3.4.4. Influence of the Surface Structure on the Secondary Emission Yield.

In this section we shall discuss the secondary emission yield of layers consisting of crystallites of very small dimensions, so that these layers do not exhibit a reflecting surface but are optically more or less black. Such a layer can be obtained by evaporating a metal through a gas atmosphere, but since the gas must not form any compound with the evaporating material, a rare gas has to be used. The reason why this process gives a black surface is that the evaporating atoms collide with gas atoms and can only reach the wall or target after having made a considerable detour. The metal forms conglomerates in the gas, which deposit as such on the surface. Evaporation across a vacuum, on the contrary, results in the deposition of individual atoms on the surface, and these form layer crystallites and a more reflecting surface.

A layer of soot, obtained from burning hydrocarbons, can be considered as having been formed by the evaporation of carbon through air. Such a layer is composed of very small particles only a few mμ in size.

The secondary emission yield of any optically black, microcrystalline layer is much smaller than the yield of a smooth coherent layer. Fig. 3.33 shows the yield from soot compared with a smooth carbon

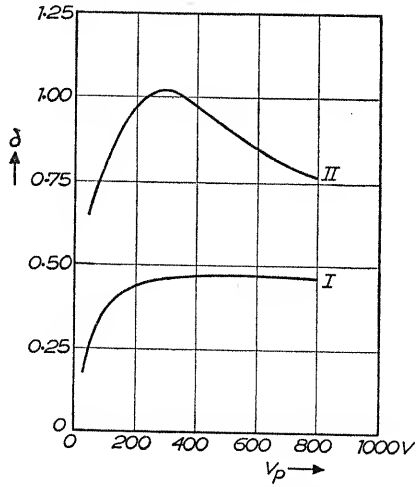

Fig. 3.33. Secondary electron emission yield of soot (I) and of a smooth carbon surface (II); according to BRUINING [171]

electrode. The latter is made by covering a metal target with ground graphite in aqueous solution ("aquadag"), and the crystallites are oriented with their natural cleavage planes parallel to the surface of the supporting target.

Fig. 3.34 shows the secondary emission yield of a black nickel layer compared with the yield of a nickel plate. If the "black" nickel is heated the secondary emission yield rises, and the original black surface shows a grey colour. The very small crystallites have united to bigger ones—a sintering has taken place. (Such a sintering can be observed with all metals. The sinter temperature is much lower than the melting point, though metals with the highest melting point show the highest sinter temperature. For example, it is possible to heat a black tungsten layer to dull red without any noticeable change in structure, whereas a black silver layer sinters at a much lower temperature.)

The explanation of the small yield from a black layer is illustrated in fig. 3.35. Once a secondary electron passes through the surface of a smooth layer it meets no more obstacles, but it is quite different

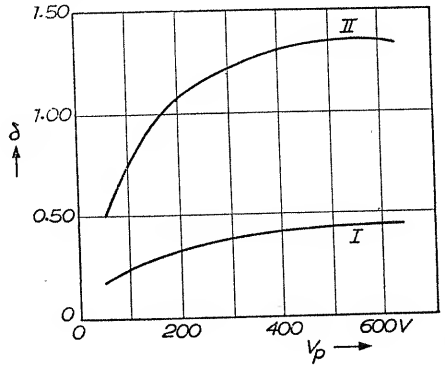

Fig. 3.34 Secondary electron emission yield from a "black" nickel layer (I) and a nickel plate (II); according to BRUINING [170]

for electrons generated in a layer with a labyrinthine structure. When these electrons leave the substance they may be again intercepted by a surrounding wall. The secondary emission yield is nearly independent of the angle of incidence of the primary

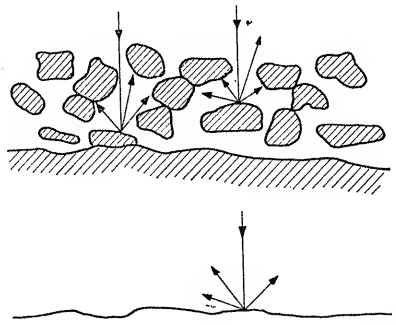

Fig. 3.35. Explanation of the low yield of a "rough" surface: the electron can leave a smooth surface unhindered but with a rough surface it may be intercepted by surrounding walls [170]

electrons, whereas a smooth surface shows an increase of the yield with increasing angle of incidence.

Black layers are useful for lowering the secondary emission where it is undesirably high. Some examples of their application will be given in Chapter 9.

3.4.5. Secondary Electron Emission at the Melting Point and Curie Point.

Several investigators have tried to find a change in the secondary emission yield at the melting point and the Curie point.

The melting point was investigated by SCHWITZKE [163] and MOROZOV [262]. SCHWITZKE found jumps in the curves of δ versus temperature for lead, tin and bismuth. For lead and tin δ is greater in the solid state, for bismuth in the liquid state. MOROSOV, too, observed a jump in δ at the melting point of lead and tin, but in the reverse direction from that found by SCHWITZKE. MOROSOV found an increase of the yield of lead passing to the molten state and practically no change for bismuth, but this result has not been confirmed.

The effects observed by these authors may be due to a change in superficial chemical condition of the target investigated and may have nothing to do with the metal itself.

Changes of δ near the Curie point have been observed by TARTAKOWSKY and KUDRJAWZEWA [91] for nickel, and also by HAYAKAWA [95] for iron, nickel and cobalt. RAO and VADACHARI [189] and TRELOAR and LANDON [191] however could not observe a noticeable effect.

3.5. TEMPERATURE DEPENDENCE OF THE SECONDARY EMISSION YIELD

Apart from changes of δ at the melting point, Curie point, and transition points, many authors have reported that they could not observe any influence of temperature on the secondary emission yield of metals.

3.6. SECONDARY ELECTRON EMISSION AT LOW PRIMARY ENERGY (< 10 eV)

Many authors have investigated the secondary emission yield δ as a function of V_p, in the lower voltage range. Many of their curves show more or less explicit maxima and minima in this range; that of FARNSWORTH [41], for copper, is given in fig. 3.36.

As was pointed out in Chapter 1 the number of elastically reflected primaries is not small compared with the total number. The interpretation of experimental data is therefore not possible unless

these are separated. From a physical point of view the experiments are not very significant. The experiments of FARNSWORTH forestalled in a way the well known DAVISSON-GERMER experiments, which will not be discussed as they are beyond the scope of this book.

The true secondary emission coefficient δ_{true} can easily be obtained by applying the correction formula (1.1). From some experiments there is considerable evidence for the conclusion that

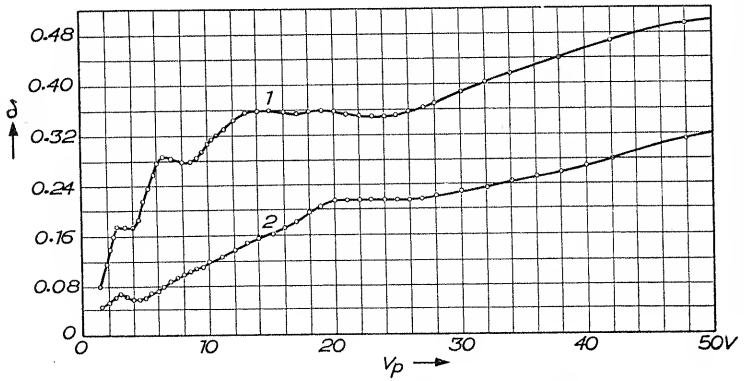

Fig. 3.36. Secondary emission yield of a copper plate (1) and an evaporated layer (2) according to FARNSWORTH [41]

δ_{true} is greater for the metals with a low work function than for those with a high work function. When V_p is small the work function is apparently a governing factor [169].

3.7. SECONDARY ELECTRON EMISSION AT HIGH PRIMARY ENERGY (> 2000 eV)

We have seen in Chapter 1 that at high primary energies the yield δ is by no means a measure of the true secondary electron emission: the secondary electron emission at high primary energies is accompanied by a considerable number of rediffused electrons.

The experimental evidence available on the secondary emission in this energy range is rather limited.

In fig. 3.37 the most recent results obtained by TRUMP and VAN DE GRAAFF [307] are collected. The full lines refer to the total yield δ, whereas the broken lines refer to the secondary electrons with an energy greater than 800 eV, evidently the sum of elastically

and inelastically scattered (rediffused) electrons. From these the factor δ_{true} can be derived by subtracting the ordinates. From the results, shown in Table 3.2, δ_{true} is apparently about inversely

TABLE 3.2. TRUE SECONDARY EMISSION YIELD ESTIMATED FROM FIG. 3.37

	δ_{true}
W	0·12
Fe	0·08
Al	0·05
C	0·025

proportional to the density of the element. We must however bear in mind the remark made by PALLUEL [304, 306], that many of the true secondary electrons are released by the rediffusing

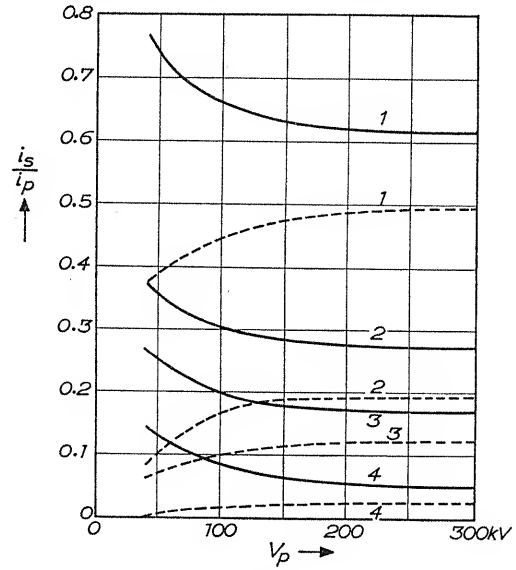

Fig. 3.37. Secondary electron emission yield at very high primary energies [307]; full line—all secondary electrons; broken lines—inelastically scattered (rediffused) electrons; curves 1, 2, 3 and 4 refer respectively to tungsten, steel, aluminium and graphite

electrons. The number of true secondary electrons liberated by the action of the impinging electrons will be much smaller still. At these high energies the true secondary electron emission has

nearly disappeared. Older measurements carried out by SCHONLAND [37] are qualitatively in agreement with the results obtained by TRUMP and VAN DE GRAAFF.

We thus see that the true secondary electron yield of metals at very low V_p is determined by the work function, at very high V_p by the density.

3.8. SECONDARY ELECTRON EMISSION ON THE EXIT SIDE OF A THIN TARGET

If a target consisting of a thin foil is bombarded with primary electrons of sufficiently high energy the electrons leaving the exit side fall into a slow group and a fast group. The slow group must be secondary electrons leaving the foil on the exit side; the fast group consists of primary electrons, which have lost a certain amount of energy.

LENARD and his pupils, in particular, have carried out a number of experiments on this subject. The most recent one is an investigation by WECKER [269]. True secondary electrons and transmitted primary electrons can be separated on the exit side just as was done on the entrance side by STEHBERGER. In Table 3.3 a survey is shown of some of the measurements on aluminium foils reported by WECKER.

It can be seen from this series of measurements that the number of transmitted primary electrons far exceeds the number of true secondary electrons when foils of this thickness are used. The increase in transmission with increasing V_p is to be expected. The decreasing true secondary emission yield per transmitted primary electron, evident in the second columns of Table 3.3, will be discussed in Chapter 6, where the energy transfer of the primary electrons is considered. As can be seen from the third columns the consequence is that the number of true secondary electrons on the exit side per primary impinging electron goes through a maximum.

It would of course be interesting to know what happens when much thinner foils are investigated. Only very few data are available but one investigation carried out by KATZ [175] may give some information. KATZ used an electron-optical method to make an image of a meshed screen, and found he could use electrons with an energy of only 1 eV, even when these electrons had been transmitted by a thin silver foil. This meant that slow electrons can

pass through the foil without any deflection. According to KATZ this high transparency cannot be ascribed to small holes, as can be proved by measuring the energy distribution and the number of transmitted electrons. In fig. 3.38 an example is shown giving the fraction of transmitted electrons able to reach a collector against a retarding field. All electrons with small initial velocities have identical final velocities after they are transmitted by the foil.

TABLE 3.3. TRUE SECONDARY EMISSION YIELD ON THE EXIT SIDE, AND TRANSMISSION OF PRIMARY ELECTRONS, FOR ALUMINIUM FOILS

3·5 μ Al

V_p(kV)	$\frac{i_{transm}}{i_p}$	$\frac{i_s\ true}{i_{transm}}$	$\frac{i_s\ true}{i_p}$
20	0·06	0·38	23×10^{-3}
30	0·44	0·20	88×10^{-3}
40	0·64	0·10	64×10^{-3}
50	0·75	0·08	60×10^{-3}
60	0·82	—	—
70	0·85	—	—
80	0·87	0·03	26×10^{-3}

9·4 μ Al

V_p (kV)	$\frac{i_{transm}}{i_p}$	$\frac{i_s\ true}{i_{transm}}$	$\frac{i_s\ true}{i_p}$
20	0	—	0
30	0	—	0
40	0·16	0·24	38×10^{-3}
50	0·40	0·17	68×10^{-3}
60	0·58	0·12	70×10^{-3}
70	0·69	0·07	48×10^{-3}
80	0·78	0·06	47×10^{-3}

When electrons impinge at higher velocities it is possible to separate the emerging electrons into two groups: one group with low velocities, the other group with an energy equal to the energy of the primary electrons.

In fig. 3.39 the fraction of the electrons transmitted without any change of velocity (the "free transparency") shows a maximum as a function of V_p. This means that any holes present have no important influence. If holes were the cause the free transparency would be independent of the energy of the primary electrons.

The slow moving electrons were considered by KATZ to be true secondary electrons on the exit side. The sum of slow and fast

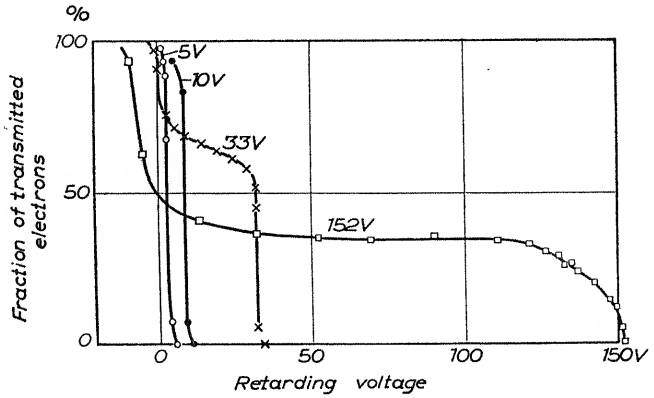

Fig. 3.38. Energy distribution of electrons leaving the "exit side" of a thin foil

electrons determines the "total transparency". It reaches as much as 10% but depends strongly on the treatment of the foil. KATZ found several foils that were initially completely opaque, but rose

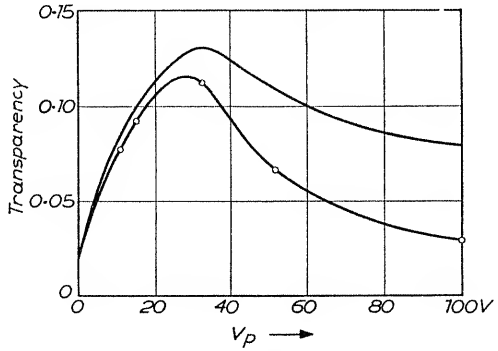

Fig. 3.39. Total transparency (upper line) and "free" transparency (lower line) of a thin foil; according to KATZ

in transparency when bombarded with electrons (fig. 3.40). This was of course a complication which made the results uncertain and irreproducible.

We must conclude that the secondary electron emission on the exit side needs still more investigation. It may be important technically if there is need to increase the true secondary current

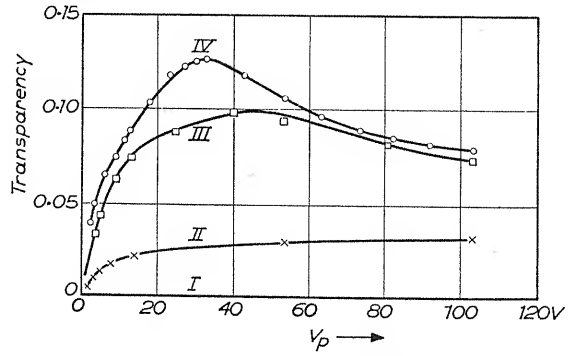

Fig. 3.40. Increase in transparency of a 1500 Å thick silver foil, as a function of time. I Start: no noticeable transparency; II after half an hour's bombardment with a current density of 2×10^{-5} A/mm², and $V_p = 300$ V; III and IV after continuing bombardment. According to KATZ

beyond the primary current. From the experimental evidence we have seen, such a possibility does not seem to exist with metal foils; other methods will have to be tried.

4

SECONDARY ELECTRON EMISSION FROM METAL COMPOUNDS; REVIEW OF RESULTS

4.1. INTRODUCTION

This chapter is devoted to the secondary electron emission from metal compounds; we shall find we have to do with an extremely complicated phenomenon. Many of the substances are not at all stable under electron bombardment. Many are electrical insulators with the consequence that surface charge phenomena have a definite influence on the secondary emission. Surface structure is also of great importance.

From a technical point of view however these substances are even more important than metals, as several of them give a high yield so that electron multiplication is possible.

It may be useful to give first a rough survey of the yields which can be obtained. We shall therefore make a classification of the metal compounds according to the maximum yields obtainable. (Table 4.1).

The highest value of δ_{max} are found with simple compounds of the alkali metals, such as oxides, halides etc. The yields are somewhat smaller from the simple compounds of the alkaline earth metals; smaller still from the oxides of aluminium, silicon etc. Low yields (comparable with metals) occur from typical semiconductors such as MoS_2, WS_2, Ag_2O etc.

$V_p^{\,I}$ and $V_p^{\,II}$ are respectively the lower and higher voltages of the primary electrons for which δ is equal to 1.

4.2. INFLUENCE OF CONDUCTIVITY ON SECONDARY ELECTRON EMISSION

We must now consider the complications connected with secondary emission from compounds. The lack of conductivity often causes the potential of the emitting surface to be ill-defined. Fig. 4.1 demonstrates how the potential of the surface of a poor conductor may arise. The current flowing to the secondary emitting

TABLE 4.1. MAXIMUM ELECTRON YIELDS FROM SOME METAL COMPOUNDS

	δ_{max}	$V_{p\,max}$ (V)	$V_p^{\,I}$ (V)	$V_p^{\,II}$	Ref.	*Method*
LiF	5·6		21		197, 90	evaporated layer
NaF	5·7		20		197, 90	
NaCl	6·8		15		197, 90	
NaCl	6	600			210a	
KCl	7·5		15		197, 90	
RbCl	5·8				197	
CsCl	6·5				197	
NaBr	5·5				197	
KI	5·5		12		197, 90	
Cs_2O*	2·3 to 11				112, 116, 134, 138, 139, 141, 149, 164, 184	
$SbCs_3$	5 to 8·3	375 450	10 20		236, 225	evaporated layer
CaF_2	3·2				197	evaporated layer
BaF_2	4·5					
BeO	3·4	2000			273	
MgO	2·4	1500			273	Mg or Ba evaporated and oxidised
MgO	4·0	400			197	
BaO	2·3	1600			273	
BaO	4·8	400			167	
CaO	2·2	500				
Al_2O_3	1·5 to 4·8	350 to 1300			167, 273	
mica	2·4	380	30	3300	229	
SiO_2	2·1 to	400 to	30			
(quartz)†	2·9	440	50	2300	229	
Ag_2O	0·98 to 1·18				119	
MoS_2	1·10				197	
MoO_2	1·09 to 1·33				119	
WS_2	0·96 to 1·04				197	
Cu_2O	1·19 to 1·25				197	

* The values of δ_{max} in the table are the highest obtained so far (1953). A layer of Cs_2O can be formed in many different ways. The well known infra-red sensitive photo-cathode (described by the symbols [Ag] — Cs_2O, Ag, Cs — Cs) consists largely of Cs_2O. This cathode is formed by oxidizing a silver layer in an oxygen gas discharge, after which the silver oxide is reduced by caesium vapour. The layer consists therefore of a silver base covered with a mixture of Cs_2O and silver and caesium atoms. Externally caesium atoms are adsorbed. With other base metals similar layers can be formed.

† Glasses mostly show a secondary emission yield of the same order of magnitude as quartz.

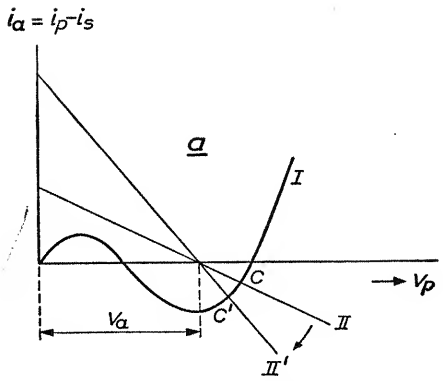

Fig. 4.1a. How an increase of conductivity affects the secondary electron current from a poor conducting substance

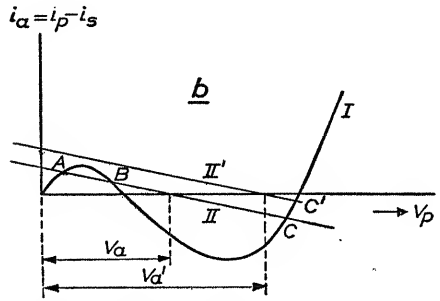

Fig. 4.1b. How an increase of the potential of the supporting target plate affects the secondary electron current from a poor conducting substance

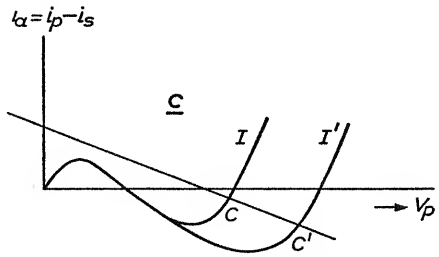

Fig. 4.1c. How an increase of the collector potential affects the secondary electron current from a poor conducting substance

electrode i_a (the difference between primary and secondary current) is determined by the "dynatron characteristic" (see 2.2).

$$i_a = f(V_p).$$

It is also determined by OHM's law and can be represented by

$$i_a = \frac{V_a - V_p}{R}$$

where $V_a - V_p$ is the potential difference between the cathode delivering the primary electrons and the plate supporting the secondary emitting layer and R is the resistance of that layer.

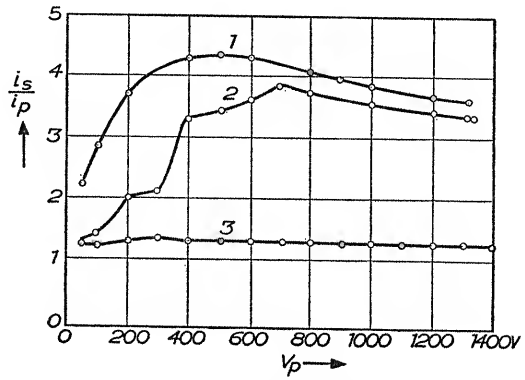

Fig. 4.2. Secondary electron yield of a [Ag] — Cs_2O, Ag, Cs — Cs surface. Curves 1, 2 and 3 show the yield with an increasing amount of oxygen absorbed. According to KHLEBNIKOW and KORSHUNOVA [176]

In fig. 4.1b the dynatron characteristic I and the resistance line II have three intersections A, B, C of which B represents the unstable, and A and C the stable state. In the low potential state A is $i_a > 0$, or $i_s < i_p$; in the high potential state C is $i_a < 0$ or $i_s > i_p$.

The figures enable different phenomena which are often found with insulating materials to be described and explained. Fig. 4.1a shows what happens when there is an increase in conductivity of the emitting material. A decrease of resistance is represented by a clockwise turn of the resistance line from position II to position II', so that the point of intersection C becomes C'. The secondary current actually increases. The results of increasing and decreasing resistance have been observed by different Russian authors. An example is given in fig. 4.2 of the secondary emission of a substance used for photoelectric emission, [Ag] — Cs_2O, Ag, Cs — Cs.

Fig. 4.1b explains the result of an increase of the potential difference V_a to a greater value V_a'. The phenomenon is most remarkable if the surface potential is in the "low" state A; on increasing V_a to V_a' both intersections A and B become imaginary and the only possibility is state C'. This transition is disclosed by a jump in i_s and by a jump of the surface potential, as has been shown by NELSON [207].

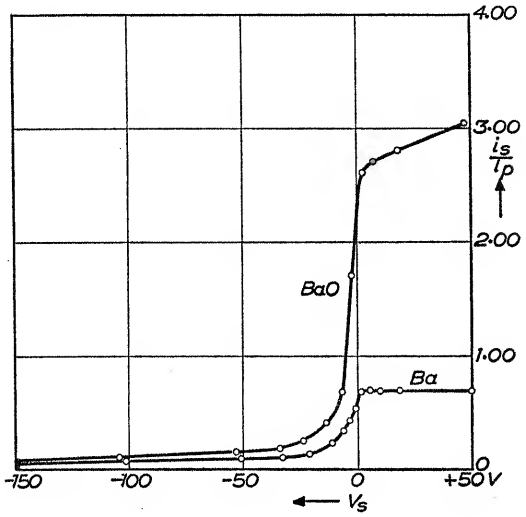

Fig. 4.3. Energy distribution of secondary electrons emitted by a barium layer and a barium oxide layer. In the range $V_s > 0$ the barium layer shows saturation, but not the oxide layer [197]

Fig. 4.1c explains the result of the increase of potential of the electrode for collecting the secondary electrons. It can easily be seen that increasing the collector potential means an extension of the dynatron characteristic to a position such as I'. The shift of the intersection point C to C' results in a greater secondary emission current; this means in practice that high emitting, poor conducting secondary emitting layers are incapable of saturation, as is very well known. An example is shown in fig. 4.3. For comparison the curve for a metal is shown, which saturates easily.

From these simple considerations the consequences of low conductivity can be seen. In some respects, however, the picture has been over-simplified. Examples of the way in which this has been done may be seen in the discussion of fig. 4.1a, where it was assumed

that a decrease in resistance did not affect the secondary emission yield; also in fig. 4.1b and 1c, where it was assumed that an increase of the potential difference $V_p - V_a$ did not affect the secondary emission yield. Another simplification was the assumption that the resistance R was well defined. In general this is not so. One has to bear in mind that in substances like these the resistance is likely to be increased by the electron bombardment itself, i.e. R is a function of i_a.

4.3. REASON FOR HIGH SECONDARY EMISSION

Why the substances mentioned in Table 4.1 should give such high yields is still being vigorously discussed. There are investigators who are of the opinion that the high secondary emission is a property of the substance itself. They have proposed a theory that allows the high secondary emission to be explained in terms of the energy level model. This theory will be discussed in Chapter 6. There are many others, however, who believe that the only reason for high yields is the positive charges left behind by the emission of the secondary electrons. These positive charges are conceived as forming an electric field which stimulates the emission. This view is held especially by the Russians, TIMOFEEW and his collaborators, who believe that the alkali atoms in the compounds with high yield, if ionized, are the actual bearers of this positive charge. Although their experimental evidence is not very convincing, it cannot be denied that there are several phenomena which so far have only been explained by the presence of an internal electric field in the layer itself [285].

The most convincing experiments showing the presence of positive and negative charges have been carried out by HINTENBERGER [202]. He showed that the surface of an insulator, if bombarded by primary electrons with V_p only slightly greater than V_p^{I}, is first charged up to the potential of the collector; but after some time the potential drops at first slowly and then abruptly to the cathode potential. For higher potentials, however, the surface remains near the collector potential. HINTENBERGER assumes that the jump of the potential with the lower V_p is due to the fact that the primary electrons, penetrating to some depth, form a negative internal space charge, whereas the surface itself remains at collector potential. The electrons arriving later hit the surface with the same

energy, but are retarded by the space charge and penetrate less deeply. The space charge extends thus to the surface. As the space charge layer increases in thickness, the depth of penetration diminishes, so that finally the yield drops below 1. When this happens the surface potential drops to the cathode potential.

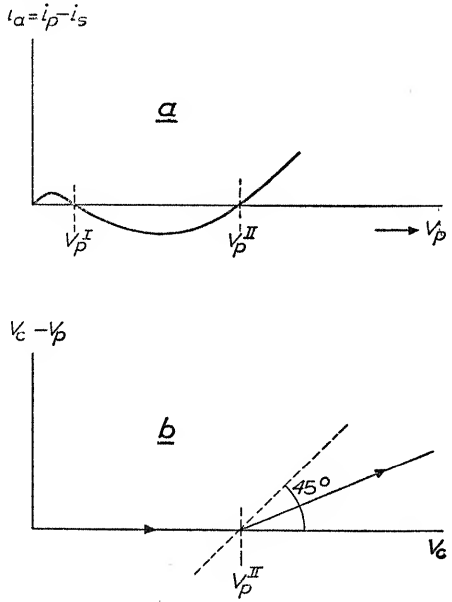

Fig. 4.4a. i_a as a function of V_c, showing that if $V_p > V_p^{II}$, $\delta < 1$
Fig. 4.4b. Potential difference between collector and secondary emitting surface when $V_c \geqslant V_p^{II}$ [201]

Although another explanation of this effect has been offered by McKay [6, p. 107], this experiment seems to be one of the few which have succeeded in demonstrating the presence of an internal field.

Other evidence for the formation of an internal field is the behaviour of the surface potential in the range beyond V_p^{II}. Fig. 4.4a shows that if $V_p > V_p^{II}$, $\delta < 1$. Let us consider a system with an electrode whose configuration is such that when $V_p = V_p^{II}$, $V_c = V_p^{II}$, V_c being the potential of the collector. If V_c is increased, V_p remains the same, because a rise would mean $\delta > 1$. Or in other words the dynatron characteristic remains independent of V_c, if $V_c > V_p^{II}$. Determining the potential difference between the

collector and the emitting surface as a function of V_c one would expect a straight line at an angle of 45° to the abscissa (dotted line in fig. 4.4b). The angle found experimentally is however smaller, which means that V_p^{II} increases slightly with increasing V_c. This is a well-known fact in cathode-ray tubes as has been shown by Hagen. There is thus a slight increase of δ, which can only be due to an internal field.

It does not follow, nevertheless, that this internal field is the only reason for the high secondary emission yield. There are numerous arguments to be brought forward against this proposition, in spite of the support it has received.

First of all there are some insulators, e.g. phosphors like willemite, zinc sulphide, etc., whose yield is not high. Another difficult fact to explain is the high secondary yield of the well-known photocathode $SbCs_3$ (see Table 4.1), although its conductivity, according to a private communication from Dr. H. J. Vink, is as high as 10Ωcm. Thirdly, if an internal field is necessary for a high δ, it seems very unlikely that multiplication of currents of the order of magnitude of one electron per second would be possible, as it is in scintillation counters.

4.4. THIN FILM FIELD EMISSION
[Malter effect; 129, 130]

A phenomenon which can only be explained by the formation of an internal field is the "thin film field emission" discovered by L. Malter in 1936. Subsequent investigations have been carried out by Mahl [159, 183], Koller and Johnson [156], Mühlenpfordt [186], Bruining and de Boer [197], Timofeew [234], and others.

The electrode used by Malter, which showed the thin film field emission, consisted of an aluminium plate with an oxidized surface layer, which after having been covered with caesium was again oxidized. Such a layer can be represented by the symbol

$$[Al] - Al_2O_3 - Cs_2O.$$

Malter himself prepared this layer electrolytically. The aluminium was the anode in a saturated solution of borax and boracic acid; the cathode was a platinum foil. The thickness depends only on the applied voltage to which it is proportional. Malter has used a thickness of about 2000 Å. More recently Piore [162] has used a

layer of silicon dioxide instead of aluminium oxide, which also gave a thin film field emission.

When such a layer is bombarded by electrons of some hundred volts, a current is found if the electrons are drawn by a suitable field. This current may be as much as one thousand times the primary current. The emission current does not reach its full value until some time after the bombardment begins. After switching off, so that the electrons fall back on the target, the field emission drops instantaneously to zero (fig. 4.5).

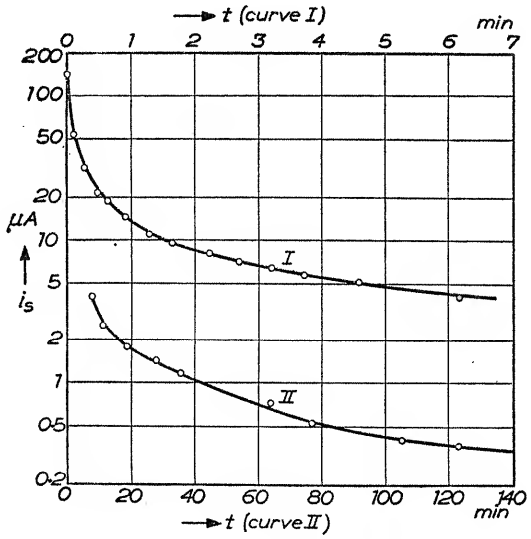

Fig. 4.5. Slowly decreasing field emission current, from a thin film, according to MALTER [130]

MALTER suggests that there may be an analogy between this field emission and the discharge as found by GÜNTHERSCHULZE* and called "Spritzentladung", or "spray discharge". This is found in a gas discharge tube, if the cathode is covered by a thin insulating layer. The dark space normally present is absent, suggesting that electrons are emitted by the insulating layer with sufficient energy to ionize the gas, so there must be an electric field inside the layer. According to GÜNTHERSCHULZE, this field is established by ions, formed in the gas discharge and which are adsorbed by the cathode

* A. GÜNTHERSCHULZE; *Z. Phys.*, **86**, 778, 1938.

surface, but MALTER thinks the field is analogous to that in his oxide layer. The positive charge is formed in his case by the high secondary emission yield of the caesium oxide, and the thin film field emission is therefore a "cold" electron emission which is exerted artificially. The internal field in the Malter effect can be observed in many ways. MALTER himself has noted that the relation between current and collector voltage is similar to the current-voltage characteristic of "thyrite", but GÜNTHERSCHULZE explains the conductivity in thyrite as a consequence of the field emission between the particles.

If the voltage is raised, spark phenomena can be observed in the oxide layer, apparently electric breakdowns. MAHL has measured the positive charge quantitatively using an electron microscope of special construction (fig. 4.6). For a 2000 Å layer potential differences between 10 and 40 V have been observed, and MAHL has concluded from energy distribution measurements that the "field electrons" are emitted by the aluminium metal base, and enter into the vacuum without loss of energy; from this it can be concluded that there is in fact some kind of a "cold" emission.

The Malter effect can be demonstrated clearly with an electron microscope. KOLLER and JOHNSON, and MAHL, showed that the "Malter" current is not emitted by the surface as a whole, but by discrete points differing in intensity. From any particular point the emission is not constant, but varies with time continuously, so that the picture shows scintillations. This is demonstrated in fig. 4.6 which is taken from one of MAHL's articles. In fig. 4.6a at the start of the primary bombardment a uniform emission is observed (the black bars in the picture are due to a thick wire mesh inserted in the primary beam). Some time after the beginning of the primary current some bright points of intensive emission emerge, increasing with time in intensity and number (fig. 4.6b and c). After switching off the primary current some emitting points remain observable (fig. 4.6d).

There are still several more phenomena left which require a further explanation as has been shown especially by MÜHLENPFORDT. He carefully investigated the correspondence between GÜNTHERSCHULZE's spray discharge and the Malter effect. He found that it is possible to change the decreasing Malter current into a spray discharge by admitting very small amounts of a rare gas, at a pressure below 10^{-5} mm Hg; and that, vice versa, the spray discharge can be altered into a Malter current by evacuation. Next

MÜHLENPFORDT showed that a decreasing thin film field emission could be evoked by bombarding a layer [Al] — Al_2O_3 — Cs_2O with positive ions. Another important discovery made by the same author was the influence of oxygen. If oxygen is admitted at a pressure of about 10^{-5} mm Hg the Malter current drops three orders of magnitude, but does not increase after evacuation. A recovery takes place only after renewed electron bombardment.

This deactivation by oxygen may prove that the caesium oxide is partially decomposed by the electron bombardment and that free caesium is essential for the appearance of the effect. It is quite likely that the Malter effect can only occur if a certain quantity of gas is present in the tube and the caesium vapour is one of the components of this residual gas. The correctness of this hypothesis has to be tested by more experiments.

PAETOW [208] has made experiments which support this hypothesis. He regards the Malter effect as a special form of the discharge which he finds if the cathode is covered with a layer of an insulating substance (Al_2O_3, MgO, glass powder, quartz powder, sulphur, bakelite etc.). PAETOW distinguishes two kinds of discharge phenomena.

(1) A high voltage discharge, which starts at some thousands of volts and a pressure of 10^{-3} to 10^{-7} mm Hg. This discharge leaves the cathode at places where the layer is thin. The discharge is very "unquiet", the particles on the cathode flying through the discharge space and falling back to the cathode because of their positive charge, and covering it with a uniform layer.

(2) A low voltage discharge, which may start, if the layer on the cathode is uniform, e.g. owing to the action of a high voltage discharge described in (1) above. The maximum current density is about 100 mA/cm². Between 10^{-6} mm and 10^{-2} mm Hg pressure the discharge current is nearly independent of the applied voltage; no discharge current is found at pressures below 10^{-6} mm Hg.

PAETOW considers the Malter current to be a low voltage discharge, basing this conclusion on the fact that the low voltage emission shows "decay" phenomena. According to MÜHLENPFORDT the Malter effect shows both a high and a low voltage discharge.

Though the above investigations seem to be the most important, yet other work on the Malter effect is worth mentioning. BOGINESCO [196a] observed a Malter effect by bombarding with negative ions, using Al_2O_3 on aluminium as a target. BRUINING and DE BOER

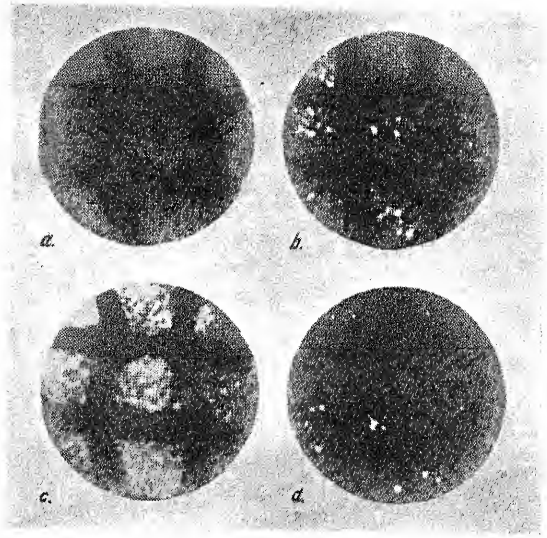

Fig. 4.6. Start and end of thin film field emission; (a) start of the primary current; (b) 10 sec. later; (c) 60 sec. later; (d) 60 sec. after stopping the primary current. According to MAHL [159]

To face page 62

observed a Malter effect with a MgO layer; the magnesium oxide was deposited on a metal plate by burning magnesium metal in air (fig. 4.7).

Finally, mention should be made of an electrode described by TIMOFEEW which is also a photocathode. It consists of a layer of the type [Ag] — Cs_2O, Ag — Cs, prepared in the normal way with the exception that the silver was evaporated on to the base when the latter was at a temperature of about 100°C. This gives the layer a rougher structure than normal. When such a layer is used as a

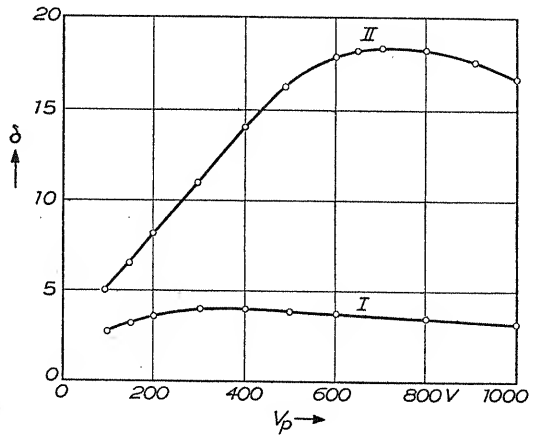

Fig. 4.7. Secondary emission yield of a magnesium oxide layer, obtained in an oxygen atmosphere (curve II); curve I shows the yield of a smooth layer (197]

photocathode it shows the same phenomena as with the Malter effect.

The time lag effects always present in the Malter effect and the lack of reproducibility of performance have up to now made it impossible to use this phenomenon for technical application.

4.5. DECOMPOSITION OF A COMPOUND WITH HIGH SECONDARY EMISSION YIELD [197]

If a layer consisting of a compound of an electropositive metal is bombarded with electrons, a decrease of the secondary emission yield can often be observed. This happens especially to layers of alkali halogenides evaporated in vacuo. If a layer with such a "spoiled" yield is oxidized, δ rises again. It thus seems correct

to assume that the decrease is caused by a separation of alkali metal (fig. 4.8).

The decomposition of the compound, with a consequent decrease in secondary emission yield, is one of the major problems when electron multiplication is required at high current densities. A complete explanation has never been given. Nevertheless we shall try to describe what actually occurs in such a layer.

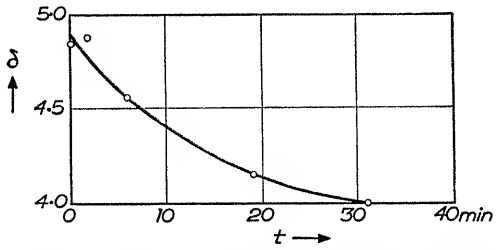

Fig. 4.8. Secondary emission yield of an evaporated sodium-chloride layer, as a function of time of bombardment [197]

As an example we take a secondary emitting layer of sodium chloride. The electrons being emitted as secondary electrons are those with the highest energy in the crystal, i.e. those occupying the highest energy band, which in sodium chloride are the $3p$-electrons. If one of these electrons is emitted, a chlorine atom is left in the crystal. We may distinguish two different cases:

(a) the chlorine atom remains in the grid;

(b) the chlorine atom escapes.

Upon the emission of an electron, a positive charge is left behind in the grid, which has to be neutralized by an electron delivered by the metal base. In case (a) the electrical neutrality is obtained by the recombination of the supplying electron with the chlorine atom so that the original situation is restored. In case (b) the chlorine atom has disappeared. Neutrality can however be achieved if the electron is caught in the hole which was left by the escaping ion. The electron now belongs to the six surrounding sodium ions. It is what is called a colour centre, and it behaves like a neutral atom in a neutral grid. When a number of chlorine atoms have escaped, an agglomeration of these colour centres takes place and colloidal metal particles are formed with conduction electrons, with the consequence that the secondary emission yield drops. From this

picture it can be seen how the salt decomposes; chlorine escapes and the remaining sodium forms metal particles, causing a discoloration.

This "printing" has a practical application in the "skiatron"; this is a cathode ray tube with the fluorescent powder on the screen replaced by an evaporated layer of one of the alkaline halides. The metallic discolouration can be used, for instance, to make a radar pattern visible. The image can be erased by heating, but this takes time, and the system seems of doubtful value for application for television projection.

The oxides of the electropositive metals decompose at a much slower rate than the halides, so that they can be used for technical purposes. The difference is that the anions of oxides have a double negative charge. On the emission of an electron a single charge is left which apparently prevents the atom from escaping.

4.6. PRACTICAL REQUIREMENTS FOR COMPOUNDS WITH HIGH YIELDS

If an electrode of high secondary emission is required, it can be seen from the previous sections that the oxides of alkali and alkaline earth metals are useful. The antimony caesium compound can also be used, but cannot be heated to higher temperatures than 50°C. The sulphides too might be stable, but sulphur is a well-known toxicum (poison) for thermionic oxide cathodes and may not be practical from this point of view.

The oxides of the alkali metals easily form carbonates, and have to be prepared inside the tube. The same applies to barium and strontium oxide. The only oxides which can be prepared outside the tube are magnesium oxide and beryllium oxide, and these oxides are stable at higher temperatures. Magnesium oxide is therefore often used in amplifier tubes, although its secondary emission yield is not as high as from the oxides of the alkali metals.

From the previous sections one can conclude that the emitting substance must have a certain conductivity, to prevent both thin film field emission and the build-up of surface charge which would make emission impossible. In general, sufficient conductivity can only be obtained by an extra amount of metal, which should not exceed a certain limit, because the secondary emission yield of the metal itself is low. This limitation of the free metal is the real problem of secondary emitting surfaces with high yield, and makes

it difficult to get reproducible targets which do not change with time.

From an industrial point of view it is most important to find an easy way of making these surfaces. One of the most elegant methods has been described by GILLE [250] and MATHES [257] and afterwards by many other authors. If an alloy of magnesium or beryllium, like silver-magnesium, nickel-beryllium, is heated in an oxygen atmosphere a superficial layer consisting of the oxide of magnesium or beryllium is formed, which will give yields of up to 16. If too high yields are aimed at, by long oxidation, a Malter effect may start, but there are many variations on this theme. To discuss the different methods for getting a proper surface we should have to

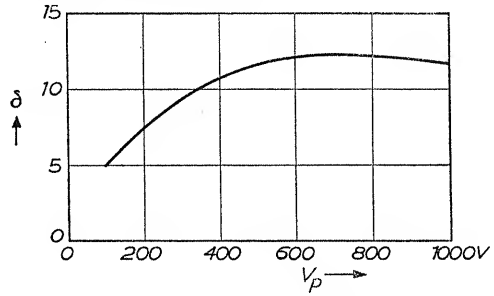

Fig. 4.9. Secondary emission yield of nickel beryllium alloy

enter the field of technical know-how, which is beyond the scope of this book. We must be content therefore to record the literature [326].

4.7. SECONDARY ELECTRON EMISSION FROM THE "OXIDE-COATED" CATHODE

Considerable work has been carried out concerning the secondary emission yield from the well-known thermionic oxide coated cathode. Such a target consists of a thin layer of barium-strontium-oxide about 50 μ thick, with a resistivity of about $10^8\Omega$ cm at room temperature, decreasing to $10^3\Omega$ cm at 800°C. The thermionic emission at high temperature is due to the formation of barium atoms, these being the actual electron sources.*

MORGULIS and NAGORSKY [185], POMERANTZ [300] and JOHNSON [297, 302] have measured the secondary emission yield from the

* J. H. DE BOER; *Electron Emission and Adsorption Phenomena*, Cambridge University Press 1935.

oxide-coated cathode as a function of temperature. All have found that δ rises with increasing temperature, and JOHNSON'S most recent results are collected in fig. 4.10. JOHNSON has used a microsecond pulse technique, the best way of eliminating resistance effects of the layer itself. It can be seen that δ has a minimum as a function of temperature. At room temperature δ is observed to decrease during the pulse period, evidently because of the positive charge on the target surface. At 400°C, where δ is minimum no resistance effect is left. At higher temperature where thermionic emission is

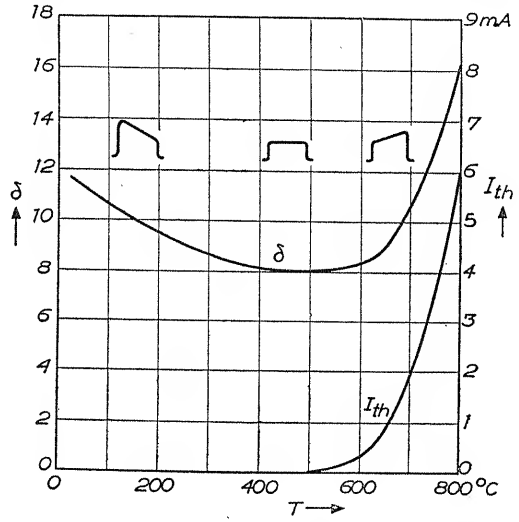

Fig. 4.10. Variation with temperature of secondary emission yield of oxide-coated cathode; according to JOHNSON [302]

already appreciable δ rises also. The secondary electron current seems to rise during the pulse and it falls with some retardation to zero after the primary current ceases. If $\Delta\delta$ is the difference between δ at any temperature above 500°C and δ at its minimum value one finds:

$$\Delta\delta = Ae^{-Q/2kT},$$

where Q is of the order of 0·7 eV. The "enhanced" yield $\Delta\delta$ is proportional to i_p, as is the ordinary secondary electron emission, but it has some characteristics which are quite different from the ordinary true secondary emission: it is practically independent of V_p beyond $V_p = 200$ V; it is about proportional to the steady thermionic current.

From these properties JOHNSON has concluded that $\Delta\delta$ is the result of an enhanced thermionic emission caused by the electron bombardment of the oxide material. Under the bombardment the emission constants apparently change. One of the changing constants may be the number of emission centres, because the number of free barium atoms may vary under electron bombardment (4.5). The proportionality with i_p, and the thermionic emission and the retardation phenomena during the pulse, fit this explanation well.

5

VARIATION OF SECONDARY EMISSION YIELD CAUSED BY THE EXTERNAL ADSORPTION OF IONS AND ATOMS

5.1. INTRODUCTION

It is well known that the photo-electric and thermionic emission from metals is increased if ions and atoms of an electropositive metal are adsorbed on the surface. The adsorbed layer reduces the work function, i.e. the energy required to liberate an electron from the metal. If the total fraction of the surface covered is small, the adsorbed particles are all ions. The decrease of the work-function is in this case proportional to the number of adsorbed ions. With increasing coverage atoms begin to be adsorbed and these, too, cause a decrease in the work-function, though in a much smaller degree. When the atoms become about as numerous as the ions the work-function rises again towards what it was for the adsorbing metal in compact form.

The change of the work-function can be observed by measuring the photo-electric and thermionic emission, for the thermionic current passes through a maximum as the covering rate increases. The photo-electric emission passes a maximum even if the surface is irradiated with light which is not absorbed by the adsorbed atoms or ions.

If however the surface is irradiated with light that is absorbed by the adsorbed atoms, these too emit electrons by the selective photo-electric effect. The curve giving the relation between photo-electric current and covering rate then has a more complicated form; two maxima may be observed. The first maximum corresponding to the lower fraction of covering is found where the work-function has its minimum value. The second maximum corresponds to the coverage where the occupation is optimum for the selective photo-electric effect.

5.2. LIBERATION OF SECONDARY ELECTRONS FROM ADSORBED ATOMS

Considering the secondary emission yield as a function of the fraction of covering one may ask whether the observed change in secondary emission yield is due to the change in the work-function or to the emission of electrons by the covering atoms. In this case we are considering a covering about one atom thick so that the number of electrons liberated from the adsorbed layer can easily be estimated by using J. J. THOMSON's well known formula:*

$$p_i^2 = \frac{e^4}{e^2 V_p^2}\left(\frac{V_p}{V_i} - 1\right) \qquad (5.1)$$

in which eV_i is the ionization energy of the adsorbed atom and p_i the distance within which the undisturbed path of the primary electron must approach the atom to be ionized. If this distance is smaller than p_i all collisions cause ionization, so that the number of ionized atoms is proportional to the area πp_i^2. With molybdenum as the base metal, covered with a monatomic layer of $3{\cdot}58 \times 10^{14}$ atoms/cm^2, and if $V_i = 5$ V, the number of atoms ionized by each primary electron is given in Table 5.1. It appears therefore that

TABLE 5.1

$V_p = 10$ V	$V_p = 20$ V	$V_p = 200$ V
0·23	0·17	0·02

for $V_p = 10$ V to 20 V the number of electrons liberated from the adsorbed layer is of the same magnitude as the yield from the uncovered metal for which $\delta \simeq 0{\cdot}3$. When $V_p = 200$ V however it is far less.

It will later be shown that the maximum increase of δ which can be observed as a result of the adsorption of foreign atoms is about 0·5.

From this it can be concluded that the change of δ, if bombarding electrons of some hundred eV are used, is in fact caused by the change of the work-function. With primary electrons of low energy a considerable number of the emitted secondary electrons may originate from the adsorbed atoms.

* J. HENGSTENBERG and K. WOLF; "Elektronenstrahlen und ihre Wechselwirkung mit Materie," *Hand-und Jahrbuch der chemischen Physik*, **VI** A page 78, 1935.

It is also possible to prove experimentally that the secondary emission yield is determined by the work-function. This can easily be done, if both δ and the work-function of the target are measured at the same time. Instead of the work-function the photo-electric emission can be measured. It has been proved by different experimenters that δ and the photo-electric emission both have a maximum as a function of the rate of covering and that these maxima are found at the same coverage (fig. 5.1). This means that the

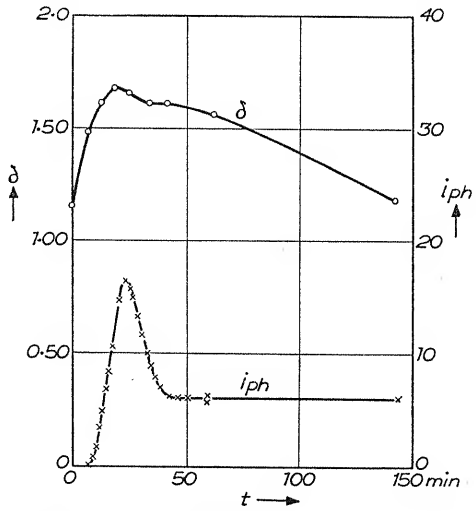

Fig. 5.1. Secondary and photo-electric current from molybdenum, as a function of time while barium is deposited at a uniform rate; $V_p = 200$ V. The photo-electric current was measured with the continuous light of an incandescent lamp [196]

secondary emission yield is in fact determined by the work-function of the target material. TRELOAR concluded from his experiments that the mean depth at which secondary electrons were liberated was 1·6 atomic layers, whereas he assumed that δ is determined by the work-function. If his conclusion were correct, the liberation of electrons from the adsorbed atoms would have to be taken into account, which was not done. We shall see however in Chapter 6 that the mean depth of liberation is much greater than 1·6 atoms.

Indeed, if the work-function is made as small as possible, practically no electrons are liberated from the adsorbed atoms. Table 5.2 shows that if a surface containing adsorbed atoms is exposed to an oxygen atmosphere, the secondary yield drops to the original

value of the uncovered metal. Now, if a considerable proportion of the secondary electrons from molybdenum with barium were contributed by the absorbed barium atoms, one would expect an increase of δ when the surface was oxidized. The fact that the yield after oxidation was nearly down to that of clean molybdenum proves that no appreciable emission from the adsorbed atoms takes place [196].

TABLE 5.2

Surface	δ (V_p = 200 V)
Molybdenum	1·21[5]
Molybdenum with barium	1·72–1·75
The same surface oxidized	1·24

5.3. INCREASE OR DECREASE OF δ WITH CHANGING WORK-FUNCTION

The relative variation of the secondary emission yield is much smaller than the variation of thermionic and photo-electric emission under similar conditions. This difference in behaviour was first observed by SIXTUS and has been confirmed by many other investigators. Fig. 5.2 shows the secondary emission yield of tungsten with three different coverages of thorium. Atoms which increase the work-function, like oxygen on tungsten, have only a slight influence on the yield. This is shown by Table 5.3, taken from the work of TRELOAR [136].

TABLE 5.3. VARIATION OF THE SECONDARY EMISSION YIELD FROM TUNGSTEN, UPON ADSORPTION OF OXYGEN (V_p = 300 V)

δ pure tungsten	1·31
δ tungsten with oxygen covering	1·06
increase of work-function due to oxygen	1·78 V

The small relative variation of the secondary emission yield can be explained, according to SIXTUS [72], on the grounds that the energy of the secondary electrons is greater than the change of the work-function, which is why its influence is much greater on thermionic than on secondary emission. This difference can be put into more quantitative form by assuming that the energy distribution of the secondary electrons is Maxwellian, with a mean energy

of 5 eV. A decrease of the work-function by 2 eV then causes an increase of the thermionic current (mean energy 0·2 eV) by a factor $e^{10} = 2{\cdot}2 \times 10^4$, whereas the secondary electron current is increased by a factor of only $e^{0{\cdot}4} = 1{\cdot}42$. The photo-electric current excited by visible light is also much more sensitive to a decrease in the work-function than the secondary electron emission. Similar results

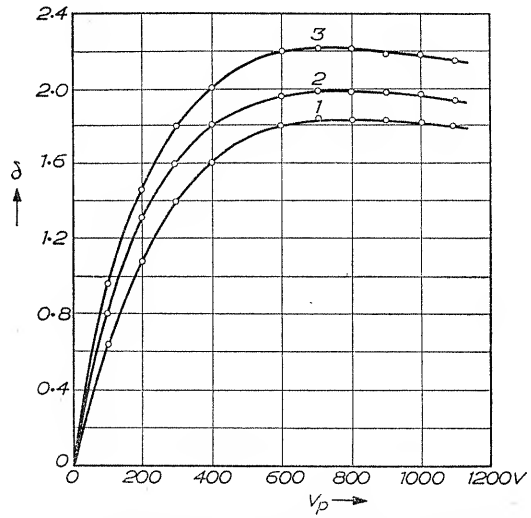

Fig. 5.2. Secondary electron emission yield of tungsten with different coverage of thorium, as a function of V_p; 1: φ = 4·52 V; 2: φ = 3·30 V; 3: φ = 2·63 V. According to SIXTUS [72]

have been obtained by MCKAY [276] with tungsten covered with sodium. He found a 60% increase in δ when the work-function was decreased by a factor 2.

5.4. RISE OF THE SECONDARY ELECTRON CURRENT WITH INCREASING COVERING RATE WITH ATOMS OF AN ELECTRO-POSITIVE METAL

Referring once more to fig. 5.1, we observe another difference between the photo-electric current and the secondary electron emission, besides the one we have just discussed. Near the left of the figure, for low coverages, the photo-electric emission rises exponentially, but the secondary emission rises linearly. This difference in behaviour, too, can be understood in terms of the difference in energy of photo-electrons and secondary electrons.

The photo-electric emission of a metal surface exposed to the radiation of a black body can be written as:

$$i_{ph} = AT^2 \exp(-e\varphi/kT) \tag{5.2}$$

where A is a constant, T the temperature of the black body and k the Boltzmann constant. If the surface is hit by a steady shower of atoms, the work-function φ changes linearly with time so long as the coverage is small; therefore

$$\varphi = \varphi_0 - ct$$

c being a constant, and i_{ph} can be written as a function of time:

$$i_{ph}(t) = AT^2 \exp\left(-\frac{e(\varphi_0 - ct)}{kT}\right) \tag{5.3}$$

As $kT \ll ect$ an exponential rise can be expected.

The secondary electron yield can be expressed by the equation

$$\delta = P \exp(-e\varphi/eV) \tag{5.4}$$

where P is a constant and eV the mean energy of the secondary electrons. Substituting again for φ, we find

$$\delta(t) = P \exp\left[-\frac{e(\varphi_0 - ct)}{eV}\right].$$

Because $eV > ect$ we may write, as a first approximation,

$$\delta(t) = P\left(1 + \frac{ect}{ev}\right) \exp\left(-\frac{e\varphi_0}{ev}\right),$$

and $\delta(t)$ is approximately a linear function of t.

5.5. SECONDARY ELECTRON EMISSION FROM METAL SURFACES COVERED WITH THICKER LAYERS

In the previous sections we discussed adsorbed layers that were only about one atom thick. We must now consider some experiments with adsorbed layers several atoms thick, which were carried out by SUHRMANN and KUNDT [284]. Knowing that the change of work-function had but a slight influence on the secondary emission yield, they wondered what would be the influence of a thicker layer. In particular they expected that a metal with an

adsorbed oxygen layer would exhibit a temperature dependent secondary emission, because the exchange between the lattices and the oxygen dissolved in the superficial metal layers also depends on temperature.

The authors carried out numerous experiments with evaporated layers of copper, gold, silver, cadmium and beryllium. The layers were evaporated at 83°K, heated up to 293°K, exposed to oxygen,

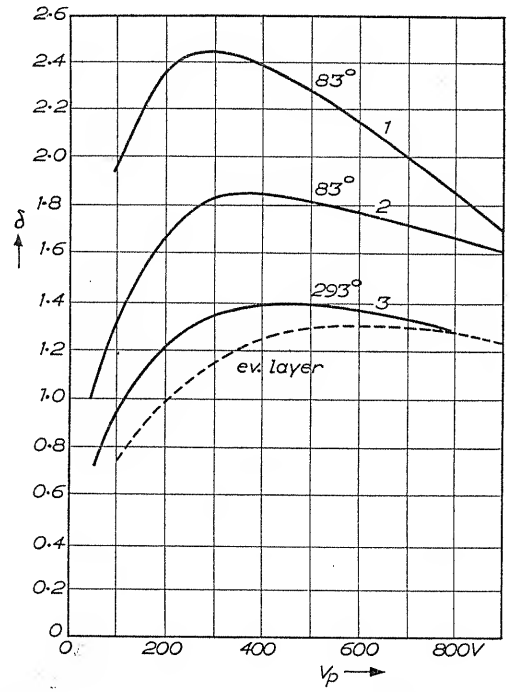

Fig. 5.3. Secondary emission yield of copper with adsorbed layer of oxygen (according to SUHRMANN and KUNDT) [284] curves 1, 2 and 3 refer to copper exposed to oxygen at room temperature

re-evacuated, cooled to 83°K, heated to 293°K, exposed to more oxygen, and so on. After each operation the secondary emission was measured (figs. 5.3 and 5.4).

The result was that copper, gold and silver showed a strong temperature dependence. The secondary emission yield of these metals at room temperature was nearly independent of the adsorbed oxygen. At 83°K however the yield was some ten per cent higher with adsorbed oxygen than without it. The metals cadmium and

beryllium, with their greater affinity for oxygen, behaved quite differently. Both metals showed an increase in yield at room temperature if exposed to oxygen. The most remarkable increase was found with beryllium, and evidently a beryllium oxide was formed. The temperature dependence of cadmium and beryllium was much smaller than that of the noble metals. SUHRMANN and KUNDT concluded from these experiments that the exchange of the

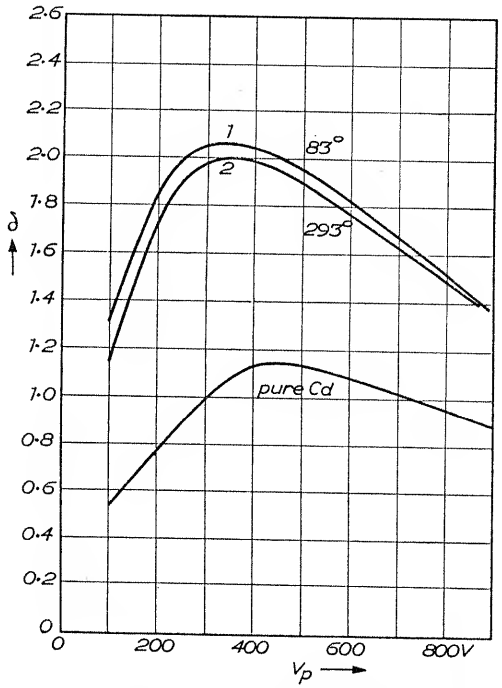

Fig. 5.4. Secondary emission yield of cadmium with adsorbed layer of oxygen (according to SUHRMANN and KUNDT) curves 1 and 2 refer to cadmium exposed to oxygen at room temperature

oxygen from the surface to the lattice is most sensitive to temperature in the cases where there is no question of oxide formation.

These experiments cannot give an important contribution to the knowledge of the mechanism of secondary emission, because the structure of the layers was not sufficiently well defined. They do however give information about the secondary emission yield from targets on which the adsorbed layer is thicker than one atom, before the formation of a complete oxide layer has taken place.

5.6. SECONDARY EMISSION YIELD OF SOOT COVERED WITH BARIUM

It was mentioned in Section 3.4.4 that the low secondary emission yield of soot is due to its finely divided form. If a soot layer is gradually covered by barium in the form of barium oxide molecules evaporating from a oxide cathode, the secondary emission yield

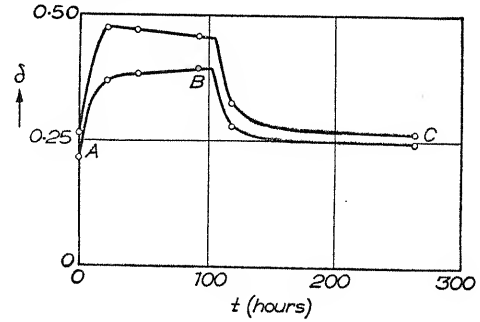

Fig. 5.5. Secondary emission yield of a soot layer as a function of time. AB, no electrons hit the anode, and δ increases; BC, the anode is bombarded by electrons, and δ drops to former value

rises. But if while the evaporation is going on the soot layer is bombarded by electrons emitted by this oxide cathode (the bombarding voltage being 300 V, and the current density about 1 mA cm^{-2}) the secondary emission yield remains constant. Under the bombardment the barium atoms are apparently migrating to a greater depth, as a result of the local heating of the soot particles by the bombarding electrons (fig. 5.5., ref. 146). This property of soot is useful in those applications where a suppression of secondary emission yield is necessary (cf. Chapter 10).

6

THEORY OF SECONDARY ELECTRON EMISSION; THE MECHANISM OF EXCITATION OF SECONDARY ELECTRONS

It is unnecessary to emphasize that the development of a theory of secondary electron emission is no simple task. Various authors have made their contributions. Some theories are more or less phenomenological; others are based on a model, either classical, or the wave mechanical model of BLOCH. No theory has yet been found which satisfactorily covers all the observed phenomena. There are views, however, which are worthy of consideration since they connect the secondary electron emission with other properties of solids.

6.1. DERIVATION OF A UNIVERSAL LAW

We shall begin by trying to calculate the secondary emission yield as a function of V_p, by applying an elementary theory [5, 229, 230].

The liberation of secondary electrons occurs by the transfer of energy from the primary electrons to the electrons of the lattice. The behaviour of the primary electron is determined by its energy loss as a function of penetration depth, its absorption and scattering. The secondary electrons are scattered, and before reaching the surface a fraction will be lost by absorption. Moreover, the work-function has to be overcome before an emission is possible.

We first will determine the amount of energy which is lost by the primary electron in a layer having the thickness dx at a depth x, fig. 6.1. We assume that WHIDDINGTON'S law is valid, so that the energy of a primary electron $eV(x)$ at a depth x can be expressed by

$$[eV(x)]^2 = e^2V_p^2 - ax \tag{6.1}$$

where a is a constant, proportional to the density of the material.

Next, we must take account of the fact that the number of primary electrons diminishes through absorption and scattering.

JONKER'S [321] argument in favour of neglecting these items is scarcely admissible, although the experimental data are too scarce to settle the matter quite definitely.

The amount of energy produced in the layer will be $-\frac{\mathrm{d}[eV(x)]}{\mathrm{d}x} i_p$; assuming that the number of secondary electrons is proportional to this differential quotient, we write $i_s = -\kappa \frac{\mathrm{d}[eV(x)]}{\mathrm{d}x} i_p$. The proportionality factor, κ, determines the yield of secondary electrons, which we will discuss later on. To describe the absorption undergone by secondary electrons on their path to the surface from where they originate, we shall assume that the number decreases exponentially with the distance x to the surface. In the next chapter it will be clear that this representation is somewhat oversimplified, but this objection does not affect the present argument.

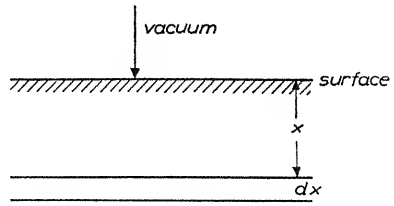

Fig. 6.1

The influence of the work-function will prevent the emission of a fraction of the electrons released inside the material. From experiments it appears that the energy distribution is largely independent of V_p. We can thus assume that the fraction which can escape is independent of V_p (Chapter 7) so that it can be included in the factor κ. Consequently we get from the layer dx at depth x a contribution to the current crossing the surface:

$$\mathrm{d}i_s = -\kappa i_p \, \mathrm{e}^{-\alpha x} \frac{\mathrm{d}[eV(x)]}{\mathrm{d}x} \mathrm{d}x. \tag{6.2}$$

By using (6.1) eq. (6.2) can be changed into

$$\mathrm{d}i_s = \tfrac{1}{2}\kappa a i_p \mathrm{e}^{-\alpha x} (e^2V_p^2 - ax)^{-\frac{1}{2}} \mathrm{d}x. \tag{6.3}$$

The range $x_{\max}$ of the primary electron follows from (6.1) by putting $eV(x) = 0$:

$$x_{\max} = \frac{e^2V_p^2}{a}.$$

The secondary current becomes therefore

$$i_s = \tfrac{1}{2}\kappa a i_p \int_0^{\frac{e^2V_p^2}{a}} (e^2V_p^2 - \alpha x)^{-\frac{1}{2}}\, e^{-\alpha x}\, dx. \qquad (6.4)$$

By the substitution $x = \dfrac{e^2V_p^2 - ay^2/\alpha}{a}$, (6.4) can be transformed into

$$i_s = \kappa i_p \sqrt{\frac{a}{\alpha}}\, e^{-r^2} \int_0^r e^{y^2}\, dy \qquad (6.5)$$

in which $r = eV_p\sqrt{\dfrac{\alpha}{a}}$.

We now calculate the value of r for which i_s has its maximum:

$$\frac{di_s}{d(eV_p)} = \kappa i_p \left(1 - 2re^{-r^2}\int_0^r e^{y^2}\, dy\right);$$

$$\frac{di_s}{d(eV_p)} = 0 \quad \text{for} \quad r = eV_p\sqrt{\frac{\alpha}{a}} = 0{\cdot}92. \qquad (6.6)$$

Baroody [315] and Jonker [324] have shown the possibility of determining a universal curve for i_s as a function of V_p. We therefore write (6.5) in a somewhat modified form

$$i_s = \kappa i_p \sqrt{\frac{a}{\alpha}}\, F(r), \qquad (6.7)$$

where $F(r) = e^{-r^2}\int_0^r e^{y^2}\, dy$. So we write

$$i_{s\,\max} = \kappa i_p \sqrt{\frac{a}{\alpha}}\, F(0{\cdot}92).$$

Using (6.6) we find, since $i_s/i_{s\,\max} = \delta/\delta_{\max}$,

$$\frac{\delta}{\delta_{\max}} = \frac{1}{F(0{\cdot}92)}\, F\left[\frac{0{\cdot}92eV_p}{eV_{p\max}}\right] = 1{\cdot}85F\left[\frac{0{\cdot}92eV_p}{eV_{p\max}}\right] \qquad (6.8)$$

Equation 6.8 represents a universal curve based on theoretical considerations only, and it is striking that a universal curve, applicable to metals, can be found in actual fact (fig. 6.2). There is, however, a marked difference between the experimental and the calculated curve, particularly at large values of V_p, where the experimental values are much higher. One of the reasons may be

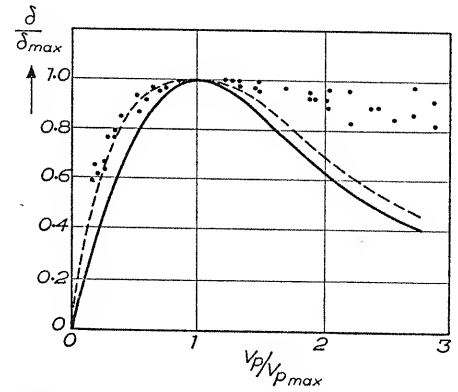

Fig. 6.2. Universal δ versus V_p curve; full line according to Baroody (eq. 6.8); dotted line according to Jonker (eq. 6.8a); the points represent measured data

that the secondary electrons are liberated by "rediffused" primary electrons (Knoll [289], Palluel [304, 305]), which means that the general depth of origination is less than one would expect from eq. (6.1).

6.2. DETERMINATION OF THE CONSTANTS a AND α

In our elementary theory of section 6.1, we left out the fact that the secondary electrons do not all set off in a direction perpendicular to the surface. We now assume with Jonker [324] that their directions are equally distributed in space at the point of origination, and we shall see in Chapter 7 that this assumption is justified. Then eq. 6.7 must be modified to read:

$$i_s = \tfrac{1}{2}\kappa i_p \sqrt{\left(\frac{a}{\alpha}\right)}\, f(r) \qquad (6.7a)$$

where $f(r) = \int_0^1 dz\, e^{-\frac{r^2}{z}} z^{\frac{1}{2}} \int_0^{\sqrt{\frac{r^2}{z}}} e^{y^2}\, dy$ and $r = \sqrt{\left(\frac{\alpha}{a}\right)}\, eV_p$.

The altered form is due to the fact that an absorption depending on the direction of the secondaries in the material has been taken into account.

The maximum value of i_s is now at $r = 0{\cdot}71$, and we can write the universal law (6.8) in the analogous form:

$$\frac{\delta}{\delta_{\max}} = \frac{1}{f(0{\cdot}71)} f\left(0{\cdot}71\,\frac{eV_p}{eV_{p\max}}\right);\ f(0{\cdot}71) = 0{\cdot}33. \qquad (6.8a)$$

The smooth curve in fig. 6.2 must now be replaced by the broken curve, and this is in somewhat better accord with the observed data.

For some metals, e.g. nickel and gold, a and α are known. The constant a of metals has been determined by TERRILL* for V_p between 25 and 50 kV and is about proportional to the density; α is known from experiments carried out by BECKER† and PARTSCH and HALLWACHS‡. For nickel, taking $3{\cdot}5 \times 10^{12}\mathrm{V}^2\,\mathrm{cm}^{-1}$ for a and $1{\cdot}5 \times 10^6\,\mathrm{cm}^{-1}$ for α, gives 1086 V for $V_{p\max}$; this is considerably higher than the experimental value which is 500 V. For gold $a = 8{\cdot}9 \times 10^{12}\mathrm{V}^2\,\mathrm{cm}^{-1}$ and $\alpha = 10^6\,\mathrm{cm}^{-1}$ gives $V_{p\max} = 2100$ V; the experimental value is 875 V. It is justifiable to doubt whether TERRILL's values of a are applicable at voltages so much lower than he used. Assuming the measured values for $V_{p\max}$ and α, the values of a for nickel and gold may be calculated to be $0{\cdot}74 \times 10^{12}\mathrm{V}^2\,\mathrm{cm}^{-1}$ and $1{\cdot}52 \times 10^{12}\mathrm{V}^2\,\mathrm{cm}^{-1}$ respectively; these are much lower than TERRILL's figures.

The lower values of a are not improbable. Obviously a primary 500 eV electron can only interact with weakly bound electrons. The faster electrons used by TERRILL would be able to interact with a larger number of electrons from the atom periphery. An electron penetrating with only a few hundred volts would thus behave like a fast electron inside elements with low atomic number, for which TERRILL himself found low values of a. The constant a must therefore depend on V_p and decrease when V_p decreases. Experiments by COPELAND [214] concerning the penetration depth of primary electrons in thin platinum layers show that, below 1000 V, the range of the primary electrons tends to be more a linear function of V_p than a quadratic function; this is essentially the same as a decreasing value of a with decreasing V_p.

Experimental data are clearly inadequate. In principle, a differentiated determination of a and α is possible by measurements on composite targets; experiments have been made with composite targets consisting of a base metal with low δ, covered by a layer with high δ, and conversely (COPELAND [214], BRUINING [5]). TRUELL's [277] experiments are of interest in the same connection. KNOLL, HACHENBERG and RANDMER [289] have investigated layers of KCl; they came

* H. M. TERRILL; *Phys. Rev.*, **22**, 161, 1922.
† A. BECKER; *Ann. Physik, Lpz.*, **2**, 249, 1929.
‡ A. PARTSCH and W. HALLWACHS; *Ann. Physik, Lpz.*, **41**, 247, 1913.

to the conclusion that the secondary electrons in a compound like KCl are much less absorbed than in metals; with insulating compounds, however, disturbing phenomena such as surface charge effects, decomposition (Chapter 4) and induced conductivity (Chapter 10) make the experimental technique still more complicated.

6.3. SECONDARY ELECTRON EMISSION FOR LOW AND HIGH V_p

(a) *Low* V_p. If $V_p \simeq 10$ V, a simplified expression can be written for the function $F(r)$. Experimental evidence indicates that $a \simeq 10^{12}\mathrm{V}^2\,\mathrm{cm}^{-1}$ and of $\alpha \simeq 10^6\,\mathrm{cm}^{-1}$. Thus $r \ll 1$ and $F(r) \simeq r$. Instead of eq. (6.5) one obtains

$$i_s = \kappa i_p e V_p. \qquad (6.9)$$

This result could have been expected, since the depth of penetration of the primary electrons and thus the depth of origination of the

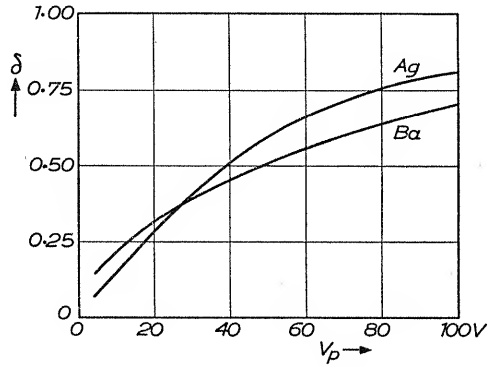

Fig. 6.3. Secondary yields of Ag and Ba, for slow primary electrons [169]

secondaries are negligibly small. Hence the yield is determined by the factor κ only.

Measurements in this range of V_p are scarce, but an example is shown in fig. 6.3. They show that a metal with a low work-function (barium) gives a higher yield than a metal with a higher work-function (silver).* Thus with low V_p a certain similarity between photo-electric emission and secondary emission is observed.

* The curves represent the true secondary emission yield since a correction has been made for elastic reflection of the primary electrons.

(b) *High* V_p. If $V_p \simeq 10$ kV, $F(r)$ can be approximated by $1/2r$. Hence eq. (6.5) becomes

$$i_s = \kappa i_p \frac{a}{2\alpha e V_p} \tag{6.10}$$

Thus i_s decreases with increasing V_p, and is proportional to a/α. Table 3.2 shows that a appears to be dominant over α, since the yield increases with the density. The correctness of our considera-

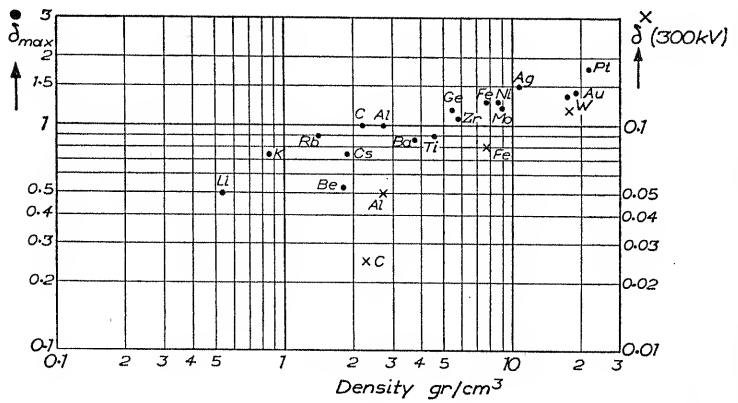

Fig. 6.4. Maximum secondary emission of metals, versus density; × δ for $V_p = 300$ kV; • δ_{max}

tions is however doubtful in this energy range, for the reasons given in the preceding section.

(c) δ_{max}. From (6.7) it follows that $i_{s\,max} = \kappa i_p \sqrt{\frac{a}{\alpha}} F(0{\cdot}92)$. Thus δ_{max} is proportional to $\kappa\sqrt{\frac{a}{\alpha}}$. Experiments show indeed (fig. 6.4) that δ_{max} has a tendency to be proportional to the square root of the density (cf. K. G. McKAY [6], where δ_{max} is plotted as a function of the work-function).

The above considerations show how far the "phenomenological" approach goes at present. It leads to a rough description of the secondary emission yield as a function of the primary energy. It even makes possible a comparison between the yields of different metals.

6.4. SOME OTHER THEORIES OF SECONDARY ELECTRON EMISSION

Several authors have developed theories of secondary emission on the basis of a model.

First mention will be given to the theories of KADYSCHEVITZ [219] and later BAROODY [315], who used the Sommerfeld model and calculated the energy transfer to the conduction electrons along classical lines. BAROODY did not follow his model consistently; he could have derived the relation between penetration depth and energy of the primary electron, but instead assumed WHIDDINGTON'S law. Nevertheless BAROODY made an important contribution to existing theories, which has already been discussed in section 6.1 (eq. 6.8).

Quantum-mechanical theories have been developed by FRÖHLICH [87], WOOLDRIDGE [212] and DEKKER and VAN DER ZIEL [323]. These authors used the Bloch model for metals and considered the collision of a single primary electron with a single metal electron. They paid special attention to the direction of the momentum transferred; thus in their model the emission of entirely free electrons is impossible, since this would be contrary to the law of conservation of momentum. We shall give here the principle of their calculations, followed by a discussion of the consequences.

The electrons in the substance satisfy the equation of SCHRÖDINGER:

$$\Delta\psi - \frac{8\pi^2 m}{h^2}[E - V(\mathbf{r})]\psi = 0 \tag{6.11}$$

in which the potential $V(\mathbf{r})$ is a function of the coordinates x, y and z, periodical with the lattice; $\mathbf{r}$ is a vector with components $\mathbf{x}$, $\mathbf{y}$ and $\mathbf{z}$.

Solutions of (6.11) exist for particular values of E, usually called E_k, when the function ψ takes the form

$$\psi_k = U_k(\mathbf{r})e^{i(\mathbf{k}\cdot\mathbf{r})} \tag{6.12}$$

$U_k(\mathbf{r})$ has the period of the lattice. Its deviations from its average value determine the binding of the lattice electron. The vector $\mathbf{k}$ is called the wave vector; its components are determined by three quantum numbers k_x, k_y and k_z, each of them having discrete values. Any set of k_x, k_y and k_z determines the components of the momentum of an electron.

These discrete values of k_x, k_y and k_z imply that the energy spectrum is discontinuous. It consists of bands, each band being split up into a number of levels. The number of levels is equal to N^3 where N is the number of elementary cells. In a lattice of cubic structure each component of $\mathbf{k}$ possesses N values, thus $\mathbf{k}$ itself has N^3 values. These N values of $\mathbf{k}$ are between $n\pi/a$ and $(n+1)\pi/a$, n being an integer characterizing a single band and a the lattice constant. If the "edge" of the band is passed, the energy "jumps", so that another band is reached. Fig. 6.5 shows the energy spectrum for one dimension. As

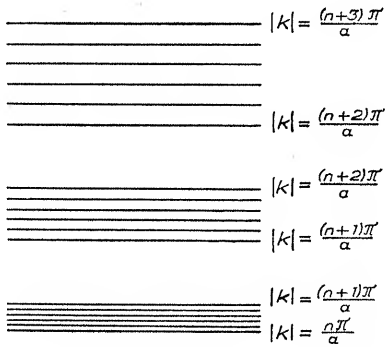

Fig. 6.5. Energy levels of electrons in a solid (one dimensional)

n increases the bands widen, and the "prohibited" areas become narrower. In the three dimensional case the scheme is more complicated, since the bands may overlap each other.

For weakly bound electrons $U_k(\mathbf{r}) \simeq 1$: The momentum $\mathbf{p}$ of the electrons can be written $\mathbf{p} \simeq h\mathbf{k}/2\pi$ and the energy $E \simeq h^2|\mathbf{k}|^2/2\pi m$.

According to WOOLDRIDGE the wave function of the primary electron is represented by $\psi_k = e^{i(\vec{\mathbf{k}} \cdot \vec{\mathbf{r}})}$. He assumes that its velocity is so high that it moves through the lattice as a free electron.

When the two electrons in positions $\mathbf{r}$, $\mathbf{R}$ interact, the perturbation potential is the Coulomb energy $e^2/|\mathbf{r} - \mathbf{R}|$. The probability of the transition of this two electron system from the state corresponding to the wave numbers $\mathbf{k}$, $\mathbf{K}$ to the state $\mathbf{k}'$, $\mathbf{K}'$ can be determined with the aid of perturbation calculus. This probability differs from zero if

(1) $$\mathbf{k} + \mathbf{K} - \mathbf{k}' - \mathbf{K}' + \frac{2\pi\rho}{a} = 0 \qquad (6.12)$$

ρ being a vector with integer components; and

(2) The total energy of the particles before and after interaction is the same. With a low binding energy this condition leads to

$$|\mathbf{k}|^2 + |\mathbf{K}|^2 - |\mathbf{k}'|^2 - |\mathbf{K}'|^2 = 0 \qquad (6.13)$$

Equation (6.12) is the law of the conservation of momentum. It differs from the expression for free electrons by the additional term $2\pi\rho/a$, which allows the vectors $\mathbf{k}'$ and $\mathbf{K}'$ to be reversed in direction, meaning that the secondary electron can be expelled from the surface. Physically it means that a reflection in a lattice plane is necessary to make emission possible. WOOLDRIDGE shows that these transitions will most probably occur if

$$\mathbf{k}' \simeq \mathbf{k} + \frac{2\pi\vec{\rho}}{a}, \text{ where } |\rho| = 1.$$

A lattice electron in this case absorbs the energy E_0 from a primary electron, where

$$E_0 = \frac{h^2}{m\pi^2}\left(\frac{2\pi}{a}\right)^2. \qquad (6.14)$$

In order to expel a secondary electron, the energy of a primary electron eV_p has thus to fulfil the following condition:

$$eV_p > E_0 - e\varphi, \qquad (6.15)$$

φ being the work-function. If V_p were smaller than this the primary electron would fall back to an already occupied level, which is impossible, by the Pauli principle. If $E_0 \simeq 25$ eV and $\varphi \sim 5$ V (silver) no secondary emission is possible while $V_p < 20$ V. The most serious objection to this theory is that the interaction of only two electrons is considered. In reality more electrons will be involved at the same time, a problem until now impossible to solve. One should also bear in mind that the interaction of primary electrons with valence electrons only is considered.

The agreement between theory and experiment is somewhat doubtful. The shape of the theoretical δ vs. V_p curve is in reasonable agreement with experimental results. However, on the other hand some experimental results are *not* in concordance with the theoretical predictions. There is for example no definite experimental evidence, that true secondary electron emission starts after V_p has exceeded a certain value. There are authors who have indicated such a limit (BECKER [39, 40], HAWORTH [125]); in other articles [61],

however, no limit could be observed.* Due to lack of information concerning the lattice fields the absolute magnitude of the secondary emission cannot be closely predicted. Similarly the energy distribution of the emitted secondary electrons cannot be accurately predicted without a detailed knowledge of the scattering and absorption processes, which affect the "true secondary electrons".

6.5. TEMPERATURE DEPENDENCE OF SECONDARY ELECTRON EMISSION

Many investigators have found the secondary electron yield of metals to be completely or almost independent of the temperature. This can be understood since the energies of the secondary electrons are large compared with kT, where k is BOLTZMANN's constant and T the absolute temperature. The energies of conduction electrons, on the contrary, for example, are smaller than kT, and conductivity depends strongly on temperature.

With compounds the situation is more complicated. Secondary electron yield may be temperature dependent because the surface charge can be removed or increased by a change of temperature; and this can cause a change of the secondary electron emission, as we saw in Chapter 4.

6.6. SECONDARY EMISSION-YIELD OF METALS AND COMPOUNDS [198]

In Chapter 4 we saw that simple compounds of the alkali and alkaline earth metals have a high secondary emission yield, but that semi-conductors—most of which are derived from metals with a high ionization energy—and the remaining metals, show a low yield ($\delta \simeq 1$). In this chapter we shall try to explain the difference between these two groups of substances, by using a simple method of representation. The method lays no claims to exactness and its correctness must be tested by still more experimental data.

We shall consider how the primary electrons may lose their energy in the substance. In compounds with high δ, generally insulators, the energy bands are either occupied entirely or not at

* This limit can, however, be observed with certainty with some metal compounds, as alkali halides; cf. 6.6.

all. A primary electron can thus only transfer its energy by bringing an electron from an occupied band to the next unoccupied band. We have to determine the probability that the excited electron will leave the substance. Now we may imagine two kinds of compounds:

A. The unoccupied band is at such a level that the electron is able to leave the substance without any additional energy.

B. The unoccupied band is too low, and the excited electrons cannot leave the substance without additional energy.

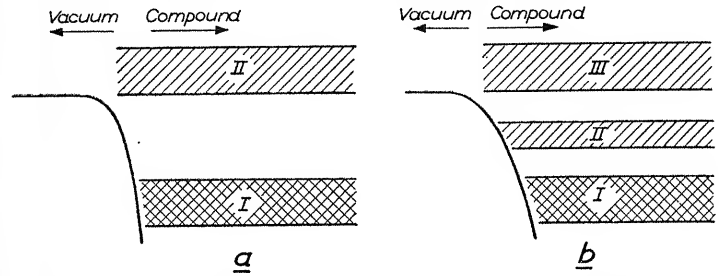

Fig. 6.6. Energy diagram of a substance, (a) with high δ, (b) with low δ

Fig. 6.6a and b shows an energy diagram. Band I is the occupied band (indicated by cross shading), the unoccupied bands II and III are indicated by single shading. Fig. 6a represents a substance with a high secondary emission yield, according to A. Fig. 6.6b, however, is for a substance with lower yield; in this case the primary electron loses its energy by transferring the lattice electrons from band I into band II, from where they cannot leave the substance, emission is only possible after transfer into band III. Thus in fig.6.6b, only a fraction of the energy of the primary electrons will contribute to secondary emission. Some experimental data support this representation. It has, for example, been shown by FLEISCHMANN* that light of the longest wavelength absorbed by KBr is able to expel electrons from the crystal. MOTT† has calculated for NaCl, KCl, and KBr the amount of energy necessary for electrons in the lowest level of band II to be emitted. This energy is not zero (as was suggested by FLEISCHMANN's experiments) but is only one tenth or less of the energy difference between the two bands.

* R. FLEISCHMANN; *Z. Phys.*, **84**, 717, 1933.
† N. F. MOTT; *Trans. Faraday Soc.*, **34**, 500, 1938. J. H. DE BOER; *Elektronenemission und Adsorptionserscheinungen* p. 182, Leipzig 1937.

An interesting example is the well known photo-cathode material, antimony caesium ($SbCs_3$). It has a high photo-electric yield (one photo-electron for ten absorbed quanta in the maximum of the absorption band at 3 eV. Now a rough estimate of the secondary emission yield can be made from the photo-electric yield. About 50 electrons can be excited by a primary electron of 150 eV. If the same percentage of these is emitted as if they were photo-electrons δ can be expected to be about 5; a figure of 4·5 has been found in fact by experimentation [236]. Thus $SbCs_3$ can be classified with the substances in type A; it differs however from the alkali halides in that the width of the energy band is much smaller.

With semi-conductors the situation is different. For Cu_2O $\delta \simeq 1$ and the work-function is 5·4 eV* but the maximum of the absorption band is found at the equivalent of 2 eV. According to experimental data the scheme of fig. 6.6b seems likewise to be valid for MoS_2.†

Metals present a more complicated situation. The energy bands are only partially filled; and occupied and unoccupied bands may overlap each other. According to the theories mentioned so far only transitions from one band into the adjacent band are possible. More accurate calculations are desirable to determine the minimum energy needed for such a transition. Experimentally acquired information for the minimum energy can be obtained from RUDBERG's data [131] by taking the distance between the maximum R and the next maximum of fig. 1.3. The table gives the results for gold, copper and silver with the corresponding work function:

	Distance between maxima in eV	*Work function* (eV)
Cu	4·2	4·30
Ag	4·0	4·74
Au	2·8	4·90

We thus see that for metals the evidence obtained from experimental data is not quite satisfactory for the support of the supposition concerning the low yield of metals.

* R. FLEISCHMANN; *Ann. Physik, Lpz.*, **5**, 73, 1930.
† J. H. DE BOER and W. CH. VAN GEEL; *Physica,'s Grav.*, **2**, 286, 1935.

6.7. EXCITATION OF ELECTRONS IN SOLIDS BY ELECTRON IMPACT

Several attempts have been made to demonstrate the presence of excitation levels in solids by electron impact. In the case of metals a superfine structure in the δ-V_p curve was observed by a number of investigators; but other investigators later proved this fine structure to be caused by adsorbed gas atoms and not due to a property of the substance itself. RUDBERG, however, using another technique has been able to measure excitation levels in metals.

6.7.1. Rudberg-Slater Experiments [131, 132].

The method used by RUDBERG is essentially a very accurate measurement of the energy loss of electrons re-emitted by the metal. These are electrons which cause the maximum U in the energy distribution curve shown in fig. 1.3. The maximum R is caused by elastically reflected primary electrons, so the distance between the maxima U and R is independent of the energy of the primary electrons. Evidently the maximum U represents primary electrons that have suffered the loss of a certain amount of energy. In fig. 6.7 the curves for Cu, Ag, Au are given on an enlarged scale, on which the maxima R are too high to be drawn. Each metal shows its own structure. All the metals show a deep minimum between the maxima U and R; this phenomenon has been observed by many authors. It can be explained by quantum mechanics.

RUDBERG and SLATER have investigated which transition of the lattice electrons corresponds with the observed amount of energy lost by the primary electrons. They obtain the same result as WOOLDRIDGE, viz. that the most probable difference in wave number before and after the interaction is $2\pi n/a$, where a is the lattice constant and n an integer. The minimum between R and U explains quite satisfactorily why electrons with an energy of some 100 eV cannot lose an arbitrary, small amount of energy. The theory goes further and shows that a comparison is possible of the spectrum of energy loss by electrons with the optical absorption spectrum. It is found for gold that these spectra have their maxima at the same $h\nu$. No correspondence has been found with copper or silver, but according to the authors this is due to an inaccuracy in the absorption spectrum.

Similar curves of energy loss have been measured for CaO and BaO. Their minimum is much wider than for metals. Thus the minimum energy which can be absorbed by electrons in these compounds is greater than in the case of metals. This agrees with the general experience that these compounds are transparent in the visible spectrum and opaque in the ultraviolet.

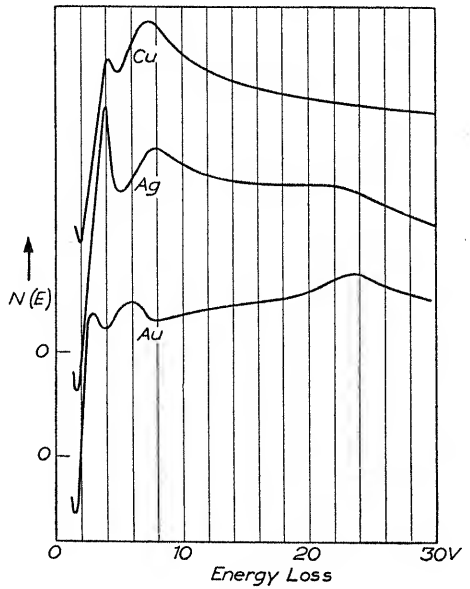

Fig. 6.7. Inelastic scattering of primary electrons by gold, silver and copper; according to RUDBERG

When considering RUDBERG's interpretation of the results, one must bear in mind that the interaction takes place in the four superficial atom layers. Thus the levels as observed in this way may not be representative for the lattice in the interior of the metal.

6.7.2. Experiments of Hilsch and Krenzien [90, 157].

Very convincing experiments have been carried out on evaporated layers of some alkali halides by HILSCH and KRENZIEN. HILSCH measured the secondary emission yield of NaCl, KCl, KI, LiF, NaF and CaF_2 for low values of V_p. The results are shown in fig. 6.8. At a certain V_p, marked with an arrow, the curves drop. Table 6.1 confirms that the value V_p, where δ drops, corresponds exactly with the limit of the transparency. Another transition, not essential

for secondary emission, is indicated for some substances by a second arrow.

Crystals of this kind are known to be entirely transparent for light of wavelengths longer than the limit given in Table 6.1. The agreement occurs in spite of the fact that electrons with an energy

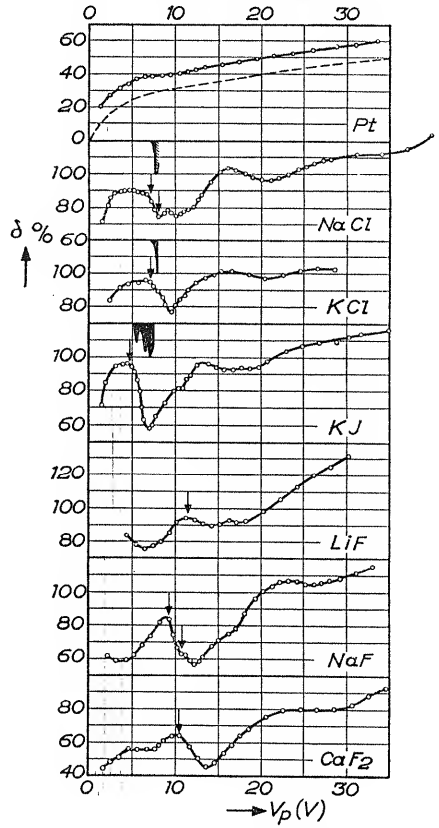

Fig. 6.8. Drop in the elastic reflection of electrons from layers of alkali halides. The position of the arrow corresponds to the long-wave side of the absorption band. According to HILSCH

below the values given in the first column of the table are not able to lose any energy by electron impact. HILSCH found in fact that such slow electrons either only penetrate into the crystal or are reflected elastically. When their energy exceeds that corresponding to the limit of transparency, the emission of slower electrons is

observed; thus true secondary emission has started or else the primary electrons have lost a fraction of their energy.

Electron transitions of the kind shown in fig. 6.8 are transitions of the outer electrons of the negative ions to the next unoccupied energy band. E.g. the $3p$-electrons of the negative chlorine ion are involved for NaCl, as was mentioned in Chapter 4.

TABLE 6.1

Compound	*Drop in yield starts at* V_p (V)	*Corresponding wavelength* (mμ)	*Limit of optical transparency* (mμ)
NaCl	7·3 ± 0·13	169 ± 3	170
KCl	7·1 ± 0·08	174 ± 2	175
KI	4·8 ± 0·15	257 ± 8	(260)
LiF	11·5 ± 0·15	107 ± 1·5	108
NaF	9·2 ± 0·08	134 ± 1·5	132
CaF_2	10·4 ± 0·05	119 ± 2	121·5

6.8. FLUCTUATIONS IN THE SECONDARY ELECTRON CURRENT

Hitherto the secondary emission yield has been indicated by the factor δ giving the average number of secondary electrons released by one primary electron. The question may arise what fractions of the primary electrons release no secondary electron, one secondary electron, two secondary electrons etc. This question cannot be answered completely; the measurement of the fluctuations of a secondary electron current gives, however, some information on this point.

Fluctuations in secondary electrons have been investigated by several authors; ALDOUS and CAMPBELL [107], L. HAYNER [111], PENNING and KRUITHOF [116], ZIEGLER [142, 143] and HAYNER and KURRELMEYER [152] all came to nearly the same result. Here we follow ZIEGLER's method.

It is well known that the electron current emitted by a thermionic cathode consists of a number of electrons with charge e emitted at random and independently of each other. Such a current therefore shows fluctuations in time. Calling the instantaneous current I, the mean current i and the frequency range in which the measurements are carried out $\Delta\nu$, their relationship

can be written

$$\overline{(I-i)^2} = 2ei\Delta\nu. \tag{6.16}$$

In order to derive an analogous relation for secondary emission, we assume that a fraction β_0 of the primary electrons releases 0 secondary electrons, a fraction β_1 one secondary electron etc. Thus

$$\sum_{n=0}^{\infty} \beta_n = 1, \tag{6.17}$$

$$i_p \sum_{n=0}^{\infty} n\beta_n = i_s. \tag{6.18}$$

The secondary electrons that are emitted in groups of n give a contribution to i_s which is subject to the same fluctuations as a group of particles each having a charge ne. For such a group we can write (by eq. 6.16).

$$\overline{(I_{ne} - i_{ne})^2} = 2nei_{ne}\Delta\nu = 2n^2e\beta_n i_p\Delta\nu.$$

The square of the fluctuations of the total secondary electron current is found by adding the squares of the fluctuations of the conglomerates. Hence

$$\overline{(I_s - i_s)^2} = \sum_{n=0}^{\infty} \overline{(I_{ne} - i_{ne})^2} = \sum_{n=0}^{\infty} 2n^2\beta_n ei_p\Delta\nu \tag{6.19}$$

$\overline{(I_s - i_s)^2}$ can be measured. There are only three equations (6.17, 6.18 and 6.19) to determine the fractions β, which would suffice only if n cannot exceed 2. A case can be imagined where a primary electron can release at the most two secondary electrons. In NaCl, where an energy of 7·3 eV is necessary for one secondary electron, not more than two electrons could be released by a 20 V primary electron.

For those cases where n exceeds 2, there is a way of indicating what values of n are to be expected.

Let us consider the quotient

$$\frac{\sum_{n=0}^{\infty} n^2\beta_n}{\sum_{n=0}^{\infty} n\beta_n} = q \tag{6.20}$$

which can be determined by measurement. Equation (6.20) may

be written as

$$\sum_{n=0}^{\infty} n^2\beta_n = q \sum_{0}^{\infty} n\beta_n$$

or

$$\sum_{n=0}^{n_q-1} n^2\beta_n + \sum_{n=n_q}^{\infty} n^2\beta_n = q \sum_{n=0}^{n_q-1} n\beta_n + q \sum_{n=n_q}^{\infty} n\beta_n \qquad (6.21)$$

in which n_q is the first integer exceeding q, i.e. $n_q > q > n_q - 1$; and hence

$$q \sum_{n=0}^{n_q-1} n\beta_n > \sum_{n=0}^{n_q-1} n^2\beta_n.$$

It follows from 6.21 that $\sum_{n=n_q}^{\infty} n^2\beta_n \neq 0$, which means that there are certainly primary electrons, which have released n_q secondary electrons.

In this way it has been found that, in a barium oxide layer, conglomerates of 10 secondary electrons are emitted, whereas the mean value δ is equal to 5.

An application of this theory will be given with the description of the electron multiplier (Chapter 8).

7

THEORY OF SECONDARY ELECTRON EMISSION; DISCUSSION OF SOME PROPERTIES OF SECONDARY ELECTRONS

7.1. ANGULAR DISTRIBUTION OF SECONDARY ELECTRONS

From recent investigations carried out by JONKER on the angular distribution of secondary electrons some insight can be gained into

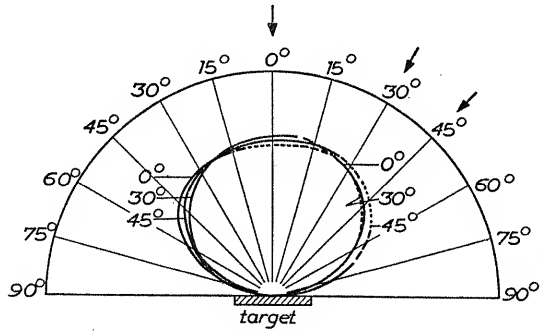

Fig. 7.1. Angular distribution of secondary electrons (5–15 eV) from polycrystalline nickel (V_p = 100 V); according to JONKER [321]

the behaviour of secondary electrons inside the material. One of JONKER's [321] most outstanding results is that the angular distribution of secondary electrons (i.e. with an energy up to half the energy of the primaries) is approximately* a cosine distribution and is *nearly independent of the angle of incidence of the primary electrons*.†

As we noted in Section 6.1, the secondaries are absorbed and scattered in the material, but in order to escape they must clear

* Approximately, since there is an indication of a slightly preferred direction contrary to that of the primary electrons. This preference is especially noticeable, if V_p is of the order of 500 V.

† Observations made with polycrystalline nickel having a flat surface.

the surface barrier. Like BARODY [317] we consider two possibilities.

(1) We suppose that the mean free path for scattering, l, is much smaller than the mean free path for absorption, λ, thus $l \ll \lambda$. This means that the secondary electrons reach the surface by a diffusion process. The angular distribution at the surface before

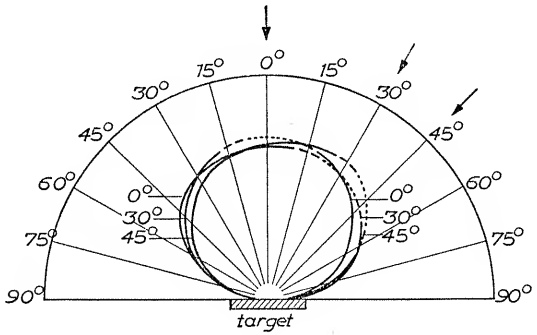

Fig. 7.2. Angular distribution of fast "secondary" electrons (45–55 eV) from polycrystalline nickel ($V_p = 100$ V) according to JONKER [321]

emission is then isotropic, resulting in an approximate cosine distribution outside, brought about by the action of the surface barrier.

(2) Another possibility is $l \gg \lambda$. In this case absorption is dominant and only a few elastic collisions take place. According to JONKER [324] the result is again an approximate cosine distribution. He assumes that the angular distribution at the point of origin is isotropic. Owing to absorption it becomes an approximate cosine distribution at the surface, but this is not altered by the action of the surface barrier.

Thus angular distribution measurements alone cannot give a definite answer to the question which of the two alternatives is correct. Other experiments, however, can give more definite information. The experiments of KATZ [175], mentioned in Chapter 3, indicate that slow electrons having pierced a silver layer about 0·15 μ thick still retain their original energy and suffer little deviation; yet a considerable fraction of the impinging electron gets lost due to absorption. This is evidence in favour of the conception $l \gg \lambda$. Combining it with the observation that the angle of incidence of the primaries does not affect the angular distribution of the secondaries, one can conclude that the angular distribution of the

secondaries *at the point of origin is isotropic.* This conclusion is based on the assumption that the results of KATZ' experiments are correct. However, this can be doubted, in view of work carried out by WAS and TOL*; a further examination of the subject is advisable.

7.2. ANGULAR DISTRIBUTION OF REFLECTED PRIMARY ELECTRONS

The angular distribution curves measured for elastically scattered primary electrons are quite different from those of the true secondary electrons. An example is shown in fig. 7.3. Actually one has to

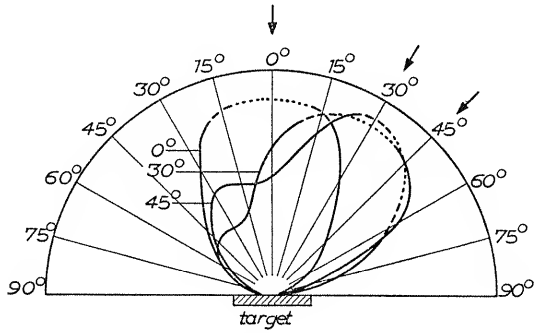

Fig. 7.3. Angular distribution of elastically and inelastically reflected electrons (80–100 eV) from polycrystalline nickel ($V_p = 100$ V); according to JONKER [321]

deal with a kind of Debye-Scherrer diagram made with 100 eV electrons. With polycrystalline targets composed of crystals of arbitrary orientation, one would expect a diagram with a shape independent of the angle of incidence and with an axis of symmetry coinciding with the direction of the primary beam. A curve giving a satisfactory approximation to this property has been found by JONKER [321], although with a sloping angle of incidence another "maximum" is added.

It is most likely that the reflected electrons contribute to the release of secondary electrons, as we supposed previously in Section 6.1. The slightly preferred direction of emission of the secondaries, mentioned in the preceding section, may be due to this effect.

---

* D. A. WAS and T. TOL; *Physica, 's Grav.*, **1**, 253, 1940.

7.3. THE INFLUENCE OF THE ANGLE OF INCIDENCE OF THE PRIMARY ELECTRONS ON THE SECONDARY EMISSION YIELD

Numerous investigators have determined the secondary emission yield with primary electrons under an oblique angle of incidence and have observed a larger yield than under normal incidence [28, 29, 41, 48, 120, 128, 160, 168, 182]. The reason for this increase is obvious. If primary electrons falling normally on the surface release secondary electrons at a mean depth x_m, when the angle of incidence changes to θ this depth becomes $x_m \cos\theta$ (fig. 7.4). Fewer secondary electrons are now absorbed before they reach the surface.

The experiments have to be carried out on a target with a smooth surface. With a rough surface the angle of incidence is not sufficiently well defined, so that the effect of a change of angle of incidence is hardly noticeable. It can be shown, for example, that the secondary emission yield of a soot layer hardly changes with varying angle of incidence, whereas the yield of a smooth nickel carbide layer shows a marked increase with an increasing angle of incidence (fig. 7.5).

Other examples are shown in figs. 7.6 and 7.7. The former gives results for different metals compared with soot, by MÜLLER [160]. Fig. 7.7 shows results obtained with lithium for different values of V_p.

It is possible to estimate the depth of origin from the measured data [120]. If Δ is the number of secondary electrons, liberated inside the metal by the action of a primary electron, x_m the mean depth of origin and δ_θ and δ_0 the yield with angles of incidence of θ and θ_0 respectively, one may write

$$\delta_0 = \Delta e^{-\alpha x_m}$$

$$\delta_\theta = \Delta e^{-\alpha x_m \cos\theta}$$

so that

$$\alpha x_m = \frac{\ln \delta_\theta/\delta_0}{1 - \cos\theta}. \qquad (7.1)$$

The correctness of the method is supported by the fact that the estimates of αx_m are nearly independent of θ. Hence x_m can be calculated; for nickel, using BECKER's value* for $\alpha = 1{\cdot}5 \times 10^6\,\mathrm{cm}^{-1}$, we find $x_m \simeq 30$ Å.

* A. BECKER; *Ann. Phys., Lpz.*, **2**, 249, 1929.

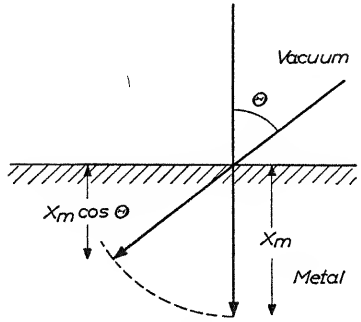

Fig. 7.4

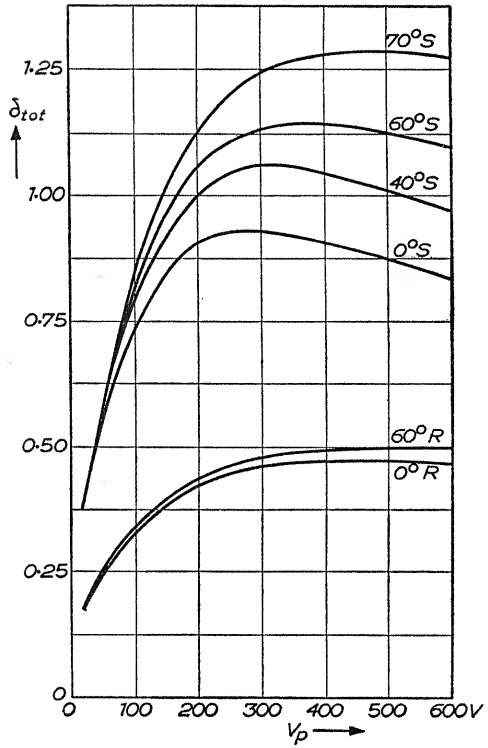

Fig. 7.5. Secondary emission yield versus V_p for different angles of incidence of the primary electrons; S smooth surface (nickel carbide) R rough surface (soot) [120]

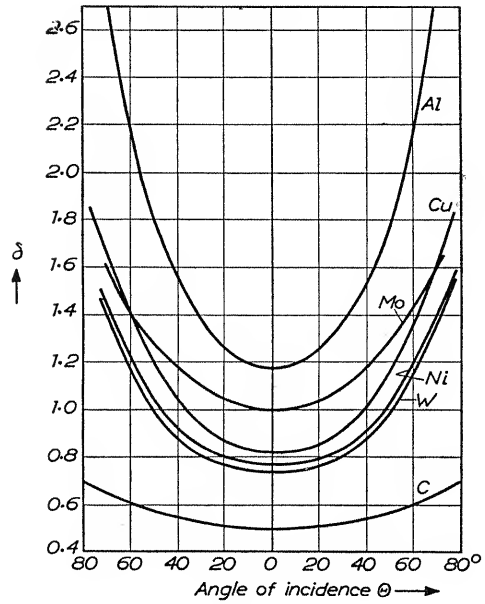

Fig. 7.6. Secondary emission yield versus angle of incidence of the primary electrons according to MÜLLER [160]

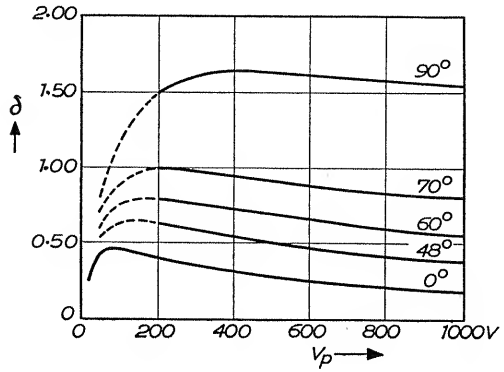

Fig. 7.7. Secondary emission yield versus V_p for different angles of incidence for lithium [168]

Formula (7.1) may also serve to calculate δ_{90}, the secondary emission yield in the case of a primary beam "falling" parallel to the surface. Absorption phenomena are eliminated in this way and one would not expect δ_{90} to show a maximum.

The experimental results with lithium however show a maximum in the δ_{90} curve, as in all the others (fig. 7.7). This unexpected result has a simple explanation (fig. 7.8). A primary electron

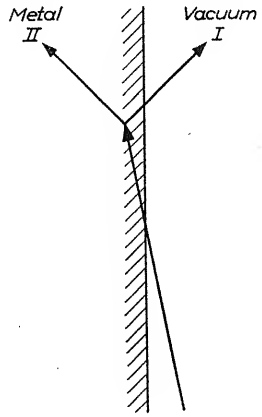

Fig. 7.8

impinging on the surface at a large angle of incidence may follow path II and remain inside the substance, or it may be scattered along path I and leave the substance. In the latter case it has only lost a fraction of its energy. Thus the observed yield with a large angle of incidence is too small, owing to losses which do not exist with normal incidence.

7.4. VALUE OF $V_{p\max}$ WITH VARYING ANGLE OF INCIDENCE OF THE PRIMARY ELECTRONS

In the preceding section we found it was correct to assume that the fraction of secondary electrons absorbed was $e^{-\alpha x \cos\theta}$ when the primary electrons were incident at an angle θ. This means that the calculations given in 6.1 can be altered by putting $e^{-\alpha x \cos\theta}$ instead of $e^{-\alpha x}$. Thus equation (6.6) becomes

$$eV_{p\max}\sqrt{\frac{\alpha\cos\theta}{a}} = 0{\cdot}71. \qquad (7.2)$$

JONKER [324] has shown that according to experimental results $eV_{p\max}$ is in fact for many metals inversely proportional to $\sqrt{\cos\theta}$.

The δ versus V_p curves, measured with a different angle of incidence can also be plotted in the form of the universal curve as has been done in fig. 6.2. The curves appear to coincide exactly.

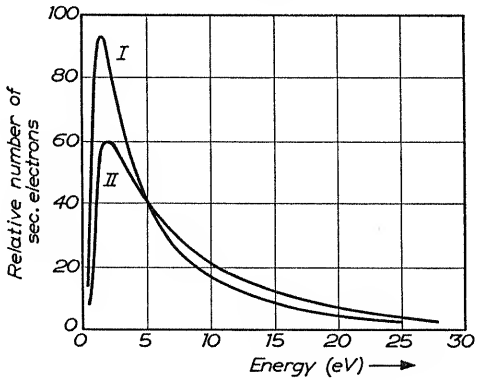

Fig. 7.9. Energy distribution of secondary electrons emitted by tantalum (I) and molybdenum (II) according to KOLLATH

7.5. ENERGY DISTRIBUTION OF SECONDARY ELECTRONS

The energy distribution of secondary electrons has been measured by several authors. In the preceding chapter we discussed the energy distribution of re-emitted primary electrons which have lost part of their energy by inelastic reflections. We shall here confine ourselves to the energy distribution of true secondary electrons.

The energy distribution has been determined both by the method of the retarding electric field and the method of deflection in a magnetic field, both of which were described in detail in Chapter 2. The magnetic method, in principle more accurate than the first one, gives the statistics of the energy distribution i.e. the number of electrons with an energy between E and $E + \mathrm{d}E$. One example [255] taken from the many available is shown in fig. 7.9. It appears that for any particular electrode an identical distribution curve is found over a large range of V_p, namely $20\ \mathrm{V} < V_p < 1000\ \mathrm{V}$. The curve shows a maximum at an energy of some volts; the absence of very slow electrons is remarkable.

This complete absence of slow elcctrons might be due to imperfections in the experimental technique, but this is improbable, because similar results have been obtained by several different authors. Again, it might be due to a much larger absorption loss for the very slow electrons. There are, however, various arguments against this supposition.

For example, the same energy distribution is found for values of V_p, where the losses due to absorption are negligibly small. Secondly, an artificial decrease of the work-function causes an increase in the secondary-emission yield not large, but quite distinct. With molybdenum δ increases by about 40%, if the work-function is lowered by 2 V through the adsorption of barium on the surface [196]. With silver the yield is increased by 75%, when the work-function of 4·7 V for a clean silver surface is lowered to about 1·4 V by the adsorption of caesium* [167]. For a final example, it has been found by Russian authors that the most probable energy decreases when the work-function is decreased [278].

It is well known from quantum mechanics that electrons approaching the metal-vacuum boundary from inside the metal have a certain probability of being reflected. The probability has been calculated by different authors for a variety of models, with the general result that the fraction of electrons reflected by the surface barrier increases if the energy of the electrons is decreased. Thus the origin of the maximum energy may be qualitatively explained as being due to internal reflection of very slow electrons at the surface.

KADYSCHEVITZ [294] has pointed out that this supposition is consistent with the results obtained for dielectrics. We saw in Section 6.5 that an electron, moving through the lattice of KBr at the lowest level of the empty energy band, can be emitted without additional energy. Thus there can be no surface barrier for these electrons. Several authors have found the most probable energy of emission for compounds with high yield to be in fact lower than that for metals. VUDINSKY [210a,b] has observed a maximum for NaCl below 1 eV, whereas for metals the maximum is between 2 and 5 V. (Cf. articles on the same subject by JOHNSON [302] and GEYER [272].)

* These figures about the change of the work-function are taken from J. H. DE BOER; *Electron Emission and Adsorption Phenomena*, Cambridge University Press 1935, p. 129.

7.6. ELIMINATION OF THE INFLUENCE OF THE WORK-FUNCTION AND ABSORPTION

From the preceding paragraphs it becomes clear that observation of the phenomena inside the secondary emitting substance is difficult if not impossible owing to the work-function and absorption. If their influence could be eliminated or reduced, more "inside" information could be obtained on the behaviour of the secondary electrons. Their influence can be reduced as follows.

I. In Section 6.1 the influence of the surface barrier on the angular distribution was briefly discussed. Since no action of a surface barrier on electrons emitted by alkali halides is observed, the shape of their angular distribution curve is of special interest.

II. In Section 6.3 we discussed a method intended to eliminate the losses due to absorption by estimating the yield δ_{90}, where δ_{90} is the secondary emission coefficient for primary electrons "impinging" parallel to the surface.

It is evident that measurements of δ for different angles of incidence of the primaries, carried out on a metal surface with the work-function lowered by the external adsorption of atoms of an alkali metal, could give some information on the "true" yield. This may lead to interesting results as is shown in the following example:

In the preceding section we showed that δ increases by about 75% if the work function of silver is lowered from 4·7 V to about 1·4 V. In the imaginary case of a "zero work-function" a yield of about twice the yield of a clean silver target can be expected (cf. Chapter 5). For $V_p = 250$ V this would be about 2·2. Assuming the absorption coefficient for silver to be the same as for nickel a yield δ_{90} of about 3·4 can be estimated for this "zero work-function" silver target. In the same way it can be calculated that $\delta_{90} \simeq 6$ for $V_p = 1000$ V.

For compounds with a high yield some data on δ_{90} are available, although these values may not be quite correct because of surface charges. For MgO and BaO, values for δ_{90} of 6·3 and 6·8 can be derived, much the same as for silver [168]. Thus, by eliminating the influence of surface barrier and absorption we may get an entirely different picture of the "true" yield of metals. At present it seems that the "true" yields of metals of high and low density (high and low work-function) are markedly different. More investigations are necessary. However, the above procedure cannot be

followed for electro-positive metals, since an artificial lowering of the work-function cannot be carried out. Perhaps the theories of Section 6.5 will provide an explanation of the low yields of these metals.

7.7. ELASTIC REFLECTION OF PRIMARY ELECTRONS

Fig. 7.10 shows the number of elastically reflected electrons per primary electron δ_{refl}, for silver, barium and barium oxide [169] for normal incidence of the primary electrons.

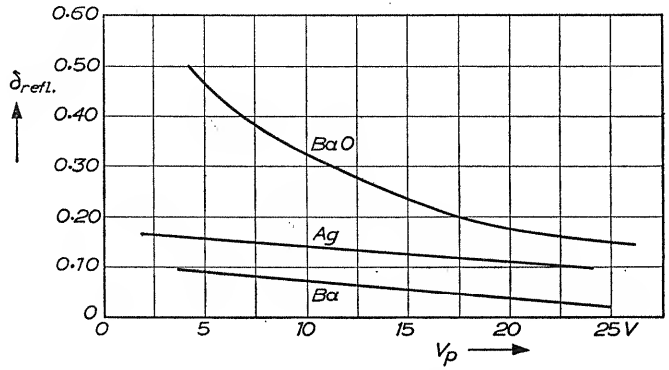

Fig. 7.10. Elastic reflection power δ_{refl} of barium oxide, barium and silver [169] for normal incidence of the primary electrons

For all three surfaces this quantity decreases with increasing value of V_p. Although silver reflects more electrons than barium, BaO reflects many more still. It is noteworthy that HILSCH (fig. 6.8, [89]) found that evaporated layers of the alkali and alkaline earth halides also possess a very high reflecting power. We have already seen that when V_p is below about 10 V the alkali halides show only elastic reflection: since no action of a surface barrier is observed (6.6), the primary electrons must all penetrate the lattice; thus the reflection must be due to elastic scattering in the lattice. With increasing V_p however the primary electron can transfer energy to the lattice electrons, so that the reflection power decreases. The high reflection power up to 90% observed by HILSCH may be due to the formation of a negative space charge, by which the electrons are pushed back. It would have been better to carry out measurements with a pulse technique.

The other curves in fig. 7.10 show the current of electrons reflected by silver and barium. This current will presumably consist largely of electrons reflected by the surface barrier. The problem of reflection of electrons against a surface barrier has been treated theoretically by MacColl* along quantum mechanical lines, on the assumption that the potential energy of an electron is constant in the interior of the metal, and taking account of the image force acting on an electron outside the metal. His results are qualitatively in agreement with the measured data, and with the result that the reflection power of a barium surface (with low work-function) is lower than that of silver (with high work-function). The measured reflection power is larger than the theoretical value, but this can be expected since in the experiment the reflected current includes electrons which are elastically reflected in the interior of the metal.

* L. A. MacColl; *Phys. Rev.*, **56**, 699, 1935.

8

APPLICATIONS OF ELECTRON MULTIPLICATION

In Chapter 4 we came across several substances with a high secondary emission yield ($\delta \simeq 10$). It is obvious that these substances make electron multiplication possible. Electron multipliers are widely used for the amplification of very small currents, photoelectric currents or secondary currents caused by bombardment with high energy particles. Electron multiplication has also proved to be useful in amplifier tubes. With the aid of substances with $\delta > 1$ it is possible to realize a tube with a negative resistance, which can be used as an oscillator.

Amplification by electron multiplication has generally the advantage of being a method, which is very simple compared with the "classical" method using d.c. amplifiers or amplifiers with a large band width. In this chapter we shall mainly consider the construction of different tubes and the requirements to be fulfilled for different applications.

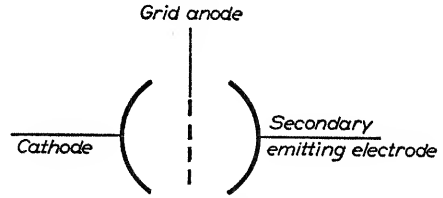

Fig. 8.1. Photo-electronic cell with single stage secondary emission amplification [331, 332]

8.1. PHOTOMULTIPLIERS

8.1.1. Photomultiplier with One Stage.

The simple multiplier in fig. 8.1 has been constructed by Penning and Kruithof [331] and Iams and Salzberg [332]. It consists of a photocathode, a secondary emitting electrode (usually called a "dynode") and a grid-shaped anode collecting the secondary electrons. Both photocathode and the secondary emitting surface are

provided with a silver-oxygen-caesium layer. The electrons emitted by the photocathode are partially caught by the anode, however the greater part will pass between the grid wires and hit the secondary emitting electrode; the secondary electrons released will be caught by the grid-anode. If the current from the photocathode is i_c and a fraction s is caught by the grid-anode, the total current to the grid-anode

$$i_a = si_c + \delta(1 - s)i_c.$$

The amplification i_a/i_c is therefore $s + \delta(1 - s)$.

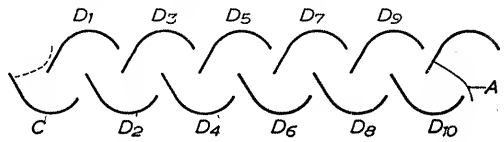

Fig. 8.2. Photomultiplier; C cathode, $D_1 \ldots D_{10}$ dynodes, A final anode. According to ZWORYKIN and RAJCHMAN [334]

8.1.2. Photomultipliers with more than One Stage

The amplification can be considerably enlarged by using several stages. If the mean secondary emission yield of one stage is δ, a gain of δ^n can be reached with n stages. The main requirement of a tube with several stages is that the secondary electrons released from one dynode must be drawn to the next one, without missing it.

This requirement has been met in different ways. ZWORYKIN and collaborators [333] have described several models. The first types were tubes with only two stages with electrostatic deflection, called the L and T types respectively. The next one was a system with magnetic deflection and electrostatic focussing. Adjustment of this tube in the magnetic field was rather critical and the system can be considered obsolete. A much simpler model was developed by ZWORYKIN and RAJCHMAN [334]. It forms the basic prototype of tubes now commercially available (fig. 8.2). The cathode is C, the different secondary emitting dynodes are $D_1 \ldots D_n$. The electrons follow zig-zag paths from C to D_1, from D_1 to D_2 etc. The shape of the dynodes can be chosen so as to obtain the desired focussing of the electrons from one dynode to the next. Typical paths and voltages are indicated in fig. 8.3.

The construction of a tube with the dynodes "lined up" as in fig. 8.2 is not very practical. In the R.C.A. tubes now available

the dynodes are arranged around a centre to economize space. Type 931A (fig. 8.4a) is provided with an internal photocathode

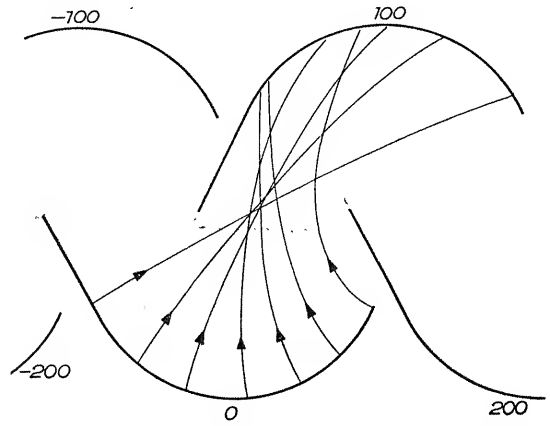

Fig. 8.3. Electron paths between dynodes in the multiplier of fig. 8.2.

and 9 dynodes. A newer type, 5819 (fig. 8.4b), contains a large photocathode on the glass envelope, from which the electrons are focussed on the first of a series of 10 dynodes. This type of multiplier has been especially designed for scintillation counting and will be referred to later [335].

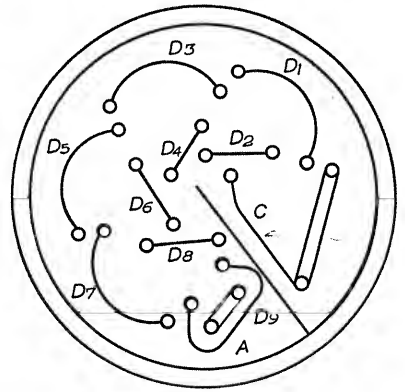

Fig. 8.4a. Photomultiplier (R.C.A. 931A), with internal photocathode [335]

There are also dynode configurations where no electrostatic focussing is applied [338]. The simplest form is the Weiss type,

where the dynodes are mesh screens with a superficial layer with high secondary emission yield. Electrons striking the wires of one

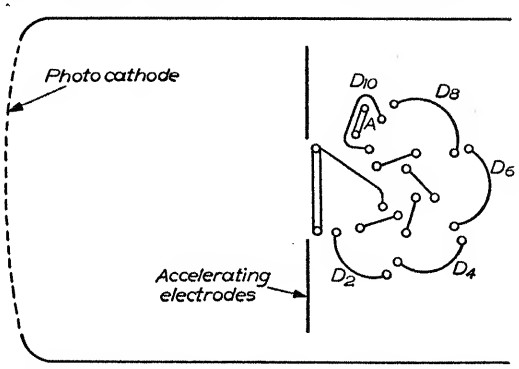

Fig. 8.4b. Photomultiplier (R.C.A. 5819), with large area photocathode on glass end of the tube; C cathode, D dynodes, A anode. According to MORTON [335]

screen produce secondary electrons, which are drawn through the screen towards the next mesh dynode. In some designs the mesh has a hollow shape in order to prevent the electrons diverging from the axis of the system (HARTMANN [336], LALLEMAND [337], fig. 8.5).

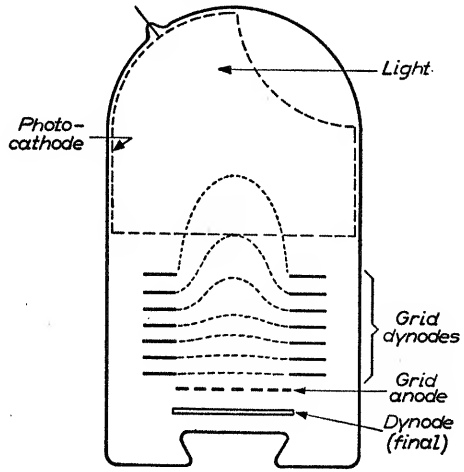

Fig. 8.5. Hollow shaped mesh screen photomultiplier; according to HARTMANN [336] and LALLEMAND [337]

Another type of unfocussed multiplier employs dynodes having a Venetian blind type of structure (E.M.I. fig. 8.6). Very fine screens

are interposed between the dynodes, the potential being equal to that of the next dynode in order to obtain the most favourable conditions for drawing away the released secondary electrons. For focussing, a hollow shaped mesh has certain advantages.

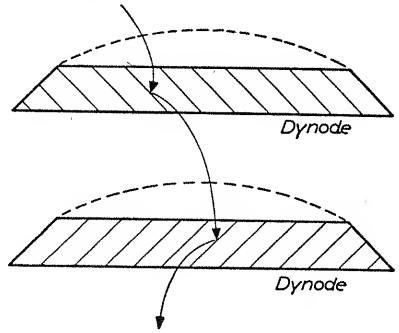

Fig. 8.6. Venetian blind type dynodes (E.M.I. photomultiplier) [338]

Table 8.1 summarizes the properties of different commercially available photomultipliers (according to G. A. MORTON [335]).

TABLE 8.1. COMMERCIAL PHOTOMULTIPLIERS

Tube type	RCA 931A	RCA 1P21	RCA 1P22	RCA 1P28	RCA 5819	EMI 4588	EMI 5060	EMI 5311
Cathode	in-ternal	in-ternal	in-ternal	in-ternal	tube end	in-ternal	tube end	tube end
area (cm^2)	1·9	1·9	1·9	1·9	11	20	0·7	5
peak response (Å)	4000	4000	4200	3400	4800	—	—	—
long wave cut-off	7000	7000	8000	7000	7000	—	—	—
sensitivity ($\mu A/L$)	10	40	3	15	40	40	20	20
number of stages	9	9	9	9	10	9	11	11
volts per stage	100	100	100	100	90	150	160	160
volts overall	1250	1250	1250	1250	1250	1500	—	—
average gain	10^6	$2{\cdot}10^6$	$2{\cdot}10^5$	$2{\cdot}10^5$	$6{\cdot}10^5$	$\sim 10^6$	10^7	10^7
Capacity: ($\mu\mu$F) collector to—								
last dynode	4	4	4	4	5	—	—	—
total structure	6·5	6·5	6·5	6·5	8	—	8	—
current collected								
max. average (μA)	1·0	0·1	1·0	2·5	0·75	1·0	1·0	1·0
dark current (μA)	0·25	0·1	0·25	—	0·05	0·03	0·01	0·1
length (cm)	9·4	9·4	9·4	9·4	15	25·4	22·3	22·3
diameter (cm)	3·4	3·4	3·4	3·4	5·7	5·1	5·1	5·1

8.1.3. Dark Current in Photomultipliers

Photomultipliers are especially appropriate for measuring very small photocurrents. The amount of "dark current" left, if there is no illumination on the photocathode, is therefore of major interest. The causes of dark current have been analysed by RAJCHMAN and ENGSTRÖM [339], who mention four different sources:

1. Insufficient insulation between the electrodes (giving leak-currents).
2. Ion currents; positive ions originating anywhere between the photocathode and final anode will be drawn towards the cathode, where secondary electrons will be released by ion bombardment.
3. Field emission at the electrodes due to the electrostatic field.
4. Thermionic emission from the photocathode.

1. The first component of the dark current can be avoided by carefully insulating the different leads to the electrodes and by an appropriate mounting of cathode and dynodes in the tube.

2. To avoid the second component requires a special shape of the dynodes. RAJCHMAN pointed out that a sufficient counter-measure is to prevent positive ions hitting the photocathode.

3. Field electron emission will be found at places with sharp edges etc. These should be avoided as much as possible. The potential difference between the dynodes must not exceed a certain value.

4. In most cases the most important component of the dark current will be the thermionic emission of the photocathode. It is well known that the long wave cut-off of the photoelectric emission band determines more or less the rate of thermionic emission. It can therefore be expected that this component is most disturbing in tubes where infra-red sensitive photocathodes are used. For this reason the blue sensitive antimony-caesium cathode is mostly used; still better is the lithium-antimony cathode which has its peak sensitivity even more towards the short-wave end of the spectrum [338].

A very useful method of avoiding thermionic emission is of course an appropriate cooling of the photocathode. It is also advisable to prepare the dynode surface so that it is not photo-emissive (TEVES [340]).

8.1.4. Fluctuations in the Output Current of a Photomultiplier.

For practical purposes it is of importance to know the fluctuations in the output current of a multiplier. We shall therefore derive the equation giving the current fluctuations using a method indicated by SHOCKLEY and PIERCE [342].

We saw in Chapter 6, p. 94, that the fluctuations in a current of secondary electrons is described by

$$\overline{\Delta i_s^2} = \overline{(I_s - i_s)^2} = 2ei_p\Delta\nu \sum_0^\infty n^2\beta_n \tag{8.1}$$

where I_s is the secondary emission current at a time t, i_s and i_p are respectively the mean secondary and primary current, e is the charge of the electron, $\Delta\nu$ is the frequency range used for the measurement and β_n the fraction of the primary electrons which release n secondary electrons.

By equation (6.16), $2ei_p\Delta\nu = \overline{(I_p - i_p)^2} = \overline{\Delta i_p^2}$. Writing $\sum_0^\infty n^2\beta_n = \overline{n^2}$, we may put equation (8.1) into the form

$$\overline{\Delta i_s^2} = \delta^2\overline{\Delta i_p^2} + 2ei_p(\overline{n^2} - \delta^2)\Delta\nu. \tag{8.2}$$

Equation (8.2) expresses the mean square of the fluctuations as consisting of two parts; the first part is due to the fluctuations of the primary current, and the second part is due to the fact that the primary electrons do not all release the same number of secondary electrons. If we write $\overline{n^2} - \delta^2 = b\delta^2$, (8.2) takes the form

$$\overline{\Delta i_s^2} = \delta^2\overline{\Delta i_p^2} + 2ei_s b\delta\Delta\nu. \tag{8.3}$$

The noise contribution of each dynode can be calculated with this formula. The total noise of the multiplier tube can be calculated if δ and b are assumed to be the same for all the dynodes. The result is

$$\overline{\Delta i^2_{\text{tot}}} = D^2\overline{\Delta i_p^2} + D^2b\overline{\Delta i_p^2}\frac{1 - 1/D}{1 - 1/\delta} \tag{8.4}$$

where D is the total gain of the multiplier.

From experimental results obtained by ZWORYKIN, MORTON and MALTER, b can be calculated to be about 0·25. This means that

only a fraction of the total noise is caused by the fact that not all the primary electrons release the same number of secondary electrons.

8.1.5. Uses of the Photomultiplier.

There are several applications where the photomultiplier has distinct advantages over the "classical" combination of a photo-cell with an amplifier. This is clearly illustrated when the signal-to-noise ratio is calculated for both systems; as an example [333] we shall determine the minimum current which can be amplified, when the signal-to-noise ratio may not be less than 5 and the frequency range is 10^6 c/s. Assuming that in the photocell-amplifier system the noise originates in the input resistance of $10^4\ \Omega$, the minimum current to the amplifier is 8×10^{-9} A. For the case of a photomultiplier, however, with $\delta = 5$ this minimum current is 4×10^{-11} A, which is lower by a factor of 200.

Another advantage of the photomultiplier is its linearity, provided that the output current is not limited by space charge, which means, for commercial multipliers, not exceeding about 1 mA. It is moreover a system which amplifies independently of frequency so long as this is below about 100 Mc/s. This upper limit is not determined by the transit time, since the transit time itself acts only as a constant delay, but by the spread in transit time of photoelectrons starting from different points on the photo-cathode at the same time. The problem has been analyzed by MORTON [335] for a nine-stage R.C.A. multiplier; the difference in transit time for the longest and shortest paths amounts to less than 6×10^{-9} sec, which is in fair agreement with frequency response measurements.

For these reasons the photomultiplier is used for amplification of light pulses in flying spot scanners, for the transmission of films by television. Electron multipliers are also used for sound film and telephone communication using modulated light. In astronomy a photomultiplier may be a useful instrument for the registration of a star passing the centre of a telescope. Astronomers consider it possible even to use the photomultiplier for photometry instead of photographic film [341].

For the measurement of extremely small amounts of light a special technique is necessary. Background currents should be reduced as much as possible; in order to reduce cold emission the potential difference between subsequent dynodes must be limited. According to equations (6.16) and (8.4) the signal-to-noise ratio

can be enlarged by using an amplification system with a limited band width.*

Using a chopped light source and analyser combined, with a band width of 1·8 c/s, ENGSTRÖM [339] was able to measure $5{\cdot}9 \times 10^{-10}$ lumen with a signal to noise ratio of 40 db at room temperature. This implies a limit of detectability of about 6×10^{-12} lumen. By reducing the temperature of the photocathode to liquid air temperatures (so that there is no thermionic emission) this lower limit can be reduced to about 6×10^{-14} lumen.

This illumination level corresponds with an emission of the photocathode of only a few electrons per second. Photomultipliers can thus be used as photon counting devices. In nuclear research photomultipliers are nowadays used as "scintillation" counters. For this special purpose tubes have been developed with a large size photocathode prepared on the glass wall of the tube. The cathode is brought into close contact with a fluorescent crystal which is excited by the α or β particles, the neutrons or γ quanta to be counted. It must be noted that equal amounts of light at the cathode do not result in equal pulses of the output current due to the statistical fluctuations in secondary emission yield throughout the stages of the tube. With scintillations of equal brightness, the pulses observed on the oscilloscope connected with the output of the multiplier are thus not equal in height. So there is a statistical distribution of secondary emission superimposed on any pulse height distribution originating from the light pulses at the input.

This can be illustrated by an example given by MORTON [335]. Suppose the crystal is bombarded with 0·6 MeV particles, and the crystal produces one photon for each 50 V of energy. Thus 12,000 photons are produced by each bombarding particle. Approximately $\frac{1}{3}$ of these reach the photocathode; if the latter has a sensitivity of 30μA per lumen, corresponding to a quantum efficiency of 6 per cent, 240 electrons will be released. Supposing that half of these, i.e. 120 on average, enter the multiplier, the standard deviation from this number can be taken as $\sqrt{120}$, i.e. 9 per cent of the average. MORTON has calculated that the "secondary emission" distribution increases this deviation by about 2·2 per cent. In other words the output pulse distribution will have an r.m.s. deviation of 11·2 per cent.

The advantage of the scintillation counter over the Geiger-Müller counter is that the pulse height obtained with the former can give

* At room temperature the noise includes fluctuations originating from both the thermionic and photoelectric current.

some information on the energy of the counted particles. Moreover the rapidity or "resolution" of the scintillation counter (10^{-8} sec) is much higher than that of the Geiger-Müller counter (10^{-4} sec). Hence it is logical to use the scintillation multiplier in combination with a fluorescent crystal with a very short decay time. As crystals with a decay time of the order of 0·1 or 0·01 μs (microsecond) have generally an emission band in the violet or the ultraviolet, it seems best to combine them with a photocathode with a peak response in the violet range, like antimony-caesium or antimony-lithium. Such cathodes have the important additional advantage of a low dark current.

8.1.6. Electron Multiplication in Image Converters.

An image converter is a tube in which the image of a photocathode is formed on a fluorescent screen by means of an electron optical lens. One use of image conversion, for example, is in the sniperscope; the photocathode is in this case sensitive to the infra-red, emitting photoelectrons from any places that are irradiated with infrared light. The phosphor on the fluorescent screen is one that has its emission band in the visible part of the spectrum, so that objects radiating in the infra-red are made visible.

In such a tube it may be advantageous to mount an electron multiplication system, especially for radiation of low intensity. The multiplication problem in this case is particularly difficult as an electron *picture* has to be imaged without distortion via several dynodes on to an anode.

Coeterier and Teves [344] provided a solution to this problem, which we shall not treat in detail. Much of the definition of the original "object" on the photocathode will unavoidably be lost, because the relatively high starting energies of the secondary electrons result in a considerable chromatic aberration. In the case of an infra-red sensitive photocathode at room temperature the "background" current will be amplified as well, so that no better contrast will be obtained. However, a brightness amplification may be useful for the convenience of the observer.

8.1.7. Multipliers Using a Secondary Emitting Cathode.

In all the preceding sections we have confined our discussion to multipliers with a photoemissive layer on the cathode. If high energy particles or high energy photons are to be counted, however,

a photocathode is not strictly necessary; secondary electrons are released from any metal, for instance, by the impact of α or β particles or γ rays. Several authors have described multipliers with a secondary emitting cathode. Allen [346, 347] has used such a multiplier for counting purposes in a mass spectrograph, Bay and Rann [345] for counting high energy photons. Recently other applications have been described by Stone.

An advantage of this kind of multiplier over those with a photocathode is that nearly all thermionic emission can be eliminated by using the silver beryllium alloy, see Chapter 4, p. 65, as a secondary emitter and by avoiding all caesium metal. A disadvantage is that the number of secondary electrons per incident particle may be far below unity, so that only a fraction of the incident particles are registered.

An important application of such a multiplier is found in the image orthicon (Chapter 10, p. 143), where the return beam, consisting of electrons of some 100 eV, is multiplied.

8.2. "DYNAMIC" ELECTRON MULTIPLIERS

The multipliers described in the preceding paragraph all use direct voltages between cathode and the dynodes. Another type of tube, described by Farnsworth [349], uses alternating voltages of very high frequency but has a simpler internal construction.

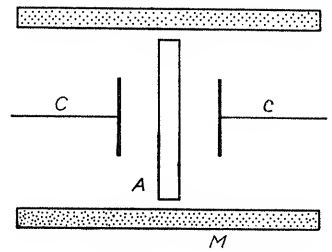

Fig. 8.7. Dynamic multiplier, according to Farnsworth [349]

Fig. 8.7 shows one of the constructions proposed by Farnsworth. It consists of two electrodes C and a cylindrical anode. The magnetic field of a coil M has to focus the secondary electrons released from one of the electrodes on to the other. Between the plates C an alternating voltage of very high frequency is applied, which accelerates the electrons from the first electrode on to the second; the

voltage is reversed as electrons are released from the second electrode, and these return accelerated to the first; and so on. The anode has such a potential as to draw a suitable proportion of the oscillating electrons to itself. The tube certainly has the advantage of simplicity, but the external circuits are necessarily rather complicated. Another disadvantage is that only a fraction of the photoelectrons are amplified, namely the electrons emitted within 32° of the optimum phase (HENNEBERG, ORTHUBER and STEUDEL [351]). If this system is used as a counting device, the quenching of the current requires special precautions. On the whole, it seems that the straightforward electron multiplier has distinct advantages over the "dynamic" type.

The internal construction of the tube we have just discussed is rather similar to that of a system which can be used as a manometer (F. M. PENNING; *Philips Techn. Rev.*, **11**, 116, 1949). This tube likewise consists of two electrodes C, both acting as cathodes, and a cylindrical anode. A similar magnetic field is used. The electrons released at the electrodes C are made to cover long distances before reaching the anode, so that their chance of hitting a gas molecule is great. Even at pressures of 10^{-5} mm a gas discharge can be developed, which opens the possibility of using this system as a manometer at extremely low pressures. The dimensions of the Farnsworth tube make it likely that an unwanted gas discharge will be excited within it.

8.3. AMPLIFIER TUBES WITH SECONDARY EMISSION AMPLIFICATION [352-355]

A surface with high secondary emission yield may also be useful in radio tubes with thermionic emitting cathodes. Fig. 8.8. shows the scheme. Basically such a tube consists of a cathode, a control grid, a secondary emitting dynode and a final anode. It can easily be shown that such a tube has a greater mutual conductance than a tube without secondary emission amplification using the same anode current. The cathode current can be expressed as

$$i_c = A(V_g + b)^p,$$

where A, b and p are constants. V_g is the potential difference between cathode and control grid. Without secondary emission amplification the mutual conductance is:

$$\frac{\mathrm{d}i_c}{\mathrm{d}V_g} = Ap(V_g + b)^{p-1} = A^{\frac{1}{p}}\, p\, i_c^{\frac{p-1}{p}}. \tag{8.6}$$

With secondary emission $i_a = \delta i_c$, so that

$$\frac{\mathrm{d}i_a}{\mathrm{d}V_g} = \delta^{1/p} A^{1/p}\, p\, i_a^{\frac{p-1}{p}}. \tag{8.7}$$

For the same anode current the mutual conductance is therefore increased by a factor $\delta^{1/p}$; e.g. if $\delta = 5$ and $p = 1{\cdot}6$ the mutual conductance is greater by a factor 2·6 than in a similar tube without secondary emission.

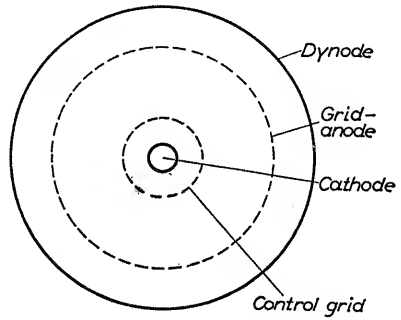

Fig. 8.8. Elementary construction of secondary emission amplifier tube

It is of importance that if secondary emission multiplication were used a higher mutual conductance would be obtained without higher input capacitance, which means that this type of tube would be useful for amplification in the high frequency range. However, the number of stages would be limited, since the construction would tend to be too complicated, and the total voltage to operate the tube to be too high. Moreover, it would be difficult to meet the requirement that contact potential differences and secondary emission yield of the dynodes must remain constant within narrow limits.

Several models of "secondary emission tubes" have been proposed. One of the simplest forms is a cylindrical construction, in which the final anode is a grid, and the dynode is a plate surrounding the internal structure (fig. 8.8). This system has the disadvantage that a fraction of the primary electrons emitted by the cathode C are caught by the grid anode and never hit the dynode, whereas the secondary electrons emitted by the dynode may pass through the openings between the wires of the grid anode, return and fall back to the dynode. Many investigations with this kind of construction have shown that barium atoms evaporating from the

oxide coated cathodes gradually cover the inner surface of the dynode so that the secondary emission yield decreases during its life. MUELLER [355] has shown that long life can be obtained by reducing the temperature of the cathode. According to unpublished data of VEENEMANS [354], caesium oxide can have a long life, provided the temperature of the dynode is below 180°C and an additional layer of finely divided nickel, capable of binding small quantities

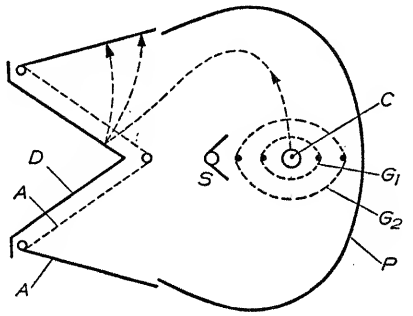

Fig. 8.9. Secondary emission tube; C cathode, G_1 control grid; G_2 screen grid; S shield; P plate; D dynode; A anode. According to JONKER and VAN OVERBEEK [353]

of caesium, is in the tube. During life the caesium-oxide is presumably replaced by barium oxide.

Both the above difficulties can be overcome by the construction illustrated in fig. 8.9, where the dynode is shielded from the cathode by a shield S. In such a tube the electrons emitted by the system [cathode C, control grid G_1 and screen grid G_2] reach the dynode D through the curved electric field formed by an additional plate P at cathode potential. The evaporating barium atoms, being neutral particles, travel in straight lines and cannot reach the dynode.

Fig. 8.10 shows the structure of a tube described by JONKER and VAN OVERBEEK [353], where the contamination of the dynode is only slight and the final anode is a plate, so that "oscillating" secondary electrons are avoided. Each of the two beams emanating from the cathode is split into two parts, one to the right and one to the left of the small ribbon shaped anode. They impinge on the inner wall of a gutter-like dynode.

There are many uses for "secondary emission tubes", but it would be going beyond the scope of this book to mention them all.

The interested reader can find a survey in a recent article written by VAN OVERBEEK [354].

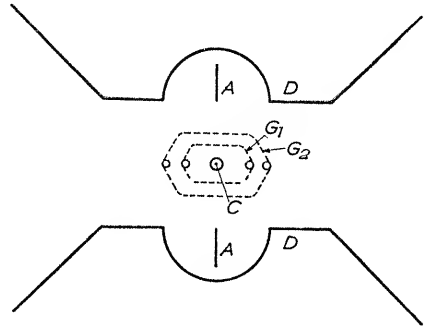

Fig. 8.10. Secondary emission tube, according to VAN OVERBEEK [354]

8.4. THE DYNATRON [356]

It was pointed out in Chapter 2 (fig. 2.8) that in a secondary emission tube the dynode current decreases as a function of the dynode voltage, if the latter is below the anode voltage. In this range the tube shows a negative resistance. By virtue of this negative resistance the tube can be used as an oscillator. In fig. 8.11 a circuit

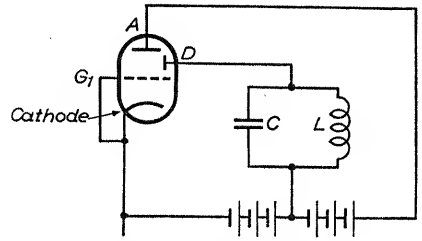

Fig. 8.11. Dynatron circuit

is shown where the dynode is connected with an inductance L and a capacitor C in parallel. If now the absolute value $|R|$ of the negative resistance is greater than the quotient L/Cr (r being the ohmic resistance of the coil) the damping of the system is negative and oscillations start. This type of oscillator is not often used since the amplitude of the oscillations depends on the secondary emission yield of the dynode surface, and no way has yet been found of keeping this suitably constant during its life.

Using a secondary emission tube with small interelectrode distances, DIEMER and JONKER [358] determined the upper frequency limit of a dynatron oscillator. They found this was 2400 Mc/sec; this means that if there is any time lag at all in the emission of secondary electrons from compounds it must be smaller than 3×10^{-11} sec. A time lag of the same order of magnitude has been found by GREENBLATT and MILLER [350].

8.5. CONTACT VALVES AND SWITCH VALVES [359, 360]

In telephone exchanges electrical contacts are nowadays generally established mechanically. Mechanical contacts are vulnerable if they are exposed to air and dust, are liable to wear, and always show a certain inertia. A low impedance all-electronic contact can be obtained with a tube with secondary emitting surfaces.

In order to explain the operation of such a contact tube we refer to the "dynatron" characteristic, mentioned in Chapter 2.

Let us assume that the dynode electrode is connected to a fixed voltage V_w, through a resistance R. We saw in Chapter 4 (fig. 4.1c) that the potential which the dynode takes up is determined by the intersection P of the dynatron characteristic and the straight line representing OHM's law (fig. 8.12). By choosing a suitable value

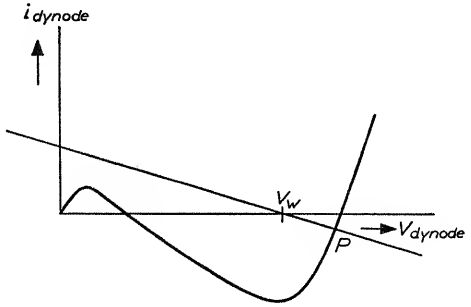

Fig. 8.12. Principle of potential stabilization in switch tube.

for R and by a proper geometry of the tube one can arrange that the dynode attains a potential V_D equal to the potential of the cathode collecting the secondary electrons. If the anode changes its potential, it is followed by the dynode, which means that a contact has been established between the two electrodes. Thus by switching on and off a primary current from the cathode, one

obtains a contact, without inertia, between the anode and dynode. Fig. 8.13 shows a practical application, where an incoming signal over the line L_1, connected with the anode, leaves the tube via the dynode, along the line L_2.

The above example makes use of a tube which makes contact unidirectionally. However, for many applications a bi-directional

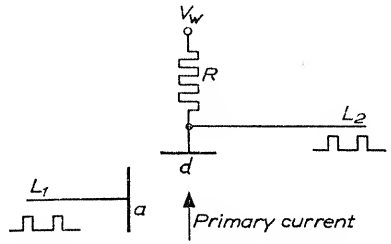

Fig. 8.13. Uni-directional switch tube; a anode, d dynode [359]

contact is required, in which case the electrodes d and a must be able to exchange roles. Fig. 8.14 shows a structure where this is arranged for, and where a signal may be passed from L_1 to L_2 just as well as in the reverse direction.

It is obvious that the internal resistance should be as small as possible, which means that the slope of the curve near the point of

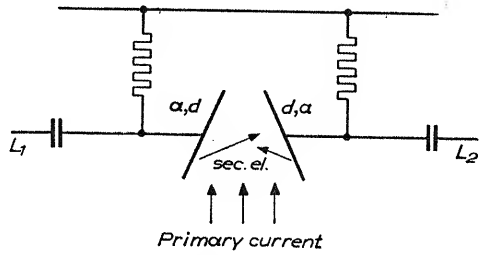

Fig. 8.14. Bi-directional switch tube. The electrodes d, a can both act as either dynode or anode [359]

intersection P (fig. 8.12) should be as steep as possible. Thus the construction of the electrodes in figs. 8.13 and 14 has to be such as to make the exchange of secondary electrons as efficient as possible. A high secondary emission yield is also favourable.

This principle of switching by means of secondary electron emission can be applied in different ways. Out of the many possible

examples we may mention a "selector" tube (fig. 8.15), where a number of electrodes n_1, n_2 . . . n_n (contacts) can be connected with an electrode r. The cathode c is the source of primary electrons; the electrodes e_1 and e_2 form a ribbon-shaped beam which is given

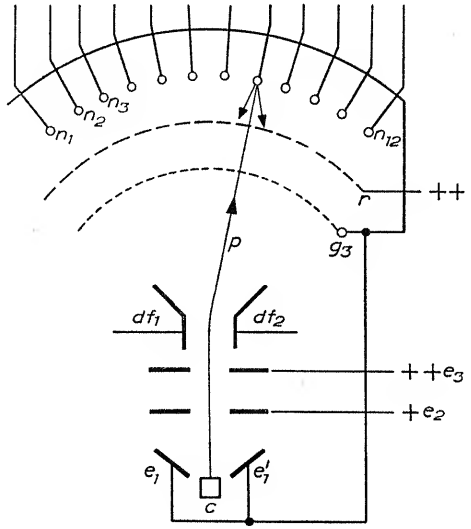

Fig. 8.15. Selector tube. The ribbon shaped primary beam p hits one of the electrodes n_1 . . . n_{12}, with high secondary emission yield; the electrode under bombardment thus assumes the potential of the screen grid r. The suppressor grid and shield g_3 is at cathode potential. Other letters: c cathode, e_1, e_2, e_3 electrodes for beam formation, df_1 and df_2 deflection plates [360]

a controlled deflection by plates d_1 and d_2 (as in an oscillograph tube). The anode r is provided with slits, each slit opposite one of the secondary emitting electrodes n_1 . . . n_n. Thus by giving the beam the right deflection any one of the electrodes n can be selected for connection with r.

9

SOME EXAMPLES OF SECONDARY ELECTRON EMISSION CAUSING DISTURBING EFFECTS

In the previous chapter we discussed the applications of surfaces with high secondary emission yield, and cases where secondary electron emission plays an essential part in the operation of a tube. There are other cases where secondary electron emission may cause disturbing effects and where it should be eliminated as much as possible. No substance has yet been discovered which is without secondary emission, though there are many with fairly low yield. Special constructions, too, can be used to avoid the transition of secondary electrons to whatever other electrode or insulating surface they must not reach.

9.1. SURFACES WITH LOW SECONDARY EMISSION YIELD [5, 361]

We have seen already that metals have a lower secondary emission yield than insulators. This can be decreased still further by superposing layers of very small particles, like soot. The lowest yield

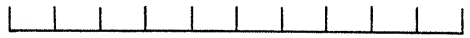

Fig. 9.1. Surface with low secondary emission yield

of all could probably be obtained with a layer of finely divided lithium, but lithium in finely divided form is very easily oxidized and the result would be the reverse of what was wanted. Soot is highly stable, and furthermore its secondary emission yield does not increase if it is exposed to barium atoms evaporating from an oxide coated cathode (Chapter 5). However, for many purposes the secondary emission yield of soot is still too high. The electrode shown in fig. 9.1 gives better results. It consists of a metal plate on which small plates are mounted perpendicularly. The surface is completely covered with a soot layer, so that the space between

the plates is not filled. Fig. 9.2 shows the dependence on V_p of the secondary emission yield of such an electrode [5].

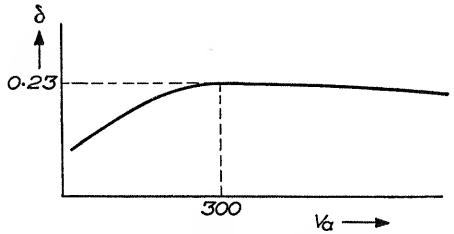

Fig. 9.2. Secondary emission yield from electrode in fig. 10.1

9.2. CHARACTERISTIC OF A DIODE

It is well known that in a diode, where the anode current is limited by space charge, the anode current i_a increases as $V_a^{3/2}$ where V_a is the anode voltage. Accurate measurements by several authors [362, 363] have shown that in the i_a, V_a characteristic a small anomaly is often present at a V_a of about 10 volts (fig. 9.3). Although

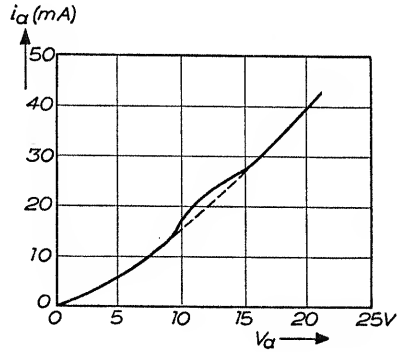

Fig. 9.3. Anomaly in diode characteristic; according to JONKER [364]

different suggestions as to the cause of this anomaly have been made, it now seems fairly certain that secondary electrons from the anode are of a considerable influence. JONKER [364] has shown that the anomaly is not found where a tungsten cathode and no getter material is used. Apparently secondary electrons originating from BaO or MgO evaporated on to the inner surface of the anode cause this effect. The energy distribution of secondary electrons at low primary voltage is of special interest since we can expect

that elastically reflected electrons can in principle reach the cathode and so contribute for a second time to the space charge round it, whereas slower moving secondary electrons cannot. Most of the substances with a high secondary emission yield show a high percentage of reflected primaries at low primary voltages, which drops suddenly at about 10 volts. Thus it can be understood that at 10 volts a slight rise of i_a is found. At higher voltages, where the true secondary emission increases rapidly, another decrease of i_a can be expected.

9.3. SUPPRESSION OF SECONDARY ELECTRON EMISSION IN TETRODES [365, 366]

An example of a case where secondary electron emission has to be suppressed as efficiently as possible, is the tetrode, especially the tetrode used for amplification of large voltages. The inner structure of such a tube consists of a cathode c, a control grid g_1, a screen grid g_2 and an anode a (fig. 9.4).

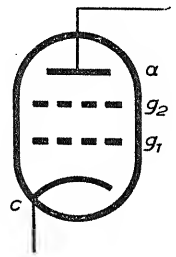

Fig. 9.4. Tetrode

Fig. 9.5a shows the anode current i_a as a function of the anode potential V_a for different values of V_{g_1} (potential difference between control grid and cathode). With increasing V_a there is a rise of i_a, since of the electrons emitted by the cathode an increasing fraction is able to reach the anode. However as V_a increases still further the anode starts to emit secondary electrons, which are caught by the screen grid so long as $V_{g_2} > V_a$, where V_{g_2} is the potential difference between screen grid and cathode. The consequence is a horizontal section of the i_a-characteristic, which in some cases may decline. When V_a becomes about equal to V_{g_2}, no secondary electrons from the anode can reach the screen

grid; i_a then rises rapidly. With $V_a > V_{g_2}$ a slow rise of i_a is observed.

We shall discuss first the situation where a resistance is inserted in the anode circuit. In this case i_a is determined by the intersection of the characteristic under consideration and the straight line

$$i_a = \frac{V_a' - V_a}{R},$$

where V_a' is the external voltage in the anode circuit and R is the load resistance. Obviously a distortion-free amplification can only be obtained if i_a is a linear function of V_a (such as in fig. 9.5b) and not as complicated as in fig. 9.5a. If the anode circuit is loaded with a self induction (e.g. a loud-speaker), current and voltage are not in phase and the straight line as in figs. 9.5a and b becomes an ellipse. In this case, too, a distortion-free amplification is obtained only if the relation between i_a and V_a is linear (fig. 9.5c).

Thus amplification without distortion can only be realized by suppressing the transition of secondary electrons from anode to screen grid and the reverse. This is possible by inserting a third grid at cathode potential (or nearly cathode potential) between the screen grid and anode. The secondary electrons, having a much lower energy than the primary electrons, cannot pass this third grid and are "pressed back" to the electrode from which they are released. The diagram of such a pentode is shown in fig. 9.5b.

If the alternating part of the anode voltage is very large, the potential in the plane of this third "suppressor" grid may be higher than the anode potential in the half wave where the anode potential is low. The consequence is that secondary electrons from the anode can still escape to the screen grid. By covering the anode surface with a soot layer (low δ) the straight part of the characteristics can be extended to a lower voltage, so that such a tube is able to yield a greater power (fig. 9.6) than a tube without soot cover [365].

The action of secondary electrons may also be disturbing in tetrodes used for high frequency amplification in radio receivers. The amplitude of the high frequency voltages is in most cases much smaller than of the audio-frequencies considered above, and the action of secondary electrons has a quite different influence. The so-called high frequency tetrode is (or has been) used with $V_a > V_{g_2}$. Under this condition the characteristic has a shape as shown in fig. 9.7a. The characteristic does not run parallel to the V_a-axis,

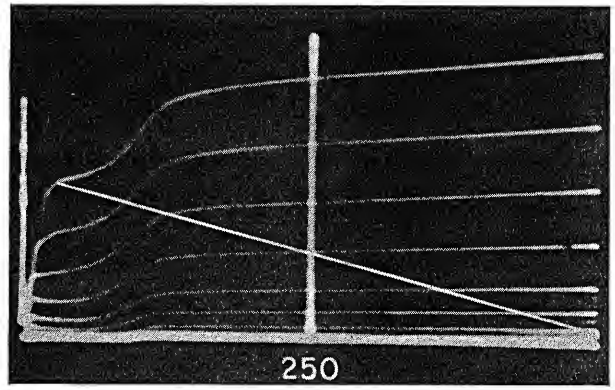

Fig. 9.5a. Anode current i_a as a function of V_a in a tetrode with different potentials V_{g_1} of the control grid, and a constant screen grid potential V_{g_2}. The straight line $i_a = (V_a' - V_a)/R$ shows that there will be distortion when the anode circuit is loaded with an Ohmic resistance R. According to JONKER [361]

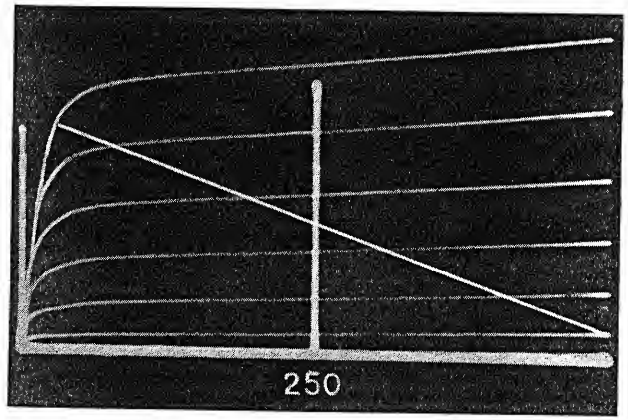

Fig. 9.5b. The same curves for a pentode

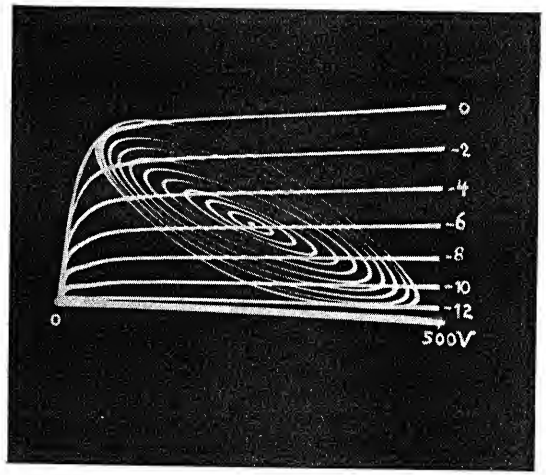

Fig. 9.5c. The same curves for a pentode. The ellipses indicate distortion-free amplification when the anode circuit is loaded with a self-induction

To face page 130

since the secondary electrons, released from the screen grid at the side facing the cathode, are drawn through the grid wires in order to reach the anode. Therefore the secondary electron current from

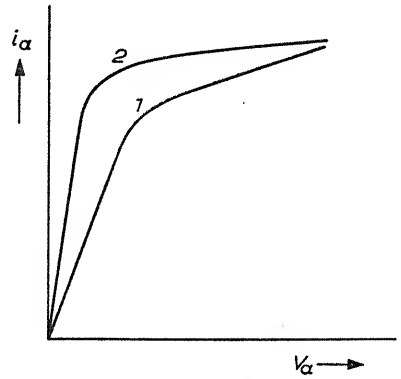

Fig. 9.6. Anode current i_a as a function of V_a. Curve 1: anode surface uncovered. Curve 2: anode surface covered with a soot layer. According to JONKER [365]

screen grid to anode cannot easily be saturated. In most of the cases the anode resistance of the tube, $\frac{\delta i_a}{\delta V_a}$, does not exceed 0·2 $M\Omega$. A high frequency tube is used with an LC circuit in the anode lead. If the tube has a low internal resistance, this circuit is damped

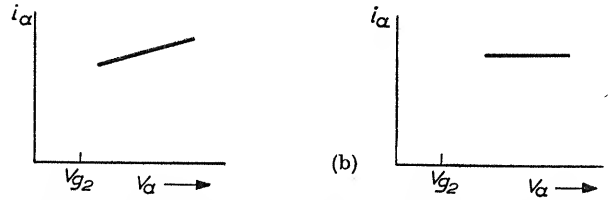

Fig. 9.7. (a) Anode current i_a as a function of V_a for a tetrode ($V_a > V_{g_2}$). (b) The same curve for a pentode

and the selectivity deteriorates. Obviously the internal resistance can be increased by preventing the transition of the secondary electrons.

For receiving purposes the tetrode has been completely superseded by the pentode, with a grid at cathode potential between screen grid and anode. The inner resistance is now of the order of 2 MΩ (fig. 9.7b), quite sufficient for tubes in common receivers.

An additional advantage is that the currents to screen grid and anode in the pentode stay in constant proportion. In the tetrode this proportion fluctuates during life because the secondary emission yield of the screen changes as it is exposed to a constant stream of barium atoms evaporating from the cathode.

In high power, high frequency tubes for transmitting purposes, a tetrode may be preferred to a pentode, since the capacitance of the anode versus the other electrodes is smaller. In this case a covering of the anode with soot gives good enough results, the requirements being less severe than in the audio-frequency range. Another method of suppressing the transition of secondary electrons is to increase the distance between screen grid and anode. With normal operating currents and voltages a space charge between these electrodes is formed, so that a potential minimum arises, which acts like the suppressor grid in the pentode [366].

9.4. SUPPRESSION OF SECONDARY ELECTRON EMISSION FROM INSULATORS

A phenomenon well known to all manufacturers of receiver tubes is the "S effect" [361]. This effect can be met in all tubes where insulated parts (metallic and non metallic) are hit by electrons. As an example we may discuss a tube with a cylindrical anode of gauze and a cathode at the axis. The electrons emitted by the cathode can hit the glass wall. In this case we can apply the same principles of potential stabilization as we shall in Chapter 10. We shall see that the inner surface of the glass wall may take either of two potentials, that of the cathode or a potential about equal to the anode potential. In the second case some disturbing effects can be observed.

This charging of the glass surface can be observed by metallizing the outside of the glass and connecting an electrostatic voltmeter to it. In German literature it is called "*Schalt-Effekt*", since the potential of the glass-wall can be influenced by changing the order of *switching* on the voltages of the anode and cathode. If the cathode voltage is switched on first, so that the cathode is emitting, without any anode voltage, the glass wall becomes stabilized at cathode potential and remains at that stable potential even after the anode voltage is switched on. However, if the order of switching is reversed, the glass wall may acquire the higher, positive, anode potential

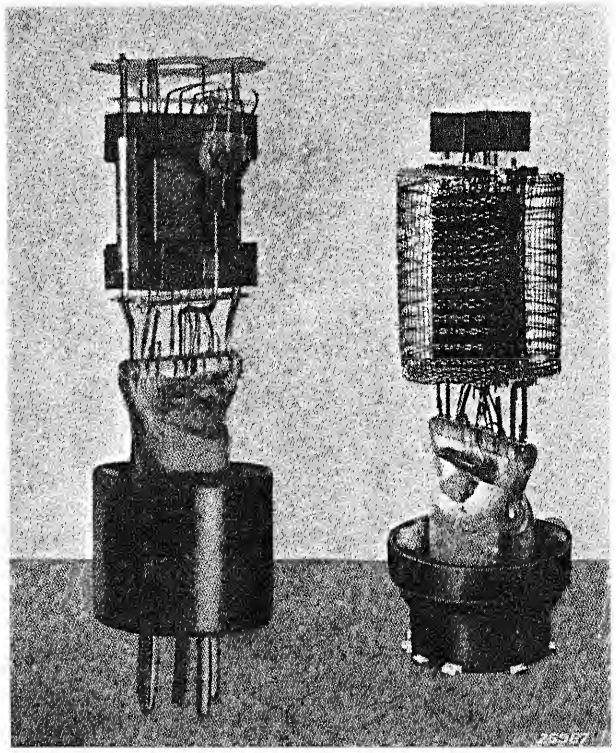

(a) (b)

Fig. 9.8a. Tube, in which mica supports and glass wall are sereened by metal plates from electron-bombardment

Fig. 9.8b. Tube, in which the anode is surrounded by a gauze cylinder at cathode potential. According to JONKER [361]

To face page 132

(especially if there is some leakage due to getter material evaporated on the wall) and may be likewise stable at this higher potential.

A positive charge on the glass wall may be a nuisance—in several ways. First, the electrons attracted to the wall can decompose insulating substances (cf. Chapter 5), so that gaseous products such as oxygen are released, and these may inactivate the oxide coated cathode.

Second, from a mere radio-technical point of view there may be a damaging influence. The internal resistance of a high frequency pentode can be considerably decreased when there is a positive charge on the glass wall. This means that there is a low resistance in parallel with the tuned circuit in the anode lead, with a consequent decrease in the selectivity and sensitivity of the amplifier. (Actually the conditions of the switch tube, described in Section 8.4 are more or less realized.)

A third phenomenon may be met in low frequency tubes used with high alternating voltages. The potential may vary jerkily, i.e. the potential of the wall jumps from one stable situation into the other. Since there is a capacitance between control grid and glass wall, these jumps cause potential differences between control grid and cathode, which are audible in the loud speaker as a crackling noise (Buzz-effect).

The charging of the glass wall and its harmful consequences can be avoided in different ways. For example it is possible to cover the glass wall with a substance, such as soot or tungsten oxide, whose secondary emission yield is less than 1. The openings between the electrodes can be closed by plates (fig. 9.8a), or the anode can be surrounded by a gauze cylinder at cathode potential (fig. 9.8b) [361].

9.5. SUPPRESSION OF SECONDARY ELECTRON EMISSION FROM THE CONTROL GRID IN AN OSCILLATING TRIODE [368]

In a transmitting tube the secondary electron emission from the control grid may have a disturbing effect. Fig. 9.9 shows the characteristic of the grid current versus the grid voltage, where the secondary emission yield of the grid material is larger than 1 (dotted line). After a rise the curve falls with increasing V_g, where V_g is the potential difference between grid and cathode. In this section

where $\delta i_g/\delta V_g$ is negative the system control grid-cathode has a negative resistance; the consequence is that it may act as a dynatron and thus be the source of undesirable oscillations.

It is therefore necessary to construct a tube without negative resistance, i.e. make a grid with a reduced secondary emission

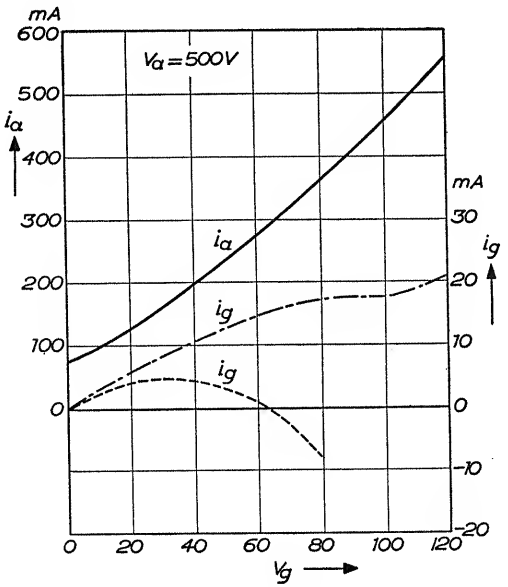

Fig. 9.9. Grid current i_g and anode current i_a as functions of grid potential V_g in transmitting tube (Philips MB 2/200). — · — · — · zirconium grid; — — — — molybdenum grid. According to BOUMEESTER [368]

yield. However it is not necessary, or even desirable, to reduce the yield to the very minimum. If this were to be done i_g would become unnecessarily large, at the cost of the anode current and hence of the effective conductance of the tube. It is best to decrease the secondary emission yield by such an amount that the $i_g - V_g$ characteristic runs nearly parallel to the V_g-axis. Zirconium, with $\delta_{max} = 1$ can be used with success (fig. 9.9, chain dotted line). Tungsten and molybdenum with a thin cover of zirconium oxide also show the same yield. Their surface too is presumably zirconium, the oxide being reduced by the underlying metal during the out-gassing process.

A thin cover of Cr_2O_3 also diminishes the secondary emission yield (German patent DRP 587386); carbon gives the same result, but it is liable to dissolve in the underlying metal at the usual high operating temperatures in this type of tube.

9.6. SECONDARY ELECTRONS IN X-RAY TUBES [369]

In X-ray tubes secondary electrons are released by the fast moving primary electrons. Investigations carried out by WAGNER and by TRUMP and VAN DE GRAAFF have shown that many of these secondary electrons are "fast" or "rediffused" electrons, the energy distribution curve having a maximum at 90% of the energy of the primary electrons. These electrons may cover long distances and so

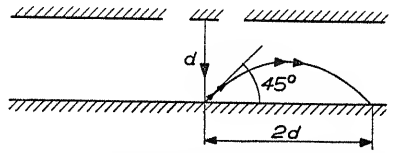

Fig. 9.10. Elimination of the disturbing influence of secondary electrons in X-ray tubes; according to BOUWERS and VAN DER TUUK [369]

give rise to disturbing effects. For instance, they can excite X-rays, cause electrolysis of glass etc.

The lowest yield for these electrons will certainly be found in metals with a low density. However one is not always free to select such a metal and in many cases the only means of elimination is by altering the geometry of the tube. BOUWERS and VAN DER TUUK have described a number of constructions of X-ray tubes in which special attention is paid preventing secondary electrons from leaving the space between cathode and anode. Fig. 9.10 shows a flat cathode and anode. The "secondary" electrons with an energy equal to the energy of the primary electrons and escaping under an angle of 45° from the anode surface have the maximum range. According to BOUWERS and VAN DER TUUK no disturbing influences are experienced, provided that these electrons are again captured by the anode surfaces; a simple calculation shows that the radius of the anode should be twice the distance between cathode and anode (fig. 9.10).

10

SECONDARY ELECTRON EMISSION IN TUBES WITH SURFACES OF AN INSULATING MATERIAL

Secondary electron emission is of essential importance in two sorts of tubes in general use today: cathode-ray tubes, and storage tubes. In both, an electron beam hits a surface of insulating material.

Although we have already discussed, in Chapter 2, the potentials at which such a surface can be stabilized, we shall now briefly reiterate these considerations, using a somewhat different picture (fig. 10.1). As before, the electron beam hits a non-conducting

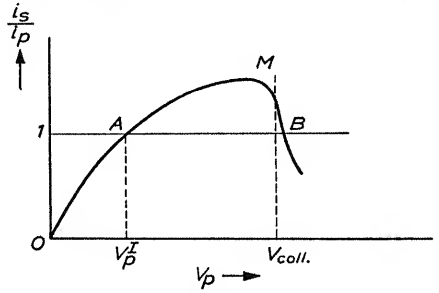

Fig. 10.1. Number of secondary electrons per primary electron reaching the collector, when $V_{coll} < V_p^{II}$. $V_p = 0$ and $V_p \approx V_{coll}$ are stable situations; $V_p = V_p^I$ is unstable

target, and we shall suppose the secondary electrons to be collected by a surrounding collecting electrode. If the target were a conductor, the current of secondary electrons as a function of the energy of the primary electrons would be according to the curve shown in fig. 10.1. The decrease of i_s/i_p near M is caused by the fact that if V_p increases while V_{coll}, the potential of the collector, remains constant, the secondary electrons cannot reach the collector owing to the retarding field. Since the target is an insulator there are two stable situations: one where $V_p = 0$, so that no electrons can reach the target; the other at such a value of V_p that i_s/i_p is

equal to 1, a situation corresponding to point B. In the latter case $V_p \simeq V_{coll}$. At A, where $V_p = V_p^I$, the situation is unstable.

If V_{coll} is made very large, the curve of fig. 10.1 tends to the curve of fig. 10.2; we have now the well-known $\delta - V_p$ relation in which the second stable situation is found at $V_p = V_p^{II}$.

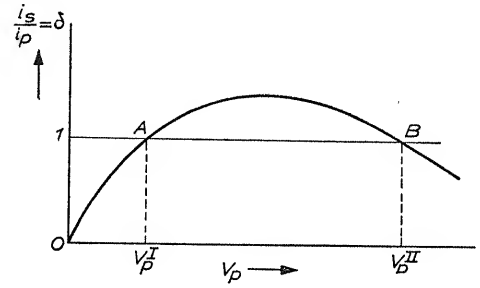

Fig. 10.2. Secondary emission yield as a function of V_p when, $V_{coll} > V_p^{II}$. $V_p = 0$ and V_p V_p^{II} are stable situations; $V_p = V_p^I$ is unstable

10.1. CATHODE RAY TUBES

In cathode ray tubes the situation at $V_p = 0$ is obviously not wanted. In this case the target, the fluorescent screen, must be brought to the stable situation B, of high potential (collector potential). If V_p is increased from zero potential, the screen may never reach the high stable potential, as $V_p = 0$ is a stable situation. This difficulty is sometimes encountered with oscilloscope tubes using a low anode voltage of a few hundred volts; in this case a conductive transparent layer under the screen material may be useful.

In the cathode ray tubes in television receivers V_p is between 5 and 15 kV, and the screen always stabilizes at high potential. This phenomenon needs actually a further explanation. Positive ions, always present in the tube, will presumably raise the screen potential gradually towards V_p. If V_p exceeds V_p^I the screen potential jumps of itself either to V_{coll} or V_p^{II}. As long as $V_p < V_p^{II}$ the potential of the screen will follow V_{coll}, if the latter is increased. It is, however, obvious from fig. 10.2 that the screen potential can never exceed V_p^{II}. V_p^{II} is therefore often called the "sticking" potential. In the case of tubes which have to be used at high voltages this can be an annoying phenomenon, as an increase of

collector potential does not increase the energy of the primary electrons and therefore does not allow any increase of light output. Secondly, the electric field between screen and collector may give rise to a distorted picture. Thirdly, by the action of this field positive ions are drawn to the screen, which can be affected chemically, and a decrease of light output can result. In rectangular tubes this phenomenon is known as "cross-burn".

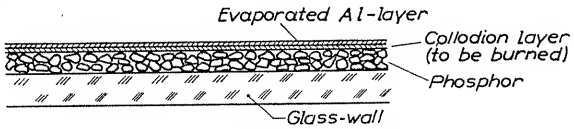

Fig. 10.3. Metal backed phosphor screen

The secondary emission yield of different phosphors is therefore of importance, and in particular the values of V_p^{II} at which they stabilize.

It is not possible to give exact data on the secondary emission yield of phosphors. In practice, it is certainly influenced by the way in which the powders are applied on the base. Moreover, the yield of the base will also contribute to the secondary emission, if the covering is not complete, as in television cathode-ray tubes. The table shows some different data taken from literature [370].

	V_p^{II} in kV
Willemite	3–7
Willemite	5–10
Willemite	20
Zinc sulphides	6–9
Calcium tungstate	3–5

By adding a mixture of oxides with a high yield (MgO, BeO) it is possible to increase the secondary emission yield.

A new way to avoid "sticking" has been developed by application of the technique called "metal-backing". Nowadays it is a well-known technique, especially important for cathode-ray tubes used in projection television, where a high voltage is needed.

Metal-backed screens are made by evaporating a very thin aluminium layer on to the phosphor layer. On account of the roughness of the powder layer itself, the aluminium is not flashed on to the powder but on a very thin intermediate layer, usually collodion (nitrocellulose), covering the tops of the phosphor grains as a sheet. The smooth surface of the latter is then covered with a layer of aluminium about 0·1 μ thick; afterwards the collodion film is destroyed by heating the screen in air (fig. 10.3).

It can easily be seen (for instance from WHIDDINGTON'S formula) that the energy loss of the electrons (H with an energy of 10 keV or more) is negligibly small. Owing to the metal-backing the screen is at V_{coll}. Moreover the light, which in normal tubes is also radiated to the inside of the tube, is now reflected to the outside. For this reason the light output of a metal-backed screen is greater.

Since ions cannot penetrate the aluminium layer, a third advantage of metal-backing is the protection of the phosphor screen against bombardment by negative ions originating from the gun-cathode; negative ions can cause a rapid discoloration ("ionspot") of the screen.

10.2. STORAGE TUBES [371]

In the introduction to this chapter we saw that the potential of the surface of an insulator can be stabilized at either of two potentials: that of the cathode delivering the primary electrons; or (about) that of the electrode collecting the secondary electrons emitted by the insulator.

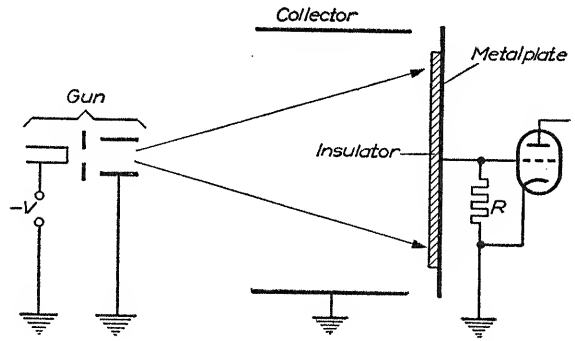

Fig. 10.4. Reading a charge pattern stored on the surface of an insulator

Let us suppose the surface to be divided into a large number of small areas, all originally at the same stabilization potential. If a charge is added to or subtracted from one of these areas its potential deviates from the stabilization potential, but can be restored by bombarding the area with electrons. If the opposite side of the insulating layer (the side not exposed to the electron beam) is covered with a continuous metallic layer, the area under consideration forms one side of a small condenser, which is charged (or discharged) by the stabilizing electron beam (fig. 10.4). The

current resulting from the stabilization of each area is conducted through an outside circuit, causing fluctuating voltages across the resistance R. If the charge is wiped out by a single scan of the stabilizing beam the amount, which was stored on the surface, can be measured. This method is used, for example, in television pick-up tubes.

In other systems only the *presence* of a charge is of interest; if in this case some of the charge is used by the exploring beam, it is supplied by electrons originating from a special gun (a "holding" gun), and the wiping out of the charge has to be carried out by a special stabilizing process.

It is clear that a surface of an insulator is able to store information in the form of electric charges.

The process of bringing information into the surface will be called writing, and the process of measuring the stored charges will be called reading. Another method of measuring the stored charges consists of controlling the intensity of a continuous electron beam, through the action of the stored charge on a grid shaped insulating electrode.

During the last decade several types of storage tubes have been described [371]. It would go far beyond the scope of this book to give a complete survey. We shall therefore restrict ourselves to a few examples.

We shall classify the tubes in the following way:

(a) tubes where writing occurs continuously and reading periodically (television pick-up tubes)
(b) tubes where writing is carried out periodically and reading continuously (viewing tubes)
(c) tubes where both writing and reading occur periodically (pick-up tubes for film transmission, and graphecons)
(d) storage tubes for computing machines.

10.2.1. Television Pick-up Tubes.

We start with tubes with an insulating target, on which electric information is written by photo-electric emission or by secondary electron emission caused by photo electrons (television pick-up tubes) [372].

A picture to be transmitted by television is divided into elementary areas. Each picture element has its own brightness. In pick-up

devices, the brightness of the elements is transformed successively, e.g. into electric currents. For the television systems now generally used the time available to transform the brightness of a single element is of the order of 10^{-7} sec. In the older devices, like the Nipkow disk and the Farnsworth dissector, the photocurrent from each element during this 10^{-7} sec had to provide the signal. If, however, the charge of a photocurrent during a frame period ($\frac{1}{25}$ or $\frac{1}{30}$ sec) can be stored, the result of an illumination of $\frac{1}{25}$ or

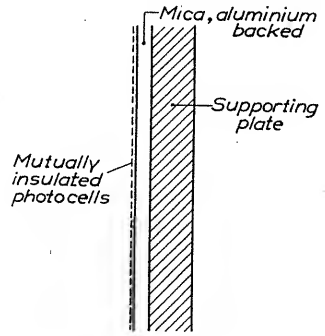

Fig. 10.5. Photosensitive target in television pick-up tube

$\frac{1}{30}$ sec can be transmitted, instead of the result of an illumination of 10^{-7} sec. Thus a gain in sensitivity of the order of 10^5 can be expected. All pick-up tubes nowadays in use are storage devices.

In television pick-up tubes the stabilization phenomena are much more complicated than in cathode-ray tubes. Pick-up tubes have been developed along various lines, but we shall first consider an elementary type.

In such a tube the photo-emissive layer is laid on the surface of an insulating material, e.g. mica. The layer consists of a very large number of mutually insulated photocells (e.g. of the type (Ag-Cs_2O, Ag—Cs)), the other side of the mica being coated with a continuous metal layer, fig. 10.5. Such an electrode is thus composed of a very large number of small condensers. If an image is projected on to the photosensitive side of the mica and if the photo-electrons can be drawn to a collector a positive residual charge is formed on each element, proportional to the amount of light absorbed. This charge is measured and at the same time neutralized by scanning the surface with an electron beam line-by-line. This occurs 25 or 30 times per second. Between two scannings a positive charge is

accumulated by an illuminated elementary condenser. These types of tubes are therefore called "storage tubes".

In television pick-up tubes we have the usual two possibilities of potential stabilization, viz. at $V_p = 0$ and $V_p \simeq V_{coll}$. Both are used; in the first case the target is hit by electrons with nearly zero velocity, and the positive charge caused by the illumination is simply neutralized. In the second case the elements are always bearers of a positive charge, which can vary in magnitude according

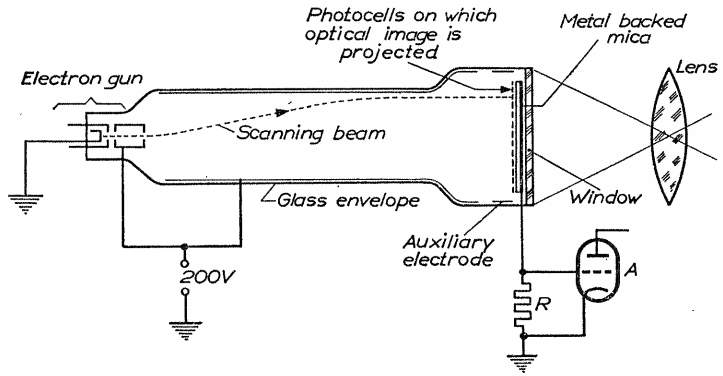

Fig. 10.6. Schematic representation of television pick-up tube with cathode potential stabilization (cf. C.P.S. emitron)

to the amount of light being absorbed. The way in which the accumulation and neutralization of the charge take place is rather complicated and will be discussed later on.

The first type of tubes are usually called tubes with low-velocity scanning or tubes with C(athode)-P(otential)-S(tabilization) [373, 374]. This system of C.P.S. scanning is applied in tubes indicated with names like orthicon, superorthicon, image-orthicon, C.P.S. emitron. Tubes of the second type (high-velocity scanning) are iconoscope, image-iconoscope, super-emitron, eriscope etc.

10.2.1.1. *Television pick-up tubes with low velocity scanning.* We shall now discuss in more details some properties of tubes with low velocity scanning. In fig. 10.6 we show the scheme of a tube, which is now manufactured by E.M.I. in England and called the C.P.S. emitron. The electron-gun delivers the beam for scanning. It is focussed by a longitudinal magnetic field and deflected by the magnetic field of two pairs of coils (the coils are not shown in the drawing).

The metal layer at the rear of the target is transparent so that the photosensitive side of the target, consisting of mutually insulated photocells which are positively charged, can be illuminated. Fig. 10.6 shows how the scanning beam discharges the elementary condensers through the resistance R, which is the input resistance of the video amplifier A.

One of the difficulties of this type of tube is that the positive charge of the target surface under conditions of strong illumination

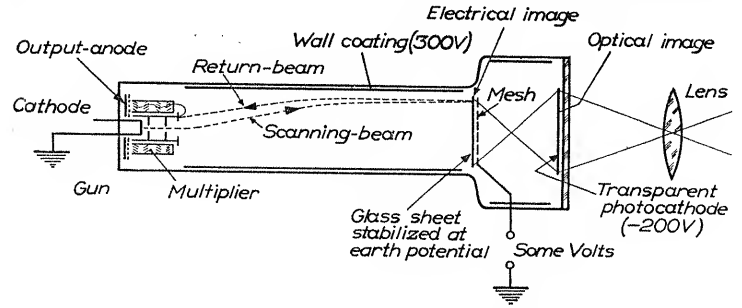

Fig. 10.7. Schematic representation of image-orthicon

may be sufficiently high to raise the potential of the surface beyond V_p^{I}. Then the potential of the surface jumps to that of the collector and a high velocity scanning is started. This instability can be avoided by inserting a very fine mesh just in front of the target and adjusting it to such a potential (of the order of 5 V) that V_p^{I} will never be reached. This mesh, however, may be the cause of disturbing effects, due to additional capacity.

The objections to this tube have led to the development of the image-orthicon [375], a pick-up tube which is now generally used in the U.S. In the C.P.S. emitron the target has a double task: it forms the photosensitive layer and it stores the electric charge due to the photo-electric emission. These functions are separated in the image-orthicon (fig. 10.7): the photocathode is a continuous transparent layer applied on a window; the photo-electrons are made to form an image on an insulating target, which is scanned by a scanning beam.

The word "image" refers to the section of the image-orthicon in which the electron optical image is formed. The advantage is obvious: the continuous photocathode is more sensitive than the broken layer in the C.P.S. emitron; apart from this the stability in this kind of tube is assured as we shall see.

The method of scanning the charge pattern is most original. The tube is divided into two sections. The left-hand part is the scanning section, as in the C.P.S. emitron, but the target is a very thin sheet of glass. The right-hand part is the image-section, in which the photocathode is imaged optically on the glass sheet. The photo-electrons form a positive charge pattern owing to secondary emission. This positive charge leaks through the glass and is neutralized on the other side by the scanning beam. On the side of the photocathode a very fine mesh is inserted, just in front of the glass sheet. Suppose the cathode of the electron gun is at earth potential; then the surface of the glass sheet is also at earth potential, the mesh is some volts above earth potential and the photocathode itself, e.g. at —200 V. The charge pattern on the glass sheet is established by the secondary electrons drawn from the glass sheet to the mesh; there is a limit to the potential of the sheet surface, in the same way as that produced by the mesh in the C.P.S. emitron.

The distance between glass sheet and mesh determines the capacity, and therefore the amount of charge which can be collected. In order to cover a sufficiently large range of illumination this capacity has to be as large as possible. If the amount of light being used is too great there is an excess of secondary electrons falling back on the target. In television pictures this can sometimes be observed as a halo-like phenomenon: white parts of the pictures are surrounded by a black area.

The video signal is taken from this tube in a different way to that from the C.P.S. emitron. To illustrate this we consider a small area on the target, i.e. the glass sheet, with a positive charge. The positive area needs a fraction of the scanning beam for neutralizing the positive charge, and we find a reduction in the returning electron beam corresponding to the neutralized amount of charge on the target. This being a low velocity system it is possible to collect the returning beam quite easily, as the returning electrons follow cycloid-shaped orbits along the magnetic lines of force similar to those of the scanning electrons. The returning beam can be collected inside an electron multiplier surrounding the electron gun; in this way an amplification of the fluctuations is obtained. The construction of the multiplier is of the "Venetian blind" type. This principle could of course also have been applied in a C.P.S. emitron.

The image-orthicon is the most sensitive pick-up tube used in practice, that is to say it has in low illuminations a greater signal to noise ratio than any other type of tube. In the image-orthicon the noise level is determined by the shot noise in the returning beam; in the other tubes, the noise level is determined by the noise originating from the coupling resistance or the first amplifier tube.

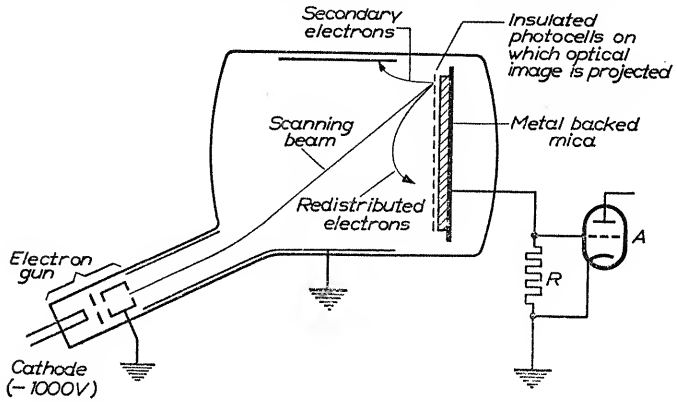

Fig. 10.8. Schematic representation of iconoscope

It can easily be seen that in the image-orthicon the returning beam is strongest in the black parts of the picture being transmitted, so the black parts show the most pronounced noise. As the depth of modulation of the return beam is as much as 20 to 30 per cent there is another contribution to the noise. To lower these noise effects the "image-isocon" [376] has been developed. In this tube the secondary electrons originating from the neutralized parts on the target are amplified and not the return beam. WEIMER has succeeded in finding a way to separate the secondary electrons from the beam of returning electrons. This type of tube, however, has not yet come into use in regular television broadcasting.

10.2.1.2. *Television pick-up tubes with high velocity scanning*, [377–380]

The simplest form of these tubes is the ordinary iconoscope (fig. 10.8). A charge pattern is formed in the same way as for the C.P.S. emitron. Here the target is scanned by a beam of electrons whose energy is about 1000 eV. The potential of an element after stabilization is therefore a few volts above collector potential and the element is not able to emit photo-electrons against the retarding field which is formed between itself and the collector, the energy of

the photo-electrons being smaller than that of the secondary electrons. It is, however, obvious that in a system where the distance between target and collector is great, compared with the distance between an element and its neighbours, the influence of the surroundings of an element will be important. The result will

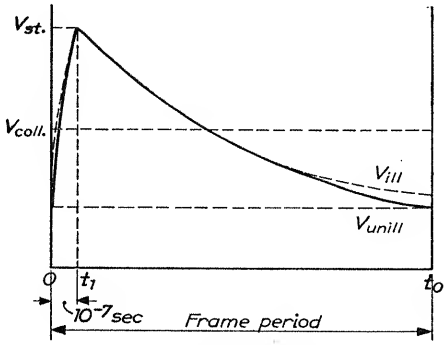

Fig. 10.9. Variation of potential of target element with time in a tube with high velocity scanning. Scanning period is between $t = 0$ and $t = t_1$. Between $t = t_1$ and $t = t_0$ the potential drops gradually owing to redistributed electrons. Full line: target dark. Broken line: target illuminated

be that during the scanning of an element only a fraction of the secondary electrons released is able to reach the collector; only a small fraction falls back on the original element, but the largest fraction will fall back on other parts of the target, where the potential may be higher than collector potential. This is called the *redistribution effect*, which is essential for the mechanism of the high-velocity pick-up tube. The mechanism can be explained roughly in the following way: Fig. 10.9 shows the variation of the potential V of an element as a function of time t. In the scanning time t_1 (about 10^{-7} sec) the potential of an unilluminated element will be brought from V_{unill} to $V_{\text{st.}}$ (lower curve). From $t = t_1$ to $t = t_0$ (approximately $\frac{1}{25}$ sec being the frame period) the potential will gradually drop, the element receiving continuously secondary electrons from other elements being scanned. This redistribution current is at its maximum just after $t = t_1$, when the potential is still high and the beam is hitting adjacent elements.

If the same element is now continuously illuminated it ought continuously to emit photo-electrons. For some time after $t = t_1$, however, the potential is high and the photo-electrons cannot

leave the element until the potential has decreased sufficiently due to the redistribution. Thus photo-emission is only possible during a fraction of the frame period, and in practice the effective time of storage is only about 5% of the frame period. As a result of the photo-electric emission the potential before the next scanning will be somewhat higher than for an unilluminated element so that the "jump" to the potential of stabilization will be smaller.

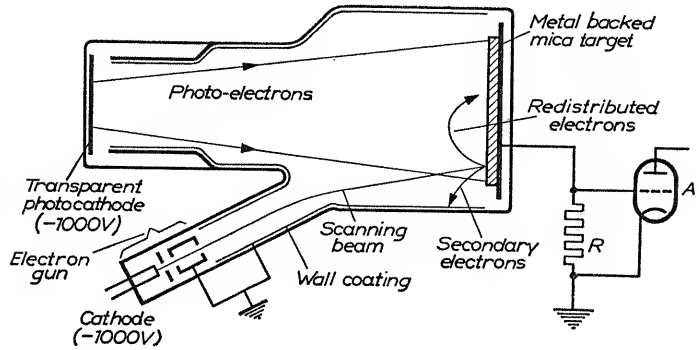

Fig. 10.10. Schematic representation of image iconoscope

We can see in this way the importance of the current of redistribution electrons in determining the properties of this kind of tube. Obviously the high velocity tube is less sensitive than the low velocity tube, since the effective time of storage in the first is about 5%, while in the latter it is 100%. The iconoscope is in fact too insensitive to be of much practical use for ordinary broadcasting purposes and is now generally replaced by the image-iconoscope, a high-velocity tube where the tasks of photosensitive layer and target are separated as in the image-orthicon.

Fig. 10.10 shows the design of this tube in principle. The photocathode is transparent and its image is electron-optically focussed on the target, so that secondary electrons are released and a charge pattern is accumulated. This is scanned by an electron beam in the same way as in the iconoscope. The image-iconoscope is more sensitive than the iconoscope for three reasons:

(a) the broken photocathode in the iconoscope is replaced by a continuous layer (3- to 4-fold gain in sensitivity); (b) there is a secondary emission multiplication on the target (3- to 4-fold gain); and (c) in the image-iconoscope the effective time of storage is

about 30% of the frame time. It is larger than in the iconoscope because the secondary electrons producing the charge pattern on the target are faster than the photo-electrons in the iconoscope (6-fold gain). Thus the image-iconoscope needs only $1/3 \times 1/4 \times 1/6 = 1/72$ of the amount of light of the iconoscope to give the same signal.

The difference in the scanning mechanism of low and high velocity tubes results in a marked difference in behaviour and picture quality:

(a) In high velocity tubes the stability of the target potential is always guaranteed; in low velocity tubes it can only be obtained with the aid of a mesh.

(b) Owing to the effective time of storage low velocity tubes may give a "blurred" image of fast moving objects; whereas a high velocity tube produces a series of more or less sharp pictures.

(c) In tubes with high velocity scanning the density of the re-distribution electrons is not uniform over all the parts of the target; different parts of the target are therefore not quite at the same potential, even without illumination i.e. without impinging photo-electrons. Signals originating from these potential differences are called "spurious signals". These spurious signals are in principle not encountered with low velocity scanning. Pictures produced by low velocity scanning are therefore "flatter" than the pictures from high velocity tubes. Spurious signals can be largely eliminated by the application of compensating signals generated in outside circuits and inserted in the video amplifier. Alternatively, an additional direct current of slow moving electrons from an extra cathode can equalize the potential differences over the target, usually with the help of extra electrodes around those places in the target area where a supply is especially needed. This is a method used in the P.E.S. photicon; it is also used in the U.S.A. in the iconoscope for film transmission.* When these precautions are not taken the intensity of the spurious signals determines the minimum light levels, at which an acceptable picture can be obtained.

(d) It would seem at first sight desirable that the generated signal should be a linear function of the amount of light. A general expression is $S = CI^{\gamma}$, where S and I are respectively signal output and illumination and C and γ are constants. Low velocity tubes

* P. SCHAGEN; Thesis, Amsterdam 1951.

deliver a signal for which $\gamma = 1$, with the restriction that the signal becomes independent of the illumination as soon as the rise of the potential on the target surface is stopped by the action of a mesh. In tubes with high velocity scanning $\gamma < 1$, and the signal gradually tends towards a saturation value with increasing illumination (fig. 10.11). Before passing judgement, however, we must consider

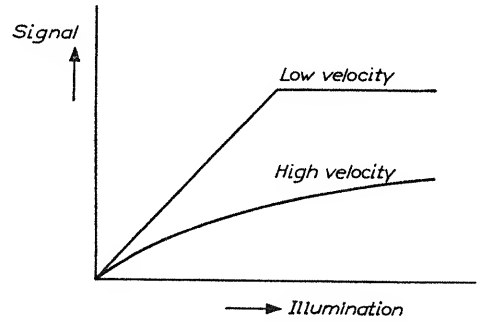

Fig. 10.11. Signal characteristics of tubes with low and high velocity scanning

the receiving end. The light output L of the cathode-ray tube depends on S according to the relation $L = C_1 S^{\gamma_1}$, where $\gamma_1 > 1$ (mostly $\gamma \simeq 5/2$) depending on the properties of the electron gun in the receiving tube. Thus $L = C_2 I^{\gamma_1 \gamma}$. For the best result $\gamma_1 \gamma$ must $\simeq 1$. In practice, without any additional γ-corrector, a high velocity tube gives a picture of better quality than a low velocity one.

The differences summarized above determine the advantages and disadvantages of the two scanning systems. In transmitting systems where a high definition is required the high velocity scanning method will be preferred, since a high resolution capacity is more easily obtained with high velocity than with low velocity electrons. Nowadays low velocity tubes (image-orthicons) are in common use in the U.S.A. In Europe both low and high velocity systems (image-iconoscope) are used.

10.2.1.3. *Monoscope*

A monoscope, as it is termed, is a tube which is often used for testing a television transmitter. This tube is provided with a target (e.g. aluminium with a thin oxide layer), on which a test pattern is drawn with carbon. The differences in secondary emission yield enable a

signal to be obtained when the target is scanned in the usual way. A similar tube has been constructed by KNOLL and THEILE [381] for the transmission of arbitrary pictures which can be drawn on the target.

10.2.2. Viewing Tubes with Storage.

In cathode-ray tubes used for television reception (kinescopes) the elements of the fluorescent screen are successively hit by an electron

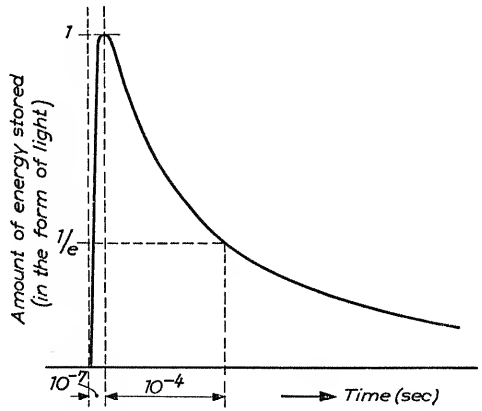

Fig. 10.12. Storing and emission of energy by a phosphor in a cathode-ray tube

beam; its intensity is determined by the signal obtained from the pick-up device. In the type of tube described in Section 10.1 an element of the fluorescent screen receives the full energy of the beam during 10^{-7} second; a fraction of this energy is emitted in the form of light during the next frame period. A cathode-ray tube is in fact a storage system, but it stores energy rather than charge (fig. 10.12).

The specific loading of an elementary area is high; extremely so in tubes for projection television [382], used in combination with an optical system and projector screen, where specific loadings of the order of 100 kW/cm² during the scanning period of 10^{-7} second are normal. Since the capacity for storing energy in fluorescent powder is limited (especially in high efficiency phosphors of the sulphide type), the amount of light as a function of the loading tends to a saturation value. Another disadvantage, demonstrated by HAANTJES and DE VRIJER [383], is that phosphors with a short

decay time (e.g. for sulphides $t \simeq 10^{-4}$ second) tend to give pictures with "flicker".

A continuous loading of the screen is preferable. This can be carried out by applying a *charge* storage principle. Examples described in the literature [371] operate on similar lines. A charge pattern is written by a writing beam on a grid, the surface of which

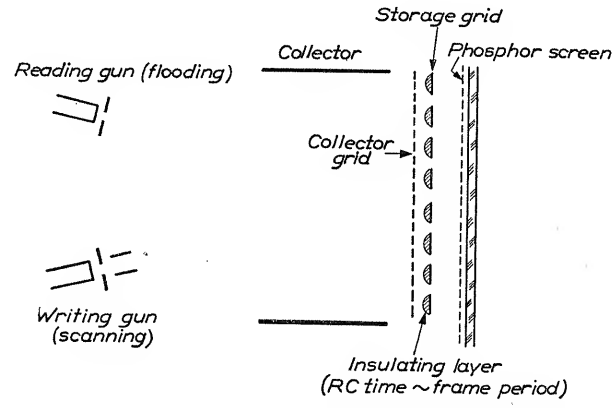

Fig. 10.13. Principle of a cathode-ray viewing-tube with storage

is covered with an insulating layer. A continuous current, originating from another gun or photocathode, "flooding" this grid is controlled by the charges. Thus the charges determine the transparency of the grid for the flooding electron current, so that a picture can be observed on a fluorescent screen placed on the other side of the grid (fig. 10.13).

The decay time of the charge pattern on the grid should be of the order of a frame period, for a longer decay time will give rise to "smeared" pictures. The decay time can be calculated, for example, as it equals the RC time of the condenser formed by the insulating layer.

In practice this principle has never been used for cathode-ray tubes with phosphor screens; direct view tubes have the advantage of being free from saturation effects, and flicker can be avoided by the choice of a phosphor with a sufficiently long decay time. Nevertheless, for a projection system where an enlarged picture is projected of the phosphor screen of a cathode-ray tube, a charge storage system could be useful to avoid saturation of the phosphor;

but charge storage has not yet been used in projection tubes, either.

There is, however, one special example in projection television [384] where application of the storage principle has given extremely good results. In this system, called "Eidophor", invented by the Swiss physicist FISCHER, a charge pattern is written in an oil film; under the action of electrostatic forces the surface is deformed. If this oil film is inserted in a "Schlieren" optical system, the deformed places in the oil film allow the passage of light originating from an external light source. The system is thus in fact a light-relay.

It is obvious that the decay time of the oil deformation is of essential importance. Let us call the frame period T and the effective time of opening of a picture element τ ($\tau < T$). Then a fraction $\frac{\tau}{T}$ of the light flux entering the element will be allowed to pass. Thus $\frac{\tau}{T}$ determines the illumination of the projection screen, which should be as great as possible. In the eidophor system the oil on which the information is written is conductive, its conductivity being chosen so that an optimum decay time is obtained. The result is an effective light storage time of about 70%.

10.2.3. Systems where Writing and Reading occur Periodically.

Many systems have been described, where writing and reading take place periodically. One well known example is the transmission of films by television with the aid of pick-up tubes. In such a system writing takes place during the frame fly back, when the scanning of the target is stopped. Reading takes place in the way described in Section 10.2.1. There are also tubes provided with two guns, one for writing, the other for reading [371]. These systems can be used, for example, to transform one television standard into another. We shall describe in more detail the "graphecon"; in this system use is made of a form of amplification, which is essentially an "internal" secondary electron amplification.

In a graphecon the radar picture known as a "plan position indicator" (P.P.I.) can be transformed into a television picture without using optical means. A P.P.I. pattern is generally written completely in some seconds, whereas in normal television systems a charge pattern is read 25 or 30 times a second. The writing system

of the transformation tube must therefore accumulate a charge of such an amount that a few hundreds or thousands of scanning periods are possible, each providing a signal of sufficient amplitude. Such a tube has been developed by PENSAK [385]. In order to get sufficient charge by the action of the writing beam, an electron multiplication effect is used, of a general type called "conductivity

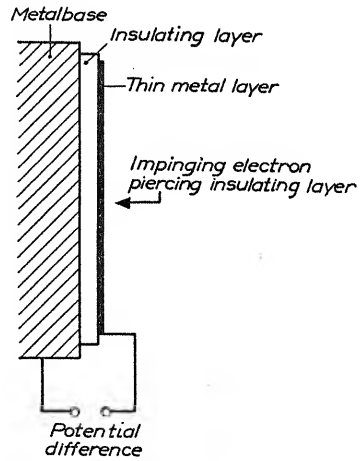

Fig. 10.14. Principle of bombardment-induced conductivity

induced by electron bombardment". This phenomenon has been studied during the last few years by several authors [386–389].

This induced conductivity can be observed, if a thin layer of an insulator like silica, aluminium oxide, or evaporated antimony trisulphide is sandwiched between two metallic electrodes and the insulating layer is pierced by a beam of fast moving electrons (fig. 10.14). If such a potential difference is applied between the two metallic electrodes as to give a field strength of the order of 10^5 to 10^6 V/cm a conduction current can be observed, which is many times larger than the bombarding electron beam. PENSAK [390] found by gradually increasing the energy of the bombarding electrons the conduction current starts when the electrons just pierce the layer. The multiplication effect is at its maximum when the amount of energy lost by bombarding electrons is also at its maximum. The amount of energy lost in the layer shows a maximum as a function of the energy of the bombarding electrons.

In the case of a 1·5 μ silica layer, for example, the maximum effect is observed at a bombarding voltage of about 14 kV. With a gradient of 10^6 V/cm a multiplication of 30 is found. The effect is still greater at higher temperature and multiplications up to 50,000 have been recently obtained.

Fig. 10.15 shows the way this effect is used in the graphecon.

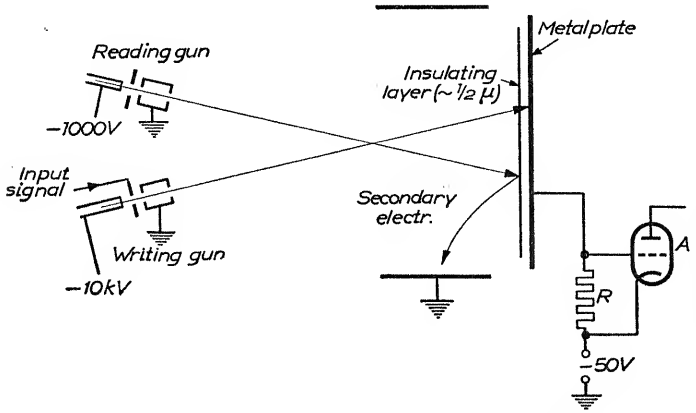

Fig. 10.15. Schematic representation of graphecon (PENSAK)

The target consists of a metal plate covered with a film of insulating material having a thickness in the order of $\frac{1}{2}$ μ. The writing gun gives a beam of 10,000 eV, which penetrates the film completely, while the reading beam of 1000 eV scarcely penetrates it. Suppose the metal base of the target to be at approximately −50 V, the collector being at zero potential. The writing beam tends to bring down the surface potential to that of the metal base; the reading beam restores it to collector potential by the emission of secondary electrons. So when a picture element is negatively charged by the writing beam it gets a small amount of positive charge each time it is being scanned, giving a signal which can be taken from the resistance inserted in the target lead. A special circuit is needed to prevent the pulse originating from the opening of the writing beam becoming visible in the television picture. Different types of tubes have been developed, including one with a double-sided target.

10.2.4. Storage Tubes for Electronic Computing Machines.

In the past few years storage tubes have become of importance for electronic computing machines. In these machines it is necessary

to write and read numbers as quickly as possible and to store them for a controllable time. Many different storage systems have been proposed, one of them being the storage of electric charges on an insulating target, i.e. an all-electronic system. We have seen already that systems with two stable potentials can easily be achieved; if one potential corresponds to the digit 0 and the other to 1, the

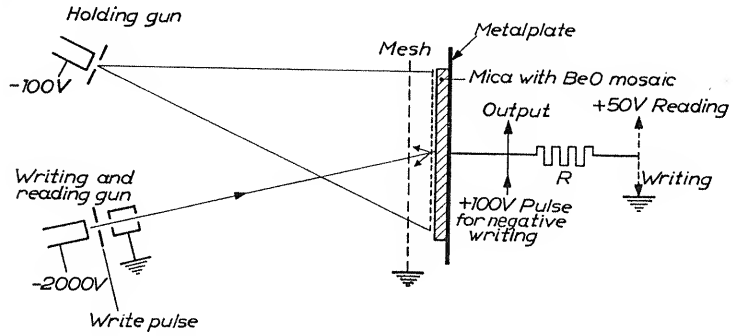

Fig. 10.16. Storage tube by DODD, KLEMPERER and YOUTH [391]

consequence will be that in this type of storage device it is practical to write numbers in the binary system.

One such tube, for example, has been developed by DODD, KLEMPERER and YOUTH (fig. 10.16). It is a kind of cathode ray tube in which the target is similar to that in the iconoscope (fig. 8.4), but its mosaic is beryllium with superficial beryllium oxide, instead of silver-caesium, and $V_p^{\,I} \simeq 50$ V. A very fine wire screen (40 meshes/cm) serving as a collector is laid in front of the target. Two guns are used, one giving a focussed beam of 2000 eV electrons for writing and reading, the other a 100 eV defocussed beam "flooding" the target for holding. By deflecting the focussed beam and by interrupting it opening at discrete deflection positions it is possible to write a pattern on the target. The authors were able to write between 256 and 1024 digits on a target of 100 cm^2.

It is obvious that in this system the writing beam always charges the target surface to collector potential (zero). The differentiation between 1 and 0 is made by the positive pulse of 100 V given to the signal plate when the beam current is opened (fig. 10.17).

It can easily be seen, that the current originating from the holding gun can retain the stored information, if the negative potential of the cathode is about equal to the positive pulse applied for negative

writing; the "positive" spots are then held at collector potential and the negative spots at the cathode potential of the holding gun. For the reading process the signal plate is gated with a special pulse of +50 V in order to obtain signals of different sign. Access to any spot is possible within 25 μs, which gives time for all the operations necessary for locating and reading or writing the information.

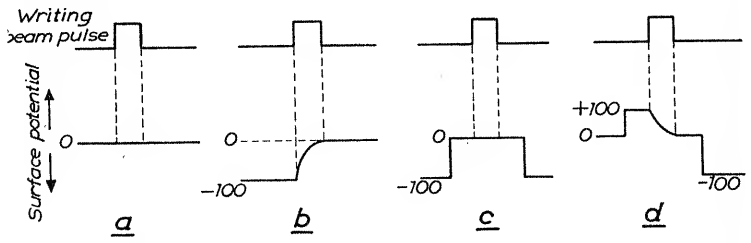

Fig. 10.17. Writing process in tube of fig. 10.16
(a) writing positive on positive spot
(b) writing positive on negative spot
(c) writing negative on negative spot
(d) writing negative on positive spot

Recently RAJCHMAN [392] has developed a tube in which a somewhat similar method of storing, reading and writing is used. The method of selecting a special spot on the target surface is, however, quite different. RAJCHMAN has used a flat cathode, which is able to emit electrons from 256 different areas, each corresponding to a different area on the target surface. By means of an ingenious grid system he is able to select one of the cathode areas for emission and to prevent emission from the rest of the cathode; this tube, therefore, does not need the deflection technique used in other systems.

WILLIAMS and KILBURN [393] have used in their computing machine the simplest form of electrostatic storage system—an ordinary cathode-ray tube with the phosphor screen acting as a storage surface. The front face has an externally applied metal coating, which serves as the signal plate. A pattern is written in the same way as in the system of DODD, KLEMPERER and YOUTH.

When the electron beam is directed at one of the points of the pattern, this point gets a positive charge and $\delta > 1$. Some of the secondary electrons are distributed over the surrounding area, causing a negative charge. Thus a potential mountain arises at a

point P as is shown in fig. 10.18a. Let us call this situation 0. If the figure 1 has to be written, the beam is moved to an adjacent area to a point Q. Now a positive charge is formed at Q and the redistributed electrons will neutralize the positive charge at P. Thus when the beam moves from P to Q the mountain moves

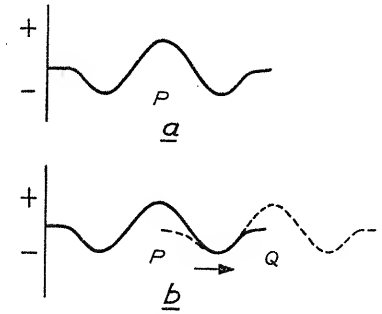

Fig. 10.18. Writing "0" and "1" in storage tube by WILLIAMS and KILBURN [393]

from P to Q as well. The situation with the mountain at Q will be called 1 (fig. 10.18b). Thus the pattern consists of pairs of points, one corresponding to 0, the other to 1.

Reading and holding occurs at the same time. Suppose the beam is directed at P. When a mountain is found at $P(0)$, nothing changes, no signal is obtained, and the beam will be blocked. If, however, there is a mountain at Q a signal will be observed at P. This signal can be used for moving the beam to Q. The old situation will then be restored and the beam be blocked.

The technique of storing numerical information in electronic tubes is quite new, and further developments can be expected.

SURVEY ARTICLES

ON THE PHYSICS OF SECONDARY ELECTRON EMISSION

[1] P. Lenard; *Quantitatives über Kathodenstrahlen*, Heidelberg 1918 and 1925.

[2] P. Lenard and A. Becker; *Handbuch der Experimentalphysik*, Bd 14, Kathodenstrahlen.

[3] R. Kollath; Sekundärelektronenemission fester Körper. *Phys. Z.*, **38**, 202, 1937.

[4] R. Warnecke; Lois principales de l'emission d'électrons secondaires par la surface des métaux. *Onde électrique*, **16**, 509, 1937.

[5] H. Bruining; *Die Sekundärelektronenemission fester Körper*. Berlin 1942.

[6] K. G. McKay; Secondary electron emission. *Advances in Electronics*, I, p. 66, New York 1948.

[7] L. R. Koller; Secondary emission, Pt. I. *Gen. Elect. Rec.*, **51**, 33, 1948.
L. R. Koller; Secondary emission, Pt. II. *Gen. Elect. Rev.*, **51**, 50, 1948.

SEPARATE ARTICLES

ON SECONDARY ELECTRON EMISSION

[8] L. Austin und H. Starke; Über die Reflexion der Kathodenstrahlen und eine damit verbundene neue Erscheinung sekundärer Emission. *Ann. Phys. Lpz.*, **9**, 271, 1902.

[9] L. Austin und H. Starke; Über die Reflexion der Kathodenstrahlen und eine damit verbundene neue Erscheinung sekundärer Emission. *Verh. dtsch. phys. Ges.*, **4**, 106, 1902.

[10] P. Lenard; Über die Beobachtung langsamer Kathodenstrahlen mit Hilfe der Phosphoreszenz und Sekundärentstehung von Kathodenstrahlen. *Ann. Phys. Lpz.*, **12**, 449, 1903.

[11] P. Lenard; Über sekundäre Kathodenstrahlung in gasförmigen und festen Körpern. *Ann. Phys. Lpz.*, **15**, 485, 1904.

[12] Ch. Füchtbauer; Über die Geschwindigkeit der von Kanalstrahlen und von Kathodenstrahlen beim Auftreffen auf Metalle erzeugte negative Strahlen. *Phys. Z.*, **7**, 748, 1906.

[13] Ch. Füchtbauer; Über die Geschwindigkeit der von Kanalstrahlen und von Kathodenstrahlen beim Auftreffe auf Metalle erzeugte negative Strahlen. *Verh. dtsch. phys. Ges.*, **8**, 394, 1906.

[14] Ch. Füchtbauer; Über Sekundärstrahlen. *Ann. Phys. Lpz.*, **23**, 301, 1907.

[15] J. Laub; Über sekundäre Kathodenstrahlen. *Ann. Phys. Lpz.*, **23**, 285, 1907.

[16] O. v. Baeyer; Über langsame Kathodenstrahlen. *Verh. dtsch. phys. Ges.*, **10**, 96, 1908.

[17] O. v. Baeyer; Über langsame Kathodenstrahlen. *Phys. Z.*, **10,** 168, 1909.
[18] O. v. Baeyer; Reflexion und Sekundärstrahlung langsamer Kathodenstrahlen. *Phys. Z.*, **10,** 176, 1909.
[19] A. Gehrts; Reflexion und Sekundärstrahlen lichtelektrisch ausgelöster Kathodenstrahlen. *Ann. Phys. Lpz.*, **36,** 995, 1911.
[20] N. R. Campbell; Delta rays produced by beta rays. *Phil. Mag.*, **24,** 783, 1912.
[21] N. R. Campbell; Ionization by charged particles. *Phil. Mag.*, **25,** 803, 1913.
[22] N. R. Campbell; The ionization of platinum by cathode rays. *Phil. Mag.*, **28,** 286, 1914.
[23] N. R. Campbell; The ionization of metals by cathode rays. *Phil. Mag.*, **29,** 369, 1915.
[24] A. W. Hull; The reflection of slow moving electrons by copper. *Phys. Rev.*, **7,** 1, 1916.
[25] H. M. Dadourian; Reflection of electrons from metal surfaces. *Phys. Rev.*, **14,** 434, 1919.

1921

[26] J. G. Barber; Secondary electron emission from copper surfaces. *Phys. Rev.*, **17,** 322.
[27] R. A. Millikan & J. G. Barber; On the reflection and re-emission of electrons from metal surfaces and a method of measuring the ionizing potential of such surfaces. *Proc. Nat. Acad. Sci. Wash.*, **7,** 13.
[28] J. T. Tate; The effect of angle of incidence on the reflection and secondary emission of slow moving electrons from platinum. *Phys. Rev.*, **17,** 394.

1922

[29] M. Baltruschat & H. Starke; Über sekundäre Kathodenstrahlung. *Phys. Z.*, **23,** 403.
[30] C. Davisson & C. H. Kunsman; The secondary electron emission from nickel. *Phys. Rev.*, **20,** 110.
[31] H. E. Farnsworth; Bombardment of metal surfaces by slow moving electrons. *Phys. Rev.*, **20,** 358.
[32] L. E. McAllister; The effect of ageing on the secondary electron emission from copper surfaces. *Phys. Rev.*, **19,** 246.
[33] F. Tank; Zur Kenntnis der Vorgänge in Elektronenröhren. *Jb. drahtl. Telegr.*, **20,** 82.

1923

[34] L. E. McAllister; Secondary electron emission from copper and copper oxide surfaces. *Phys. Rev.*, **21,** 122.
[35] I. Langmuir; A new photo electric effect: reflection of electrons induced by light. *Science*, **58,** 398.
[36] Balth van der Pol jr.; Over electronenbewegingen in trioden. *Physica, Haag.*, **3,** 108.
[37] B. F. I. Schonland; The passage of cathode rays through matter. *Proc. Roy. Soc. Lond.*, **A104,** 235.

1924

[38] O. Stuhlmann; The minimum velocity of impact to produce secondary electron emission from tungsten. *Phys. Rev.*, **23,** 296.

1925

[39] A. Becker; Über die Geschwindigkeit der sekundäre Kathodenstrahlung. *Ann. Phys. Lpz.*, **78,** 228.
[40] A. Becker; Über die Rückdiffision, Reflexion und Sekundärstrahlerregung langsamer Kathodenstrahlen. *Ann. Phys. Lpz.*, **78,** 253.
[41] H. E. Farnsworth; Electronic bombardment of metal surfaces. *Phys. Rev.*, **25,** 41.
[42] A. W. Hull & N. H. Williams; Determination of elementary charge from measurements of shot-effect. *Phys. Rev.*, **25,** 147.
[43] H. Lange; Über die Sekundärstrahlung in Elektronenröhren. *Jb drahtl. Telegr.*, **26,** 38.
[44] R. L. Petry; Critical potentials in secondary electron emission from iron, nickel and molybdenum. *Phys. Rev.*, **26,** 346.
[45] Balth van der Pol jr.; Über Elektronenbahnen in Trioden, *Jb. drahtl. Telegr.*, **25,** 121.
[46] E. L. Rose; Soft X-rays and secondary electrons. *Phys. Rev.*, **25,** 883.
[47] O. Stuhlmann; The excitation of the M-series in iron by electronic impact. *Phys. Rev.*, **25,** 234.
[48] C. Tingwaldt; Über den Einfluss der Entgasung einer von Kathodenstrahlen getroffenen Metallplatte auf die ausgelöste Elektronenstrahlung. *Z. Phys.*, **34,** 280.

1926

[49] H. E. Farnsworth; Secondary electrons from iron; critical potentials. *Phys. Rev.*, **27,** 243.
[50] H. E. Farnsworth; Secondary electrons from iron. *Phys. Rev.*, **27,** 413.
[51] R. L. Petry; Secondary electron emission from tungsten, copper and gold. *Phys. Rev.*, **28,** 362.

1927

[52] J. B. Brinsmade; Reflected and secondary electrons from an aluminium target. *Phys. Rev.*, **30,** 494.
[53] D. Brown & R. Whiddington; Electron "reflection" in vacuo. *Nature, Lond.*, **119,** 427.
[54] D. Brown & R. Whiddington; Mitteilung über die "Reflexion" von Elektronen von Oberflächen in Vakuum. *Proc. Leeds Phil. Lit. Soc.*, **1,** 162.
[55] H. E. Farnsworth; *J. Opt. Soc. Amer.*, **15,** 290.
[56] H. E. Krefft; O and N energy levels in the secondary emission of hot tungsten. *Phys. Rev.*, **29,** 908.
[57] H. E. Krefft; Critical primary velocities in the secondary electron emission of tungsten. *J. Franklin Inst.*, **204,** 537.
[58] H. E. Krefft; Kritische Geschwindigkeiten für die durch Elektronen an Wolfram ausgelöste sekundäre Kathodenstrahlung. *Ann. Phys. Lpz.*, **84,** 639.

[59] C. F. Sharman; The application of the method of the magnetic spectrum to the study of secondary electron emission. *Proc. Cambridge Phil. Soc.*, **23,** 523.

60] C. F. Sharman; A differential retarding potential method for the study of the energy distribution of slow electron emission. *Proc. Cambridge Phil. Soc.*, **23,** 922.

1928

[61] H. E. Farnsworth; Energy distribution of secondary electrons from copper, iron, nickel and silver. *Phys. Rev.*, **31,** 405.

[62] H. E. Farnsworth; Large angle scattering of low velocity electrons from copper, iron, nickel and silver. *Phys. Rev.*, **31,** 414.

[63] H. E. Farnsworth; Secondary electron current as a function of crystal structure. *Phys. Rev.*, **31,** 419.

[64] J. M. Hyatt; Secondary electron emission produced by positive caesium ions. *Phys. Rev.*, **32,** 922.

[65] J. M. Hyatt & H. A. Smith; Secondary electron emission from molybdenum. *Phys. Rev.*, **32,** 929.

[66] A. Joffé; Über den Brechungsquotienten der De Broglie-Wellen des Elektrons. *Z. Phys.*, **48,** 737.

[67] O. Klemperer; Über den Brechungsquotienten der De Broglie-Wellen des Elektrons. *Z. Phys.*, **47,** 417.

[68] H. E. Krefft; Critical primary velocities in the secondary electron emission of tungsten. *Phys. Rev.*, **31,** 199.

[69] O. W. Richardson; The emission of secondary electrons and the excitation of soft X-rays. *Proc. Roy. Soc. Lond.*, **A119,** 531.

[70] K. H. Stehberger; Über Rückdiffusion und Sekundärstrahlung mittelschneller Kathodenstrahlen an Metallen. *Ann. Phys. Lpz.*, **86,** 825.

[71] D. A. Wells; Energy distribution among secondary electrons from nickel, aluminium and copper. *Phil. Mag.*, **5,** 367.

1929

72] K. Sixtus; Untersuchungen über Sekundäremission. *Ann. Phys. Lpz.*, **3,** 1017.

1930

[73] P. L. Copeland; Secondary electrons from contaminated metal surfaces. *Phys. Rev.*, **35,** 293.

[74] P. L. Copeland; Secondary electrons from contaminated surfaces. *Phys. Rev.*, **35,** 982.

[75] F. Obolensky; Über die Wirkung der Sekundärelektronen auf dem statischen Arbeitszustand der Eingitter. *Arch. Elektrotechn.*, **52,** 834.

[76] S. R. Rao; Total secondary electron emission from polycrystalline nickel. *Proc. Roy. Soc. Lond.*, **A128,** 41.

[77] S. R. Rao; Total secondary electron emission from a single crystal face of nickel. *Proc. Roy. Soc. Lond.*, **A128,** 57.

[78] O. W. Richardson; The emission of secondary electrons and the excitation of soft X-rays. *Proc. Roy. Soc. Lond.*, **A128,** 63.

[79] E. Rudberg; Characteristic energy losses of electrons scattered from incandescent solids. *Proc. Roy. Soc. Lond.*, **A127,** 111.

[80] T. Soller; The velocity distribution of secondary electrons from molybdenum. *Phys. Rev.*, **36,** 1212.

[81] P. B. Wagner; Secondary electrons of high velocity from metals bombarded with cathode rays. *Phys. Rev.*, **35,** 98.

1931

[82] A. J. Ahearn; The emission of secondary electrons from tungsten. *Phys. Rev.*, **38,** 1858.

[83] P. L. Copeland; Thesis, University of Iowa.

[84] L. J. Haworth; Secondary electrons from molybdenum. *Phys. Rev.*, **37,** 93.

[85] S. Kalaschnikoff; Über den Aufladungsprozess an der Oberfläche der Dielektrika bei der Beschiessung mit langsamen Elektronen und positiven Teilchen. *Z. Phys.*, **69,** 380.

1932

[86] P. L. Copeland; Total secondary emission of electrons from metals as a function of primary energy. *Phys. Rev.*, **40,** 122.

[87] H. Fröhlich; Theorie der Sekundärelektronenemission von Metallen. *Ann. Phys. Lpz.*, **13,** 229.

[88] L. J. Haworth; Energy distribution of secondary electrons from molybdenum. *Phys. Rev.*, **42,** 906.

[89] R. Hilsch; Die Reflexion langsamer Elektronen an Ionenkristallschichten zum Nachweis optischer Energiestufen. *Göttinger Nachr.*, **2,** 203.

[90] R. Hilsch; Der Elektronenstoss an kristallschichten zum Nachweis optischer Energiestufen. *Z. Phys.*, **77,** 427.

[91] P. Tartakowsky & W. Kudrjawzewa; Sekundäre Elektronenemission von Nickel und Ferromagnetismus. *Z. Phys.*, **75,** 137.

1933

[92] P. L. Copeland; The variation of secondary emission with heat treatment. *J. Franklin Inst.*, **215,** 435.

[93] P. L. Copeland; Secondary emission of electrons from molybdenum. *J. Franklin Inst.*, **215,** 593.

[94] P. L. Copeland; Surface condition and stability of characteristic in screengrid tubes. *J. Franklin Inst.*, **216,** 417.

[95] K. Hayakawa; Studies on the transformation of metals by secondary electron emission. *Sci. Rep. Tohoku Univ.*, (1) **22,** 934.

[96] C. J. de Lussanet de la Sablonière; Die Sekundärelektronenemission in Elektronenröhren, namentlich Schirmgitterröhren. *Hochfrequenztechn.*, **41,** 195.

[97] S. R. Rao; Total efficiencies of soft X-ray excitation and secondary electron emission from metal faces. *Current. Sci.*, **2,** 93.

[98] S. R. Rao; The efficiency of secondary electron emission. *Proc. Roy. Soc. Lond.*, **A139,** 436.

1934

[99] P. L. Copeland; Secondary emission of electrons from complex targets *Bull. Amer. Phys. Soc.*, **9,** 31.

[100] P. L. Copeland; Secondary emission of electrons from complex targets. *Phys. Rev.*, **45**, 763.
[101] P. L. Copeland; Correlation between variation of secondary electron emission and atomic number. *Phys. Rev.*, **46**, 167.
[102] E. B. Moullin; Measurements of shotvoltage used to deduce the magnitude of secondary thermionic emission. *Proc. Roy. Soc. Lond.*, **A147**, 100.
[103] E. Rudberg; Inelastic scattering of electrons from metals. *Phys. Rev.*, **45**, 764.
[104] H. Schwarzenbach; Bestimmung der Primärelektronenströme in Trioden durch Energiemessungen. *Helv. Phys. Acta.*, **7**, 108.
[105] J. C. Turnbull & P. L. Copeland; Secondary emission of electrons from gold and aluminium. *Phys. Rev.*, **45**, 763.
[106] R. Warnecke; Recherches expérimentales sur l'emission secondaire du tantale. *J. Phys. Radium*, **5**, 267.

1935

[107] W. A. Aldous & N. R. Campbell; The effect of secondary emission upon the fluctuations of the current in a triode (Shot-effect). *Proc. Roy. Soc. Lond.*, **A151**, 694.
[108] H. Bruining; *Secundaire electronenemissie.* Handel. 25e. Ned. natuuren geneesk. Congr. 119.
[109] P. L. Copeland; Secondary emission of electrons of complex targets. *Phys. Rev.*, **48**, 96.
[110] L. J. Haworth; The energy distribution of secondary electrons from molybdenum. *Phys. Rev.*, **48**, 88.
[111] L. J. Hayner; Shot effects of secondary electron currents. *Physics*, **6**, 323.
[112] H. Iams & B. Salzberg; The secondary emission phototube. *Proc. Inst. Radio Engrs (N.Y.)*, **23**, 55.
[113] M. Knoll; Aufladepotential und Sekundäremission elektronenbestrahlter Körper. *Phys. Z.*, **36**, 861.
[114] M. Knoll; Aufladepotential und Sekundäremission elektronenbestrahlter Körper. *Z. techn. Phys.*, **16**, 467.
[115] H. W. Langenwalter; Über Rückdiffusion und Sekundärstrahlerregung langsamer Kathodenstrahlen an dünnen Metallschichten. *Ann. Phys. Lpz.*, **24**, 273.
[116] F. M. Penning & A. A. Kruithof; Verstärkung von Photoströmen durch Emission von Sekundärelektronen. *Physica, Haag*, **2**, 793.
[117] M. Ziegler; Shot effect of secondary emission. *Physica, Haag*, **2**, 415.

1936

[118] A. Afanasjèwa, P. Timofeew & A. Ignaton; Sekundäre Elektronenemission dünner auf Glas niedergeschlagene Metallfilme. *Techn. Physics USSR.*, **3**, 1011.
[119] A. Afanasjèwa, P. Timofeew & A. Ignaton; Die sekundäre Elektronenemission von oxydierten Silber- und Molybdänoberflächen. *Phys. Z. Sowjet*, **10**, 831.

[120] H. Bruining; The depth at which secondary electrons are liberated. *Physica, Haag*, **3**, 1046.
[121] Chlebnikow & Nalimow; Die Sekundärelektronenemission. *Fortschr. phys. Wiss.*, **16**, 467.
[122] F. Coeterier & M. C. Teves; An apparatus for the transformation of light of long wave length into light of short wave length. III Amplification by secondary emission. *Physica, Haag*, **4**, 33.
[123] A. Dobroljubski; Über die Wechselbeziehung zwischen der Sekundärelektronenemission mit der fotoempfindlichkeit und dem Thermioneneffekt. *Z. Phys.*, **102**, 626.
[124] A. Drobroljubski; On the correlation of the secondary emission of electrodes, possessing photosensibility and the thermo-effect of ions. *Phys. Z. Sowjet.*, **10**, 242.
[125] L. J. Haworth; The energy distribution of secondary electrons from columbium. *Phys. Rev.*, **50**, 216.
[126] M. Knoll; Änderung der sekundären Elektronenemission von Isolatoren und Halbleitern durch Elektronenbestrahlung. *Naturwiss.*, **24**, 345.
[127] I. F. Kwarzchawa; Sekundäremission und Ermüdungserscheinungen bei lichtempfindlichen Sauerstoff-Caesium-Elektroden. *Phys. Z. Sowjet.*, **10**, 809.
[128] S. Lukjanov & W. N. Bernatovitch; *J. Exper. Theor. Physics* (russ.), **7**, 856.
[129] L. Malter; Anomalous secondary electron emission, a new phenomenon. *Phys. Rev.*, **49**, 478.
[130] L. Malter; Thin film field emission. *Phys. Rev.*, **50**, 48.
[131] E. Rudberg; Inelastic scattering of electrons from solids. *Phys. Rev.*, **50**, 138.
[132] E. Rudberg & J. C. Slater; Theory of inelastic scattering of electrons from solids. *Phys. Rev.*, **50**, 150.
[133] H. Strübig; Das Potential eines im Hochvakuum isolierten Auffangschirmes bei Beschiessung mit Elektronen. *Phys. Z.*, **37**, 402.
[134] P. W. Timofeew & A. I. Pjatnitzki; Die sekundäre Elektronenemission einer Sauerstoff-Caesium-Elektrode. *Phys. Z. Sowjet.*, **10**, 518.
[135] L. R. G. Treloar; A method of measuring secondary emission of filaments. *Proc. Phys. Soc. Lond.*, **48**, 488.
[136] L. R. G. Treloar; Relation between secondary emission and workfunction. *Nature, Lond.*, **137**, 579.
[137] R. Warnecke; Emission secondaire des metaux purs. *J. Phys. Radium*, **7**, 270.
[138] G. Weiss; Über Sekundärelektronen-Vervielfacher. *Fernsehen-Tonfilm.*, **7**, 41.
[139] G. Weiss; Über Sekundärelektronenvervielfacher. *Z. techn. Phys.*, **17**, 623.
[140] V. K. Zworykin; Elektronenoptische Systeme und ihre Anwendung. *Z. techn. Phys.*, **17**, 170.
[141] V. K. Zworykin, G. A. Morton & L. Malter; The secondary emission multiplier, a new electronic device. *Proc. Inst. Radio Engrs. (N.Y.)*, **24**, 351.

[142] M. Ziegler; Shot effect of secondary emission. I. *Physica, Haag*, **3**, 1.
[143] M. Ziegler; Shot effect of secondary emission. II. *Physica, Haag*, **3**, 307.

1937

[144] A. Afanasjèwa & P. W. Timofeew; Sekundärelektronenemission von mit dünnen Alkalimetallschichten bedecktem Gold, Silber Platin. *Techn. Physics USSR*, **4**, 953.
[145] P. R. Bhawalkar; An explanation of the maximum in secondary electron-emission of metals. *Proc. Indian Sci.*, **6**, 74.
[146] H. Bruining, J. H. de Boer & W. G. Burgers; Secondary electron emission of soot in valves with oxidecathode. *Physica, Haag*, **4**, 267.
[147] H. Bruining, J. H. de Boer & W. G. Burgers; Secondary electron emission of metals with a low work-function. *Physica, Haag*, **4**, 473.
[148] P. L. Copeland; Secondary emission of electrons from sodium films on tantal. *Bull. Amer. Phys. Soc.*, **12**, 12.
[149] A. Dobroljubski; Einige Daten zur Frage des Verhältnisses von sekundärer Elektronenemission und Fotoempfindlichkeit. *Phys. Z. Sowjet*, **11**, 118.
[150] General Electric Company; Secondary emission photocell. *J. Sci. Instrum.*, **14**, 250.
[151] C. Hagen & A. Bey; Aufladepotential elektronenbestrahlter Körper. *Z. Phys.*, **104**, 681.
[152] L. J. Hayner & B. Kurrelmeyer; Shot effect of secondary electrons from nickel and beryllium. *Phys. Rev.*, **52**, 952.
[153] H. Katz; Durchgang langsamer Elektronen durch Metallfolien. *Wiss. techn. Ber. Osram*, **17**, 75.
[154] H. Katz; Durchgang langsamer Elektronen durch Metallfolien. *Z. techn. Phys.*, **18**, 555.
[155] R. Kollath & B. Mrowka; Elektronenemission. *Jb. AEG-Forschung*, **5**, 53.
[156] L. R. Koller & R. P. Johnson; Visual observation of the Malter effect. *Phys. Rev.*, **52**, 519.
[157] O. Krenzien; Auslösung von Sekundärelektronen in Adsorptionsschichten. *Z. techn. Phys.*, **18**, 568.
[158] I. F. Kwarzchawa; Secondary emission and fatigue photoelectric surfaces. *J. Exper. Theor. Phys.*, **7**, 68.
[159] H. Mahl; Feldemission der geschichteten Kathoden bei Elektronenbestrahlung. *Z. techn. Phys.*, **18**, 559.
160] H. O. Müller; Die Abhängigkeit der Sekundärelektronenemission einiger Metalle vom Einfallswinkel des primären Kathodenstrahls. *Z. Phys.*, **104**, 475.
[161] D. M. Myers; The division of the primary electron current between grid and anode of triode. *Proc. Phys. Soc. Lond.*, **49**, 264.
[162] E. R. Piore; Thin film field emission. *Phys. Rev.*, **51**, 1111.
[163] W. Schwitzke; Das Verhalten der Sekundärelektronenemission von Metalle in der Umgebung des Schmelzpunktes. *Diss.*, Berlin.

[164] P. W. Timofeew & A. Pjatnitzki; Die Sekundärelektronenemission von Rb und K-Komplex-Kathoden. *Techn. Physics USSR*, **4**, 945.
[165] L. R. G. Treloar; Secondary electron emission from complex surfaces. *Proc. Phys. Soc. Lond.*, **49**, 392.

1938

[166] Z. Bay; The electron multiplier as an elcctron counting device. *Nature, Lond.*, **141**, 1011.
[167] H. Bruining & J. H. de Boer; Secondary electron emission, Part I. Secondary electron emission of metals. *Physica, Haag*, **5**, 17.
[168] H. Bruining; Secondary electron emission, Part II. Absorption of secondary electrons. *Physica, Haag*, **5**, 901.
[169] H. Bruining; Secondary electron emission, Part III. Secondary electron emission caused by bombardment with slow primary electrons. *Physica, Haag*, **5**, 913.
[170] H. Bruining; *Philips Techn. Rev.*, **3**, 80.
[171] H. Bruining; Thesis, Leiden.
[172] P. L. Copeland; Secondary emission of electrons from sodium on tantal. *Phys. Rev.*, **53**, 328.
[173] A. Dobroljubski; Photosensitivity and secondary electron emission from the oxygen caesium layers at diffusion. *J. Techn. Phys. USSR*, **8**, 266. Ref. *Phys. Ber.*, **20**, 206 (1939).
[174] W. Engbert; Das Rauschen der Sekundäremission. *Telefunkenröhre*, **13**, 127.
[175] H. Katz; Elektronenoptische Versuche zum Durchgang langsamer Elektronen. *Ann. Phys. Lpz.*, **33**, 160, 169.
[176] N. Khlebnikow & Korshunova; Secondary emission of composite surfaces. *Techn. Physics USSR*, **5**, 363.
[177] N. Khlebnikow & Korshunova; The influence of gases on the secondary emission of certain metals. *Techn. Physics USSR*, **5**, 593.
[178] R. Kollath; Die Sekundärelektronenausbeute an Aufdampfschichten von Beryllium. *Fernsehen. Tonfilm.*, **1**, 4.
[179] R. Kollath; Der Einfluss der geometrischen Anordnung der Atome auf die Sekundärelektronenemission. *Naturwiss.*, **4**, 60.
[180] R. Kollath; Über die Sekundärelektronenemission des Berylliums. *Ann. Phys. Lpz.*, **33**, 285.
[181] R. Kollath; Einige Versuche zur Sekundärelektronenemission. *Phys. Z.*, **39**, 916.
[182] S. Lukjanov; On the dependence of the coefficient of the secondary emission on the angle of incidence of the primary electrons. *Phys. Z. Sowjet*, **13**, 123.
[183] H. Mahl; Feldemission aus geschichteten Kathoden bei Elektronenbestrahlung. *Z. techn. Phys.*, **19**, 313.
[184] N. Morgulis & A. Nagorsky; A conference on the photoelectric effect and secondary emission. *Techn. Physics USSR*, **5**, 244.
[185] N. Morgulis & A. Nagorsky; Secondary electron emission from oxide-coated cathodes. *Techn. Physics USSR*, **5**, 864.
[186] J. Mühlenfordt; Über die Feldelektronenemission an dünnen Isolatorschichten. *Z. Phys.*, **108**, 698.

[186a] H. Nelson; Phenomenon of secondary emission. *Phys. Rev.*, **55**, 985.
[187] W. H. Rann; *Nature, Lond.*, **141**, 410.
[188] J. Rajchman; Le courant résiduel dans les multiplicateurs d'électrons-electrostatiques. *Thèse*, Genève.
[189] S. R. Rao & P. S. Vadachari; Secondary electron emission of nickel at the Curie-Point. Ref. *Chem. Abstr.*, **32**, 8916.
[190] E. G. Schneider; Secondary emission of beryllium. *Phys. Rev.*, **54**, 185.
[191] L. R. G. Treloar & D. H. Landon; Secondary electron emission from nickel, cobalt and iron as a function of temperature. *Proc. Phys. Soc. Lond.*, **50**, 625.
[192] L. R. G. Treloar; The measurements of secondary emission in valves. *Wireless Engr.*, **15**, 535.
[193] J. C. Turnbull & H. E. Farnsworth; The inelastic scattering of slow electrons from a silver single crystal. *Phys. Rev.*, **54**, 509.
[194] M. M. Vudinsky; The investigation of secondary electron emission from dielectrics by a thermal method. *J. Techn. Phys. USSR*, **8**, 790. Ref. *Phys. Ber.*, **20**, 437.
[195] R. Warnecke & M. Lortie; Relation entre le coefficient d'émission secondaire et le travail d'extraction électronique de surfaces métalliques. *Bull. Soc. franç. Phys.*, **412**, 8.

1939

[196] J. H. de Boer & H. Bruining; Secondary electron emission, Part VI. Influence of external adsorbed ions and atoms on the secondary electron emission of metals. *Physica, Haag*, **6**, 941.
[196a] A. Bojinesco; Electronic field emission after bombardment of aluminium oxide by electrons or negative ions H^-, N^-, O^-, O_2^-. *C.R. Acad. Sci., Paris*, **209**, 1800.
[197] H. Bruining & J. H. de Boer; Secondary electron emission, Part IV. Compounds with a high capacity for secondary electron emission. *Physica, Haag*, **6**, 823.
[198] H. Bruining & J. H. de Boer; Secondary electron emission, Part V. The mechanism of secondary electron emission. *Physica, Haag*, **6**, 834.
[199] E. A. Coomes; Total secondary electron emission from tungsten and thorium-coated tungsten. *Phys. Rev.*, **55**, 519.
[200] P. L. Copeland; Secondary electrons from sodium films contaminated by gas. *Phys. Rev.*, **55**, 1270.
[201] C. Hagen; Aufladepotential, Sekundäremission und Ermüdungserscheinungen elektronenbestrahlter Metalle und Leuchtsubstanzen. *Phys. Z.*, **40**, 621.
[202] H. Hintenberger; Über Sekundärelektronenemission und Aufladungserscheinungen an Isolatoren. *Z. Phys.*, **114**, 98.
[203] M. Knoll & R. Theile; Elektronenabtaster zur Strukturbildung von Oberflächen und dünner Schichten. *Z. Phys.*, **113**, 260.
[204] H. Mahl; Beobachtungen über Sekundärelektronenemission von Alkali-Aufdampfschichten mit einer oszillographischen Methode. *Jb. AEG-Forschung*, **6**, 33.
[205] W. Majewski; Contribution à la technique des mesures de l'émission secondaire d'électrons. *Acta phys. polon.*, **7**, 327.

[206] S. T. Martin & L. B. Headrick; Light output and secondary emission characteristics of luminescent materials. *J. Appl. Physics*, **10**, 116.
[207] H. Nelson; Phenomenon of secondary emission. *Phys. Rev.*, **55**, 985.
[208] H. Paetow; Über die als Nachwirkung von Gasentladungen an den Elektroden auftretende spontane Elektronenemission und die Feldelektronenemission an dünnen Isolatorschichten. *Z. Phys.*, **111**, 770.
[209] A. Pjatnitzki; Distribution of the energy of secondary electrons emitted by a composite caesium cathode. *Phys. Ber.*, **20**, 437.
[210] R. Suhrmann & W. Kundt; Die Sekundärelektronenemission reiner Metalle in ungeordnetem und geordnetem Zustand. *Naturwiss.*, **27**, 548.
[210a] M. M. Vudinsky; Mechanism of secondary electron emission from thin dielectric layers. *J. Techn. Phys. USSR*, **9**, 271.
[210b] M. M. Vudinsky; On the velocity distribution of secondary electrons emitted by sodium chloride. *J. Techn. Phys. USSR*, **9**, 1583.
[211] R. Warnecke & M. Lortie; Sur l'émission secondaire du beryllium. *C.R. Acad. Sci. Paris*, **208**, 429.
[212] D. E. Wooldridge; Theory of secondary emission. *Phys. Rev.*, **56**, 562.
213] D. E. Wooldridge; Secondary emission from evaporated nickel and cobalt. *Phys. Rev.*, **56**, 1062.

1940

[214] P. L. Copeland; Secondary emission from films of platinum on aluminum. *Phys. Rev.*, **58**, 604.
[215] A. I. Frimer; A study of the secondary electron emission from copper oxide, pure or treated with alkali metals. *J. Tech. Phys. USSR*, **10**, 394.
[216] A. Gubanov; The effect of a charge on an electron beam during secondary emission. *J. Exp. Theor. Phys. USSR*, **2**, 161.
[217] A. E. Hastings; Secondary emission from films of silver on platinum. *Phys. Rev.*, **57**, 695.
[218] W. Heimann & K. Geyer; Direct measurement of the secondary electron yield from insulators. *Elekt. Nachr.-Tech.*, **17**, 1.
[219] A. E. Kadyschevitsch; Theory of secondary electron emission from metals. *J. Phys. USSR*, **2**, 115.
[220] H. Kamogawa; Secondary emission and electron diffraction on the glass surface. *Phys. Rev.*, **58**, 660.
[221] I. D. Kirvalidze; A method for determining the charging potential of dielectrics and the lower limit of secondary electron emission from a monocrystal of NaCl. *C.R. Acad. Sci. USSR*, **26**, 635.
[222] R. Kollath; A new method for the measurement of the energy distribution of secondary electrons. *Z. techn. Phys.*, **21**, 328.
[223] N. D. Morgulis; The mechanism of secondary electron emission from composite surfaces. *J. Tech. Phys. USSR*, **10**, 79.
[224] N. D. Morgulis; On the nature of secondary emission from composite cathodes. *J. Tech. Phys. USSR*, **10**, 1710.
[225] N. D. Morgulis & B. I. Dyatlovitskaya; On the emission from antimony-caesium cathodes. *J. Tech. Phys. USSR*, **10**, 657.
[226] H. Nelson; Field enhanced secondary electron emission. *Phys. Rev.*, **57**, 560.

[227] E. R. Piore & G. A. Morton; The behaviour of willemite under electron bombardment. *J. Appl. Phys.*, **11**, 153.
[228] W. Reichelt; Influence of temperature on the secondary emission of metals. *Ann. Phys. Lpz.*, **38**, 293.
[229] H. Salow; On the secondary electron yield of electron bombarded insulators. *Z. techn. Phys.*, **21**, 8.
[230] H. Salow; Angular dependence of the secondary electron emission from insulators. *Phys. Z.*, **41**, 434.
[231] K. Scherer; Charging and secondary electron emission. *Arch. Elektrotech.*, **34**, 143.
[232] H. Schnitger; The properties of secondary emitting layers of magnesium oxide. *Z. techn. Phys.*, **21**, 376.
[233] P. W. Timofeew & A. V. Afanasjèwa; Secondary emission from oxides of metals. *J. Tech. Phys. USSR*, **10**, 28.
[234] P. W. Timofeew & P. M. Aranovich; Barium oxide and magnesium oxide emitters of secondary electrons. *J. Tech. Phys. USSR*, **10**, 32.
[235] P. W. Timofeew & J. Lunkova; Electron emission from caesium oxide cathodes with gold particles in the intermediate layer. *J. Tech. Phys. USSR*, **10**, 12.
[236] P. W. Timofeew & J. Lunkova; Antimony-caesium emitters. *J. Tech. Phys. USSR*, **10**, 20.
[237] P. W. Timofeew & A. I. Pyatnitski; Secondary electron emission from oxygen-caesium emitters at different primary current densities. *J. Tech. Phys. USSR*, **10**, 39.
[238] P. W. Timofeew & K. A. Yumatov; Secondary electron emission from oxygen-caesium emitters at low velocities of primary electrons. *J. Tech. Phys. USSR*, **10**, 8.
[239] P. W. Timofeew & K. A. Yumatov; Secondary electron emission from sulphur-caesium emitters. *J. Tech. Phys. USSR*, **10**, 24.
[240] P. S. Varadachari; Secondary electron emission of nickel at the Curie point. *Proc. Indian Acad. Sci.*, **A12**, 381.
[241] D. E. Wooldridge; Temperature effects on the secondary electron emission from pure metals. *Phys. Rev.*, **57**, 1080.
[242] D. E. Wooldridge; Temperature effects in secondary emission. *Phys. Rev.*, **58**, 316.
[243] D. E. Wooldridge & C. D. Hartmann; The effects of order and disorder on secondary electron emission. *Phys. Rev.*, **58**, 381.
[244] N. Yasnopol'ski; On the "jumps" observed in emitters of poor conductivity caused by the blocking effect. *J. Tech. Phys. USSR*, **10**, 1813.

1941

[245] G. Bekow; Secondary emission from copper single crystals at small primary velocities. *Phys. Z.*, **42**, 144.
[246] H. A. Bethe; On the theory of secondary emission. *Phys. Rev.*, **59**, 940.
[247] H. Bruining; Secondary electron emission from metals with low work function. *Physica, Haag*, **8**, 1161.
[248] R. M. Chaudri & A. W. Khan; Secondary electron emission from nickel. *Phil. Mag.*, **31**, 382.

[249] J. Friedheim & J. G. Weiss; Secondary electron yield of silver-magnesium alloys. *Naturwiss.*, **29**, 777.
[250] C. Gille; Secondary electron emission by a nickel-beryllium alloy. *Z. techn. Phys.*, **22**, 228.
[251] P. Görlich; Contribution to the problem of secondary electron emission of condensed alkali-earth metal films. *Phys. Z.*, **42**, 129.
[252] M. S. Joffe & I. V. Nechaev; The secondary electron emission from potassium. *J. Exp. Theoret. Phys. USSR*, **11**, 93.
[253] A. E. Kadyschevitsch; Theory of secondary electron emission from dielectrics and semiconductors. *J. Phys. USSR*, **4**, 341.
[254] R. Kollath; On the influence of temperature on the secondary electron emission of metals. *Ann. Phys. Lpz.*, **39**, 19.
[255] R. Kollath; On the energy distribution of secondary electrons. *Ann. Phys. Lpz.*, **39**, 59.
[256] Yu. M. Kushnir & M. I. Frumin; The dependence of the energy distribution function of secondary electrons on the angle of emergence. *J. Tech. Phys. USSR*, **11**, 317.
[257] I. Mathes; Secondary electron emission properties of some alloys. *Z. techn. Phys.*, **22**, 232.
[258] G. Maurer; The secondary electron emission from semiconductors and insulators. *Z. Phys.*, **118**, 122.
[259] E. Mishibori; Secondary electron emission from magnesium oxide. *Proc. Phys.-Math. Soc. Japan*, **23**, 570.
[260] N. D. Morgulis; The emission of electrons by active semi-conducting surfaces. *Bull. Acad. Sci. USSR*, **5**, 536.
[261] P. M. Morozov; The effect of temperature on secondary electron emission. *J. Exp. Theoret. Phys. USSR*, **11**, 402.
[262] P. M. Morozov; Secondary electron emission from lead, tin and bismuth in the solid and liquid state. *J. Exp. Theoret. Phys. USSR*, **11**, 410.
[263] Yu. A. Nemilov; A new method for studying secondary electron emission. *J. Tech. Phys. USSR*, **11**, 854.
[264] H. Paetow; A new form of field emission at very low pressures from metallic surfaces covered by a deposit of insulating material. *Z. Phys.*, **117**, 399.
[265] H. Randenbusch; Some investigations on the technical uses of secondary emission surfaces. *Z. Tech. Phys.*, **22**, 237.
[266] M. Tanaka; After effect of metal bombarded by electrons. *Proc. Phys.-Math. Soc. Japan*, **22**, 899.
[267] H. Teichmann & K. Geyer; The occurrence of structure dependent selectivity in secondary electron emission. *Z. ges. Nature*, **7**, 313.
[268] M. M. Vudinsky; The stability of secondary electron emission from alkali halide cathodes. *J. Tech. Phys. USSR*, **11**, 1066.
[269] F. Wecker; New measurements on the absorption, back diffusion and secondary emission in aluminum and gold. *Ann. Phys. Lpz.*, **40**, 405.
[270] H. Wolff; Secondary electron and photoelectron emitting semiconductors. *Ann. Phys. Lpz.*, **39**, 591.
[271] V. K. Zworykin, J. E. Ruedy & E. W. Pike; Silver-magnesium alloy as a secondary emitting material. *J. Appl. Phys.*, **12**, 696.

1942

[272] K. H. Geyer; On the properties of yield and energy distribution of secondary electrons from evaporated layers of increasing thickness. *Ann. Phys. Lpz.*, **41,** 117.

[273] K. H. Geyer; Observations on the secondary electron emission from nonconductors. *Ann. Phys. Lpz.*, **42,** 241.

[274] P. Görlich; On the secondary emission of evaporated layers of antimony. *Phys. Z.*, **43,** 121.

[275] O. Krenzien; The elementary processes in the secondary electron emission of polar crystals. *Wiss. Veroff. Siemens-Werk*, **20,** 91.

[276] K. G. McKay; Total secondary emission from thin films of sodium on tungsten. *Phys. Rev.*, **61,** 708.

[277] R. Truell; Range of secondary electrons in magnesium. *Phys. Rev.*, **62,** 340.

1943

[278] J. Bronstein; *Techn. Phys. USSR*, **13,** 176.

[279] K. H. Geyer; Contribution to our knowledge of the fundamental process of secondary electron emission. *Ann. Phys. Lpz.*, **42,** 337.

[280] I. Gimpel & O. Richardson; The secondary electron emission from metals in the low primary energy region. *Proc. Roy. Soc.*, **A182,** 17.

[281] W. R. Kennedy & P. L. Copeland; The temperature coefficient of the secondary emission yield and the work function of molybdenum coated with beryllium and treated with HCl. *Phys. Rev.*, **63,** 61.

[282] H. Schlechtweg; Quantum theory of secondary electron emission of transition metals. *Naturwiss.*, **31,** 204.

[283] R. Suhrmann & W. Kundt; The secondary emission of pure metallic films in the ordered and unordered states and their transparency for secondary electrons. *Z. Phys.*, **120,** 363.

[284] R. Suhrmann & W. Kundt; On the effect of adsorbed oxygen on the secondary emission of vaporized metal films at 293°K and 83°K. *Z. Phys.*, **121,** 118.

[285] F. Trey; Review on the effect of field emission on secondary electron emission. *Phys. Z.*, **44,** 38.

1944

[286] A. V. Afanasjèwa; Stable emitters of secondary electrons. *Univ. M.V. Lomousova*, **74,** 114.

[287] J. H. O. Harries; Secondary electron radiation. *Electronics*, **10,** 100 (Sept.).

[288] J. B. Johnson; Enhanced thermionic emission. *Phys. Rev.*, **66,** 352.

[289] M. Knoll, O. Hachenberg & J. Randmer; Mechanism of secondary emission in the interior of ionic crystals. *Z. Phys.*, **122,** 137.

[290] I. F. Kwarzchawa; Change of conductivity of aluminum oxide upon electron bombardment. *Bull. Acad. Sci. USSR*, **8,** 373.

[291] S. J. Lukjanov; Secondary electron emission of solids. *Bull. Acad. Sci. USSR*, **8,** 330.

[292] D. V. Zernov, M. I. Elinson & N. M. Levin; Investigation of Auto-electronic emission of thin dielectric films. *Bull. Acad. Sci. USSR, Classe sci. tcch.* 166.

[293] D. V. Zernov; On the influence of strong electric fields on the secondary electron emission of dielectric films. *Bull. Acad. Sci. USSR*, **8,** 352.

1945

[294] A. E. Kadyschevitsch; The velocity distribution of secondary electrons of various emitters. *J. Phys. USSR*, **9,** 431.

[295] A. E. Kadyschevitsch; On the measurement of the depth of generation of secondary electrons in metals. *J. Phys. USSR*, **9,** 436.

[296] C. W. Mueller; The secondary emission of "Pyrex" glass. *J. Appl. Phys.*, **16,** 453.

1946

[297] J. B. Johnson; Secondary emission of thermionic oxide cathodes. *Phys. Rev.*, **69,** 693.

[298] L. R. Koller & J. S. Burgess; Secondary emission from germanium, boron and silicon. *Phys. Rev.*, **70,** 571.

[299] A. Lallemand; Application of secondary emission of electrons to multiplier tubes. *Rev. Sci. Paris*, **84,** 131

[300] M. A. Pomerantz; Secondary electron emission from oxide coated cathodes. *J. Franklin Inst.*, **241,** 415; **242,** 41.

1947

[301] A. I. Frimer; Study of secondary emission at low temperatures. *J. Tech. Phys. USSR*, **17,** 71.

[302] J. B. Johnson; Secondary electron emission from targets of barium-strontium oxide. *Phys. Rev.*, **73,** 1058 (1948).

[303] H. E. Mendenhall; Secondary emission from conducting films of tin oxide. *Phys. Rev.*, **72,** 532.

[304] P. C. R. Palluel; Rediffused component of secondary radiation from metals. *C.R. Acad. Sci. Paris*, **224,** 1492.

[305] P. C. R. Palluel; On the mechanism of rediffusion of electrons from metals. *C.R. Acad. Sci. Paris*, **224,** 1551.

[306] P. C. R. Palluel; The true secondary emission coefficient in metals. *C.R. Acad. Sci. Paris*, **225,** 383.

[307] J. G. Trump & R. J. van de Graaff; High voltages in vacuum. *J. Appl. Phys.*, **18,** 327.

[308] D. V. Zernov and B. S. Kuljvarskaya; Investigations of the temperature dependence of the electronic emission of dielectric films under the influence of the field of positive surface charge. *J. Tech. Phys. USSR*, **17,** 309.

1948

[308a] J. B. Johnson; Secondary emission from targets of Ba-Sr-oxide. *Phys. Rev.*, **73,** 1058.

[309] H. E. Mendenhall; Secondary emission from thoria on platinum and tantalum. *Phys. Rev.*, **74,** 1265.

1949

[310] G. W. Hees & H. Jacobs; Secondary emission from barium oxide as a function of temperature. *Phys. Rev.*, **75**, 1312.

[311] H. E. Mendenhall; Secondary emission from silicon and germanium oxides. *Phys. Rev.*, **76**, 458.

[312] E. J. Sternglass; An interpretation of secondary electron emission data for homogeneous solids. *Phys. Rev.*, **76**, 189.

[313] F. C. Todd & L. J. Rueger; Secondary emission from oxides at high temperatures. *Phys. Rev.*, **76**, 189.

[314] J. G. Trump & R. J. van de Graaff; The secondary emission of electrons by high energy electrons. *Phys. Rev.*, **75**, 44.

1950

[315] E. M. Baroody; A theory of secondary electron emission from metals. *Phys. Rev.*, **78**, 780.

[316] E. S. Sternglass; Secondary electron emission and atomic shell structure. *Phys. Rev.*, **80**, 925.

1951

[317] E. M. Baroody; Application of Wooldridge theory of secondary emission. *Phys. Rev.*, **83**, 857.

[318] J. J. Brophy; Secondary emission of electrons from liquid metal, surface. *Phys. Rev.*, **83**, 534.

[319] J. J. Brophy; Comparison of theories of secondary emission. *Phys. Rev.*, **82**, 757.

[320] H. Jacobs; Field dependent secondary emission. *Phys. Rev.*, **84**, 755.

[321] J. L. H. Jonker; The angular distribution of the secondary electrons of nickel. *Philips Res. Repts.*, **6**, 372.

1952

[322] F. Brand, H. Jacobs & J. Freely; Mechanism of field dependent secondary emission. *Rep. 12th Annual Conf. Phys. Electronics*, p. 74.

[323] A. J. Dekker & A. van der Ziel; Theory of the production of secondary electrons in solids. *Phys. Rev.*, **86**, 755.

[324] J. L. H. Jonker; On the theory of secondary electron emission. *Philips Res. Repts.*, **7**, 1.

[325] Masaki Hirashima; Secondary emission valves. *Wireless Eng.*, **29**, 246.

[326] P. Rappaport; New methods of processing silver magnesium secondary emitters. *Rep. 12th Annual Conf. Phys. Electronics*, p. 18.

[327] J. Woods & D. A. Wright; Secondary electron emission of barium oxide. *Brit. J. Appl. Physics*, **3**, 323.

[328] J. B. Johnson & K. G. McKay; Secondary electron emission from germanium. *Phys. Rev.*, **85**, 390.

[329] H. Jacobs, J. Martin & F. Brand; Secondary emission from composite surfaces. *Phys. Rev.*, **85**, 441.

[330] R. R. Law; Decay time of secondary electron emission. *Phys. Rev.*, **85**, 391.

LITERATURE ON THE APPLICATION OF SECONDARY ELECTRON EMISSION

	SECTION	
[331]	8.1.1	F. M. Penning & A. A. Kruithof; *Physica, Haag*, **2**, 793, 1935.
[332]		H. Iams & B. Salzberg; *Proc. Inst. Rad. Eng.*, **23**, 55, 1935.
[333]	8.1.2 8.1.3 8.1.5	V K. Zworykin, G. A. Morton & L. Malter; *Proc. Inst. Rad. Engrs.*, **24**, 351, 1936.
[334]		V. K. Zworykin & J. A. Rajchman; *Proc. Inst. Rad. Engrs.*, **27**, 558, 1939.
[335]		G. A. Morton; *R.C.A. Review*, **10**, 525, 1949.
[336]		W. Hartmann *Hausmitt. Fernseh. GmbH*, **1**, 226, 1939.
[337]		A. Lallemand; *le Vide*, **4**, 618, 1949.
[338]		N. Schaetti; *Z. angew. Math. Phys.*, **2**, 153, 1951.
[339]		R. W. Engström; *Rev. Sci. Instrum.*, **18**, 587, 1947. *J. Opt. Soc. Amer.*, **37**, 420, 1947.
[340]		M. C. Teves; *Philips Techn. Rev.*, **5**, 261, 1940.
[341]		G. E. Kron; *Astrophysical J.*, **103**, 326, 1946.
[342]	8.1.4	W. Shockley & J. R. Pierce; *Proc. Inst. Rad. Engrs.*, **26**, 321, 1938.
[343]	8.1.6	G. Holst, J. H. de Boer, M. C. Teves & C. F. Veenemans; *Physica, Haag*, **1**, 297, 1943.
[344]		F. Coeterier & M. C. Teves; *Physica, Haag*, **4**, 33, 1937.
[345]	8.1.7	Z. Bay; *Rev. Sci. Instrum.*, **12**, 127, 1941.
[346]		J. S. Allen; *Phys. Rev.*, **55**, 966, 1939.
[347]		J. S. Allen; *Rev. Sci. Instrum.*, **12**, 484, 1941.
[348]		R. P. Stone; *Rev. Sci. Instrum.*, **20**, 935, 1949.
[349]	8.2	P. T. Farnsworth; *J. Franklin Inst.*, **2**, 411, 1934.
[350]		M. H. Greenblatt & P. A. Miller; *Phys. Rev.*, **72**, 160, 1947.
[351]		W. Henneberg, K. Orthuber & E. Steudel; *Z. techn. Phys.*, **17**, 115, 1936.
[352]	8.3	J. L. H. Jonker & M. C. Teves; *Philips Techn. Rev.*, **3**, 137, 1938.
[353]		J. L. H. Jonker & A. J. W. M. van Overbeek; *Wireless Eng.*, **15**, 150, 1938.
[354]		A. J. W. M. van Overbeek; *Wireless Eng.*, April 1951, p. 114.
[355]		C. W. Mueller; *Proc. Inst. Rad. Engrs.*, **38**, 159, 1950.
[356]	8.4	A. W. Hull; *Phys. Rev.*, **7**, 141, 1916.
[357]		H. Barkhausen; *Elektronenröhren* (III) p. 71, Leipzig 1935.
[358]		G. Diemer & J. L. H. Jonker; *Philips Res. Repts.*, **5**, 161, 1950.
[359]	8.5	J. L. H. Jonker & Z. van Gelder; *Philips Techn. Rev.*, **13**, 1, 1951.

[360] J. L. H. JONKER & Z. VAN GELDER; *Philips Techn. Rev.*, **13**, 33, 1951.
[361] 9.1 J. L. H. JONKER; *Philips Techn. Rev.*, **3**, 215, 1938.
[362] 9.2 BALTH VAN DER POL & TH. J. WEYERS; *Physica, Haag*, **1**, 481, 1934.
[363] W. KLEEN; *Telef. Röhre*, **9**, 1934.
[364] J. L. H. JONKER; *Philips Res. Repts.*, **2**, 331, 1947.
[365] 1.3 J. L. H. JONKER; *Philips Techn. Rev.*, **10**, 346, 1948.
[366] E. G. DORGELO & P. ZIJLSTRA; *Philips Techn. Rev.*, **12**, 161, 1950.
[367] 9.4 K. A. MACFADYEN; *Wireless Eng.*, **15**, 310, 1938.
[368] 9.5 H. G. BOUMEESTER; *Philips Techn. Rev.*, **2**, 115, 1937.
[369] 9.6 A. BOUWERS & J. H. VAN DER TUUK; *Physica, Haag*, **12**, 274, 1931.
[370] 10.1 K. G. MCKAY; *Advances in Electronics*, I, p. 98, New York 1948.
[371] 10.2 M. KNOLL & B. KAZAN; *Storage Tubes and their Basic Principles*, New York 1952.
[372] 10.2.1 J. D. MCGEE; *Electronics and their Application in Industry and Research*, edited by B. LOVELL, p. 135, Pilot Press, London 1947.
[373] 10.2.1.1 J. D. MCGEE; *Proc. Inst. Elect. Engrs.*, **97**, 377, 1950.
[374] A. ROSE & H. IAMS; *Proc. Inst. Radio Engrs.*, **27**, 547, 1939.
[375] A. ROSE, P. K. WEIMER & H. B. LAW; *Proc. Inst. Radio Engrs.*, July 1946, p. 424.
[376] P. K. WEIMER; *R.C.A. Review*, **10**, 366, 1949.
[377] 10.2.1.2 V. K. ZWORYKIN; *J. Inst. Elect. Engrs.*, **73**, 437, 1933.
[378] P. SCHAGEN; *Philips Res. Repts.*, **6**, 135, 1951.
[379] J. D. MCGEE and H. G. LUBSZYNSKI; *J. Inst. Elect. Engrs.*, **84**, 468, 1939.
[380] P. SCHAGEN, H. BRUINING and J. C. FRANCKEN; *Philips Techn. Rev.*, **13**, 119, 1951/52.
[381] 10.2.1.3 M. KNOLL & R. THEILE; *Z. Phys.*, **113**, 260, 1939.
[382] 10.2.2 J. DE GIER; *Philips Techn. Rev.*, **10**, 97, 1948/49.
[383] J. HAANTJES & F. W. DE VRIJER; *Philips Techn. Rev.*, **13**, 55, 1951/52.
[384] E. BAUMANN; *J. Brit. Inst. Radio Engrs.*, **12**, 69, 1952.
[385] 10.2.3 L. PENSAK; *R.C.A. Review*, **10**, 59, 1949.
[386] F. ANSBACHER & W. EHRENBERGER; *Nature, Lond.*, **164**, 144, 1949.
[387] *Proc. Phys. Soc.*, **64**, 362, 1951.
[388] E. J. RITTNER; *Phys. Rev.*, **73**, 1212, 1948.
[389] K. G. MCKAY; *Phys. Rev.*, **74**, 1606, 1948.
[390] L. PENSAK; *Phys. Rev.*, **75**, 472, 1949.
[391] 10.2.4 S. H. DODD, H. KLEMPERER & P. YOUTH; *J. Inst. Elect. Engrs.*, **69**, 990, 1950.
[392] J. RAJCHMAN; *R.C.A. Review*, **12**, 53, 1951.
[393] F. C. WILLIAMS & T. KILBURN; *Proc. Inst. Elect. Engrs.*, Pt. 2, **96**, 183, 1949.

INDEX

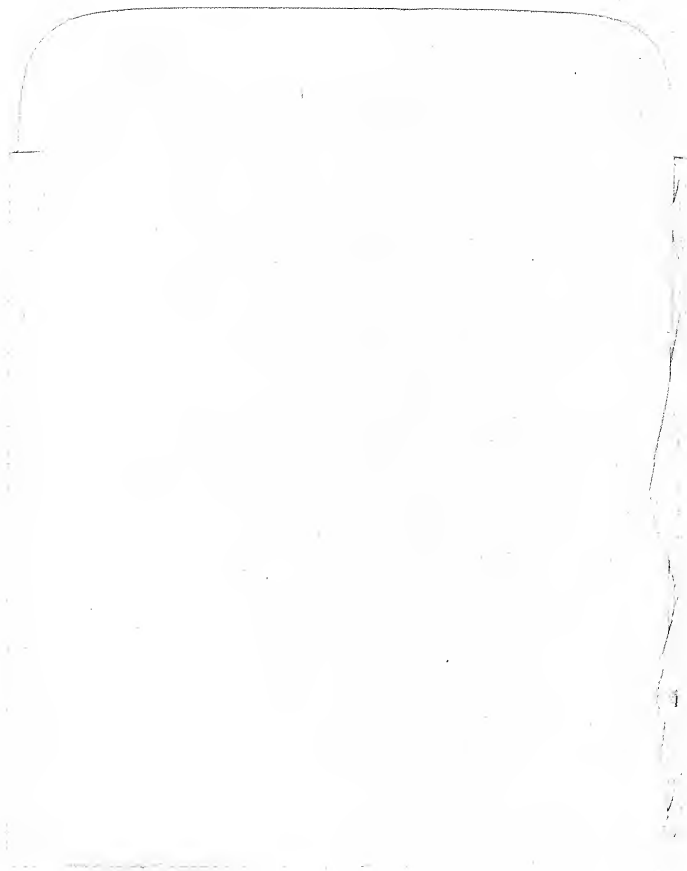

Balint